12-2001

Characterization of Chitosan Films for Cell Culture Applications

Michael Katalinich

CHARACTERIZATION OF CHITOSAN FILMS FOR CELL CULTURE APPLICATIONS

By

Michael Katalinich

B.S. University of Colorado, Boulder, 1997

A THESIS

Submitted in Partial Fulfillment of the

Requirements for the Degree of

Master of Science

(in Chemical Engineering)

The Graduate School

The University of Maine

December, 2001

Advisory Committee:

Amyl Ghanem, Assistant Professor of Chemical Engineering, Advisor

Douglas Bousfield, Professor of Chemical Engineering

Rebecca Van Beneden, Professor of Biochemistry and Marine Sciences

CHARACTERIZATION OF CHITOSAN FILMS FOR CELL CULTURE APPLICATIONS

By Michael Katalinich

Thesis Advisor: Dr. Amyl Ghanem

An Abstract of the Thesis Presented
in Partial Fulfillment of the Requirements for the
Degree of Master of Science
(in Chemical Engineering)
December, 2001

Chitosan (β-(1,4)-2-amino-2-deoxy-D-glucose) is a naturally occurring, abundant biopolymer exhibiting desirable biomaterial properties of biodegradability, low toxicity and good biocompatibility. These properties indicate the suitability of chitosan as a surface for mammalian cell growth. The goal of this thesis is to explore the potential for using chitosan as a surface for NIH 3T3 fibroblast attachment and growth. A standard, reproducible film-formation technique, based on other researchers techniques was established. The reproducibility of this technique, through characterization of the physical and chemical properties of these films, was good. The attachment and growth of NIH 3T3 fibroblasts on chitosan films and controls was measured. These films were modified by physical and chemical means to optimize the attachment and growth of the NIH 3T3 fibroblasts. Physical properties, including film tensile properties, surface roughness of films, and chemical properties including the degree of deacetylation (measure of number of acetylated amino groups in the chitosan polysaccharide) and surface free energy (SFE) estimated by contact angle measurements were performed to characterize the chitosan films.

Chitosan films of 0.5, 1.5 and 3.0% (w/v) support the attachment and proliferation of NIH 3T3 fibroblasts at rates lower than polystyrene controls. The film tensile properties, surface roughness and surface free energies indicate that the film-formation technique gives films with reproducible physical and chemical properties. The sterilization of films with ultraviolet and infrared lamps (UV-IR) over time changes the water-in-air contact angle (WIA) and increases the overall SFE of the films. This is an important result because the WIA contact angle has been shown influential to the rate of cell attachment, and the SFE has been shown to affect the degree of fibroblast spreading. Our results indicate that UV-IR treatment of chitosan films can change the WIA contact angle and SFE of the films, and can potentially be used to optimize the attachment and spreading of fibroblasts on these films.

The ability of these chitosan films to support cell attachment and growth indicates their potential use as biomedical surfaces. Good attachment and growth results in rapid and efficient wound repair. This research may result in the development of biodegradable tissue-engineering matrices. This development requires an understanding of the basic cell-chitosan surface interactions.

DEDICATION

This paper is dedicated to my father, David Katalinich. He was a significant driving force in the continuation of my education after high school. This work is a direct reflection of his influence on my professional career. He is my real-life hero and a wonderful father.

ACKNOWLEDGEMENTS

The author would like to thank his advisor, Dr. Amyl Ghanem, for her guidance, and support on all aspects of this project throughout the duration of this study. Dr. Ghanem's considerable effort towards the review and correction of papers and presentations was both beneficial and enlightening. The author would also like to thank Dr. Douglas Bousfield for his input on various aspects of this project, especially advice concerning the characterization of the films utilized in this study. The author is pleased to thank Dr. Rebecca Van Beneden for her support of the author and the project over the last two years. Dr. Van Beneden's input regarding cell culture-related project aspects was very helpful.

The author thankfully acknowledges all of those individuals who assisted with the completion of this project. Specifically, thanks to Manish Giri for his assistance with rheology testing of samples, Yang Xiang for help with image capture and analysis, Jong Tae Youn for help with tension tests of samples, Ben McCool for help with surface area and porosity measurements, and Brian Ninness for help with FTIR testing of samples. Additionally, thanks to Dr. Thompson for the donation of the UV-IR oven used to sterilze samples, Dr. Co and Amos Cline for IT support, and Mark Paradis for the use of vital testing equipment. Thanks to Angel Hildreth and Cathy Dunn for help with department-related issues. Also, thanks to Dan Jolicoeur for help with obtaining supplies and with the fabrication and repair of tools integral to this project.

Finally, a special thank you is extended to Scott Delcourt, Director of the Graduate School, and Chet Rock, Dean of the College of Engineering, for much-needed financial support towards the end of this project.

TABLE OF CONTENTS

LIST OF FIGURES

LIST OF TABLES

LIST OF EQUATIONS

Chapter 1

INTRODUCTION

1.1. Project Objective

The goal of this research project is to explore the potential use of chitosan as a surface for cell attachment and growth. Ultimately, this research may lead to the development of a technology for three dimensional (3-D) implantable chitosan scaffolds for use in tissue engineering of damaged tissues and wound repair. This research is an initial investigation on the subject of chitosan as a biomaterial for tissue engineering and serves as the foundation for future work in this field. To establish the potential of chitosan as a surface for cell culture with fibroblasts, this study considers primarily two-dimensional (2-D) applications with chitosan films. The goal of this project is to develop and characterize chitosan-based films for cell culture applications. Specific project objectives include the development of a reproducible chitosan film formation technique based on established methods, testing the reproducibility of this technique through characterization of the physical and chemical properties of these films, measurement of the attachment and growth of NIH 3T3 fibroblasts on chitosan films, and modification of these films by physical and chemical means to optimize the attachment and growth of the NIH 3T3 fibroblasts.

1.2. Chitin and Chitosan

Chitosan or β-(1,4)-2-amino-2-deoxy-D-glucose, is a hydrophobic biopolymer obtained industrially by hydrolyzing the amino acetyl groups of chitin, which is the main

component of shells of crab, shrimp and krill, by an alkaline treatment [104]. The structure of chitosan is shown in Figure 1.

Figure 1. Chemical structure of chitosan

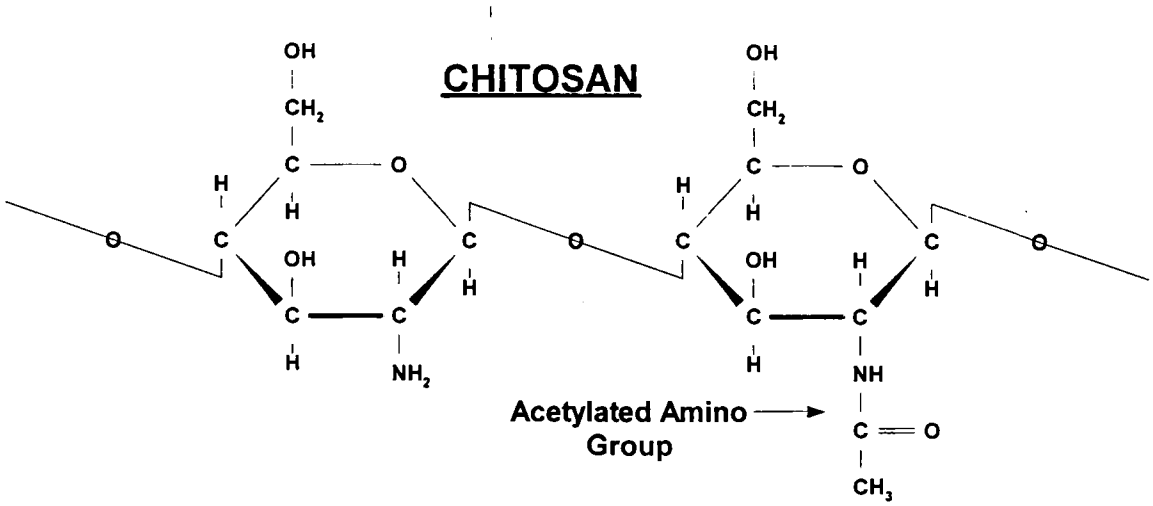

The main driving force in the development of new applications for chitosan lies in the fact that the polysaccharide is not only naturally abundant, but is also nontoxic and biodegradable [123]. Chitosan is also easily processed into films and membranes, microparticles and beads, and 3-D scaffolds.

The primary reason for utilizing chitosan in this study is its desirable properties of biocompatibility and biodegradability. Chitosan has been reported to be nontoxic and bioresorbable when used in human and animal models [116]. Chitosans with high degrees of deacetylation support the attachment of different cell lines[177], indicating good biocompatibility. Since both chitin and chitosan have excellent biocompatibility, these materials have become of interest in the field for medical materials in recent years [200]. Chitosan is also of interest because it is readily available. The structural polysaccharide chitin is the most abundant polymer found in nature after cellulose [26]. Chitosan is easily

prepared from chitin by N-deacetylation with alkali [145]. From 1970 to 1974, about 22,740 kilotons of chitinaceous material were globally harvested from sources of shellfish, krill, clams, oysters, squid, and fungi, resulting in the potential harvest of 150 kilotons of chitin per year [153]. Chitosan is commercially available through various manufacturers worldwide. Depending on the source and preparation procedure, molecular weight may range from 300-kilo Daltons (kDa) to over 1000 kDa [129]. Commercially available preparations have degrees of deacetylation (DDA) ranging from 50 to 98%. A polysaccaride with greater than 50% of the amino groups depicted in Figure 1 deacetylated is termed chitosan, and one with less is termed chitin.

Yet another reason to utilize chitosan for biomedical use is its similarity in chemical structure to glycosaminoglycans. Glycosaminoglycans (GAGs) including heparin, heparin sulfate (glucosaminoglucuronoiduronans), hyaluronic acid (glucosaminoglucuronan) shown in Figure 2, and keratin sulfate (glycosaminogalactan). These GAGs are remarkable derivatives of 2-amino-2-deoxy-D-glucose and are present in nearly all parts of the mammalian body.

Figure 2. Chemical structure of hyaluronic acid

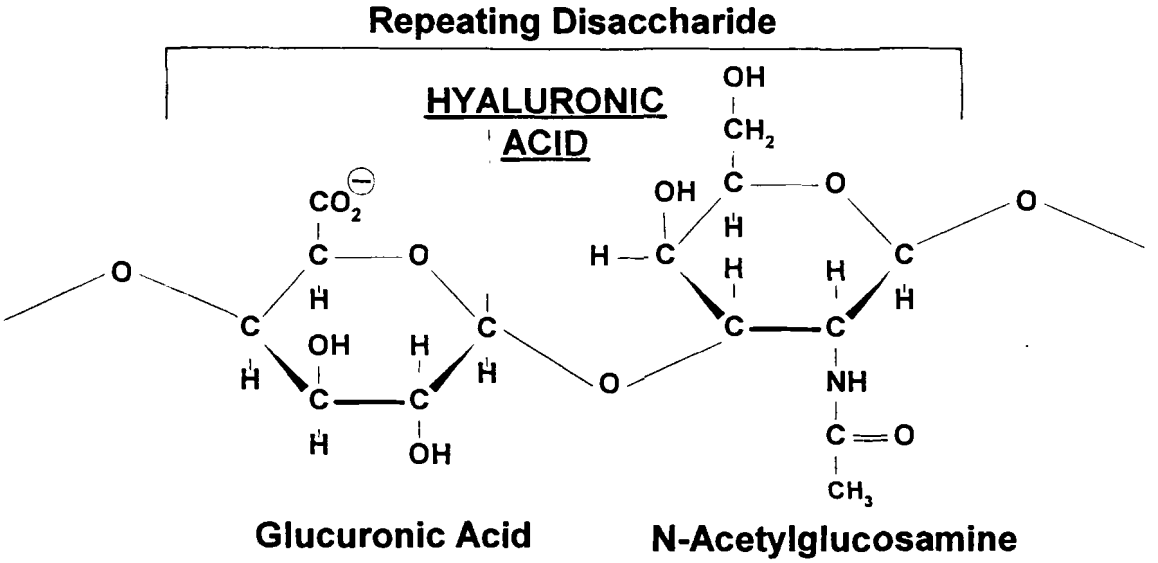

Glycosaminoglycans are among the essential building blocks of the macromolecular framework of connective and other tissues [149]. Interestingly, fetal wounds heal without fibrosis or scar formation due partly to the presence of hyaluronic acid. The healing processes of fetal wounds are mediated in part through the fetal ECM, which is rich in the GAG hyaluronic acid. Prolonged presence of hyaluronic acid in the matrix of fetal wounds creates an environment that promotes fetal fibroblast movement. Chitosan is structurally similar to hyaluronic acid and could exhibit similar effects [189].

The ability of chitosan to promote wound healing may also be attributed to its tendency to form polyelectrolyte complexes with the GAG and cellular attachment protein heparin, which possesses anticoagulant as well as angiogenic properties (promotes tissue vascularization). Heparin enhances mitogenesis (transit through the cell cycle) by the induction and stabilization of fibroblast growth factor (FGF). Chitosan

promotes tissue growth and wound healing by forming a complex with heparin and acting to prolong the half-life of growth factors [116]. Fibroblast growth factor is especially effective in wounds showing impaired healing, for example in diabetic ulcers, venous ulcers and pressure sores. Wound healing is supported by basic FGF's (bFGF) potency to promote migration and proliferation of capillary endothelial cells which are essential for the formation of new blood vessels in the damaged area [11].

1.3. Tissue Engineering and Biomaterials

Tissue engineering combines living cells, biochemicals and synthetic or natural materials into functional implants for the human body. Tissue engineering encompasses many disciplines including chemical engineering, cell biology, chemistry and medicine with inputs from genetics and surgery. Many approaches to tissue engineering have utilized naturally occurring polymers, including collagen and chitosan [35, 221, 161, 31, 31, 129, 161, 221]. Chitosan has the potential to accelerate the reformation of connective tissues and promote the vascularization of tissues [147]. Furthermore, the presence of chitosan benefits wound healing, bone repairs, vascular graft implantation and cell tissue cultures [158].

Chitosan also has the desirable properties of being easily processed and developed into films and membranes, microparticles and beads, and 3-D scaffolds. It is important that materials utilized in tissue engineering be biocompatible with tissues both *in vitro* and *in vivo*, especially when the resorption of the material is required. The resorption of a material is its ability to be incorporated harmlessly back into the host during degradation. Chitosan satisfies these biocompatibility requirements [159, 196, 45]. The field of tissue engineering and the use of chitosan as a biomaterial will be discussed in further detail in Chapter 2.

1.4. Cell Culture. Use of NIH 3T3 Fibroblasts

Fibroblasts are connective tissue cells that play an integral part in the wound repair process. This project utilizes a strain of 490N3T 3T3 fibroblasts obtained Don Blair of the National Institute of Health (NIH) and generously donated by Dr. Rebecca Van Beneden of the University of Maine. While these cells do not display identical behavior to fibroblasts *in vivo*, they are a standard model system for wound repair processes. There are numerous studies that have used fibroblast cells as model systems for wound repair. For example, L929 fibroblasts have been used as model systems on chitosan membranes [37 177]. Zielinski and others studied R208N.8 and R208F fibroblast cell lines as standard fibroblast models with chitosan as a cell-immobilizing matrix[232].

It is currently accepted that fibroblasts follow the inflammatory cells into the sites of tissue injury and contribute to wound healing through the synthesis of structural proteins. The most important of these structural proteins is collagen, which itself plays a critical role in the wound repair process and will be discussed in Chapter 2. Fibroblasts also facilitate wound contraction and the reorganization of the extracellular matrix (ECM) [147]. Tissue engineering approaches must support the attachment, speading and growth of fibroblasts for successful wound repair applications. Currently, many approaches to tissue engineering attempt to incorporate collagen or other growth factors to increase or maximize the activity of fibroblasts in the wound repair process. Thus, it is important that tissue engineering matrices successfully interact with the fibroblast and structural proteins to promote the natural process of wound repair.

Fibroblasts are also regarded as target cells of cytokines (intercellular mediators secreted by inflammatory cells) and growth factors, and recent investigations focused on

the role of fibroblast-secreted cytokines. Reports show that fibroblasts are capable of secreting a broad range of cytokines [147]. Full thickness wounds (wounds involving damage to both epidermis and dermis) heal by epithelialization, wound contraction and scarring. The fibroblast synthesizes and deposits a collagen-rich ECM. Early migration of fibroblasts and their proliferation in the wound area is implicated in wound scarring through the presence of fibroblast-produced collagen [189].

Another reason to consider fibroblasts as a model cell type, is that they are the most easily cultivable of mammalian cells. Serial cultivation of disaggregated cells from a piece of tissue from almost any location soon leads to predominance of the fibroblasts and the emergence of strains of homogeneous appearance [69]. There have been numerous studies of fibroblast interaction and function with biomaterials, including chitosan, which will be further discussed in Chapter 2. For these reasons, this project utilizes the NIH 3T3 fibroblast as a model system for an important stage of the wound repair process.

Chapter 2

BACKGROUND

2.1. Tissue Engineering and Biomaterials

2.1.1. Tissue Engineering: Applications and Approaches

Tissue engineering is a relatively new and rapidly growing field in today's society. Tissue engineering combines living cells, biochemicals, and synthetic or natural materials into functional implants for the human body. The goal of tissue engineering is to replace or restore the function of damaged or lost tissue. Furthermore, tissue engineering encompasses many disciplines. This research project focuses on developing bioresorbable materials with more favorable tissue interactions during degradation than current commercially available materials. Some long-term goals of this project are to manipulate the healing environment to control the structure of the regenerated tissue around a wound, as well as producing cells and tissues for transplantation into the body and stimulating the *in vitro* construction of transplantable vital tissue.

Tissue engineering has evolved due to a lack of affordable and effective medical therapies for treating various wounds and diseases. The limited surgical materials and treatments currently available are very expensive. Thus, one of the goals of tissue engineering is to help alleviate the high costs related to current medical procedures. A major aspect of tissue engineering is the development of cost-effective biomedical devices from biomaterials with applications to surgery and wound repair. Approximately 100,000 patients in this country die each year because organs are not available, and many of those who are saved by transplantation ultimately die because donor organs are rejected [44]. Additionally, well over 10 million Americans carry at least one major

implanted medical device, and the medical industry has topped $50 billion in annual sales. But despite the trade's large size, most medical device designers have been forced to work with a small handful of classic biomaterials such as stainless steel and chromium alloys, ceramics, a few composites and industrial plastics [99]. These materials often trigger unwanted or harmful immune responses at the implant site. Thus, a need has arisen for biocompatible biomaterials for use in tissue engineering both *in vitro* and *in vivo*, and for biomedical devices.

There are many approaches to tissue engineering. The development of artificial skin for severely burned patients is among the most advanced tissue-engineering attempts to date. Studies have shown the successful application of an artificial chitosan dermis applied to rats [40]. Human foreskin fibroblasts and keratinocytes were cultured in a chitosan-GAG-chondroitin matrix and used as a dermal equivalent. Keratinocytes proliferated and differentiated into a multi-layered epithelium [196]. Further detail on these studies is discussed in Section 2.3.1. These are a few of the encouraging studies with chitosan which have influenced the pursuit of the current project.

Other tissue engineering methods include attempts to control cellular responses to biomaterial implants. Cell adhesion, spreading and growth have been stimulated in biomaterials through the incorporation of the amino acid sequence arginine-glycine-aspartic acid (RGD), which is integral in the attachment of many cell types to surfaces [91]. Arginine-glycine-aspartic acid is a domain commonly found in many adhesion proteins and binds to numerous integrin receptors. One advantage of incorporating oligopeptides like RGD into biomaterials is imparting selectivity to the biomaterial. It may be possible to make one material selective to certain cell types, while rejecting the adhesion of others.

This concept could also be employed in the manipulation of the healing environment around an implanted biomaterial to control the structure of regenerated tissue [90].

Another approach to tissue engineering is the immobilization of active biological substances (epidermal growth factor, FGF, bone morphongenetic proteins) in polymer matrices (such as collagen) for soft wound healing or the repair of hard tissues [138 164]. One disadvantage of collagen matrices is their rapid degradation *in vivo*. Chitosan may exhibit slower degradation than collagen *in vivo*. The biodegradability can be reduced by the introduction of cross links between the polypeptide chains. Also, collagen matrices are prone to contraction and weight loss when exposed to cell culture conditions. These phenomena can be limited by the addition of GAGs or chitosan [35]. Fibroblasts cultured in collagen gels modified with a GAGs and chitosan displayed higher collagen synthesis than those cultured in collagen alone [45].

Chitosan films and matrices may be employed as a biomaterial on which growth factors or attachment proteins may be immobilized. In addition, several enzymes and proteins have been successfully attached to chitosan membranes. One example produced chitosan membranes with immobilized urease. These membranes have applications in enzymatic reactors such as artificial kidneys for the removal of urea from aqueous solutions [113]. Chitosan membranes can also be prepared with the GAG heparin, which plays in important part in cell adhesion as well as binding various growth factors and modulating phases of wound repair [114 32]. Soft and flexible fleeces of methylpyrrolidinone chitosan were freeze dried and combined with basic FGF (bFGF). The combination of bFGF and methylpyrrolidinone chitosan may improve impaired wound healing by two additional mechanisms. Methylpyrrolidinone chitosan can prevent

excessive scar formation and bFGF induces faster wound closure. Also, methylpyrrolidinone chitosan is biodegradable by lysozyme, which is found in wound fluids, so that the wound dressing can naturally degrade over time and resorb back into the body [11].

Another tissue engineering approach involves the *in vitro* construction of transplantable vital tissue. This approach to tissue engineering is among the long-term goals of the present study. Intensive research has been focused on the generation of artificial cartilage and bone to treat articular joint diseases or injuries, and to augment defects of the neck. The *in vitro* construction of transplantable tissue has also found applications in treatment the nose and ear in plastic surgery. One approach for the development of functional tissue equivalents is the bioreactor cultivation of isolated cells on biodegradable polymer scaffolds [56 208]. There are also studies on the development of an *in vitro* bone tissue substitute for the purpose of grafting regenerate deficient bone back into the host. One study utilized three different bone substitutes of collagen type I, a porous poly (lactide/glycolide)/hydroxyapatite 3-D matrix, and a poly(lactic-co-glycolic acid) foam for the development of bone tissue *in vitro*. All three biomaterials were shown to encourage the development of bone tissue *in vitro* [27, 117, 117 97]. However, these biomaterials have several disadvantages. One problem is that they degrade at variable rates and are very weak in terms of structural characteristics. Furthermore, tissues showed difficulty diffusing completely into these scaffolds and elicited a major immune response in the host. Also, these materials are limited in the types of matrices that they can be formed into. Chitosan may have advantages over these materials as a scaffold for the *in vitro* development of bone.

Chitosan has been incorporated into 3-D matrices by various methods. Chitosan/tricalcium phosphate (TCP) sponges were developed as 3-D tissue engineering scaffolds for bone formation with osteoblast culture [121]. Chitosan is biodegradable and can improve wound healing and enhance bone formation. Furthermore, chitosan is non-toxic and doesn't evoke a serious immune response [121]. Chitosan can be prepared in many forms including films, 3-D scaffolds and fibers, and its degradation may be controllable. Future studies should investigate the potential to control the degradation rate of 3-D matrices.

Future challenges of tissue engineering include the development of resorbable materials with more favorable tissue interactions during degradation [90], the construction of liver organoids for bridging comas and the development of an artificial kidney on the basis of cultured cells [144]. Other challenges lie in the improvement of current research and clinical methods for the development of artificial skin grafts, 2-D and 3-D biocompatible and biodegradable materials, as well as pioneering the field of repairing all sorts of damaged or diseased tissues.

2.1.2. Biomaterials

The ability of a material to be resorbed into the body over time is an important feature for certain implantable biomaterials. In engineered matrices, degradation and resorption of the matrix permits the gradual in-growth and ultimately the complete replacement of the regeneration matrix by normal tissue. Additionally, the risk of complications that may be associated with the long-term presence of a foreign material may be avoided by using resorbable biomaterials. Resorbable materials used in tissue engineering include protein and polysaccharide-based biomaterials, biopolymer gels of

polysaccharides, and amorphous protein polymers. Many substances that are both non-resorbable and resorbable are currently used as biomaterials. They include metals (titanium), ceramics (alumina), synthetic polymers [polyurethanes, silicones, polyglycolic acid (PGA), polylactic acid (PLA), copolymers of lactic and glycolic acids (PLGA), polyanhydrides, polyorthoesters, and natural polymers (chitosan, glycosaminoglycans, collagen) [35]. Some tissue engineering applications involve tissue responses that may vary with position or by patient. The use of materials that are degraded in response to cellular activities can be advantageous to the performance of the biomaterial in these applications. For example, biopolymer gels and other synthetic biomaterials degrade in response to specific cellular proteases. Specific tissues might be employed to determine the rate of degradation and resorption of these materials [90]. Regardless of the intended applications, candidate materials for implant use must be evaluated carefully for toxicity, because any material degradation may result in the release of potentially harmful components into a patient's body [99].

Many of the synthetic resorbable polymers such as PGA, PLA and ϵ-caproic acid have been developed for use in biomedicine, including applications in surgery, drug delivery, and tissue engineering. The structures of a PLA and PGA are illustrated in Figure 3.

Figure 3. Chemical structures of PLA and PGA

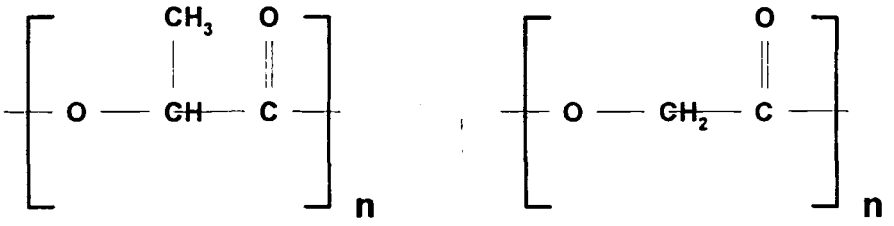

PLA: Poly-lactic Acid **PGA: Poly-glycolic Acid**

These polyesters have been successfully employed as matrices for cell transplantation and tissue generation [90]. Synthetic degradable sutures of PGA have been available commercially since the 1970's. Poly-lactic acid, PGA and their copolymers have been commercialized more than any other degradable polymer because of their long history of use as biomaterials. Disadvantages of products made from PLA and PGA include a fast degradation rate and loss of mechanical strength in just two to four weeks, which is much too rapid for some tissue engineering applications. Also, some inflammation is typically associated with degradation of these hydrophobic polymers. Furthermore, many cell types do not attach or grow efficiently on PLA or PGA materials, suggesting that these substances are not ideal materials for tissue engineering scaffolds [99]. Conversely, chitosan exhibits good attachment, spreading and growth towards many cell types [161 31, 31]. Also, chitosan can be modified to increase its stability against degradation by cross-linking [232]. Thus, chitosan appears to be a more suitable material for tissue engineering than PLA or PGA.

Collagen has been tested and used extensively as a biomaterial. It possesses many of the desired traits of a functional biomaterial. Collagen substrates modify the morphology, the migration, the adhesion, and, in certain cases, the differentiation of cells. Collagen types I, II, and III are also known to be chemotactic (a compound that produces positive directed migration of one or more kinds of leukocytes, cells that help the body fight infections and diseases). This phenomenon, as well as the action of collagen on cellular development, illustrates the role and significance of collagen in tissue reconstruction. Fibroblasts produce collagen as an extracellular matrix protein. Fibrillar collagens provoke the adhesion of platelets and subsequent aggregation leading to clotting. Collagen is a biodegradable molecule, broken down in tissue by catabolic processes, including degradation by specific collagenases and phagocytosis (uptake of collagen by cells). Collagen can be obtained from several sources, including the dermis, tendons, bone, blood vessels, pericardium, and placenta. Some insoluble fibrillar collagens are useful for the manufacture of mechanically stronger biomaterials [35]. Although collagen possesses many desirable traits as a biomaterial, it also has some disadvantages. Collagen is rapidly degraded *in vivo*. Some applications require a slow degradation of the biomaterial, including the regeneration of periodontal defects and the reconstruction of the dermis and epidermis [160 40 196]. Also, although cross-linking the polypeptide chains can stabilize collagen, cross-linking collagen by glutaraldehyde (GTA) promotes an undesired rapid calcification of tissue after implantation due to a lack of nutrients. This may be a result of GTA tightly cross-linking the collagen as to inhibit nutrient migration within the collagen matrix. Also, there are limitations on the preparation capabilities of collagens into films and 3-D scaffolds [35]. It is unclear whether

these limitations are from the source of collagen. The presence of chitosan oligomers to a wound can stimulate the proper deposition, construction and orientation of collagen fibrils that are incorporated into ECM components [159]. Chitosan-collagen-GAG is also beneficial for skin substitutes because it provides insolubility and increases the production of collagen and regulatory factors by fibroblasts. The addition of chitosan to skin substitutes provides better adhesion than collagen alone, and encourages fibroblast and keratinocyte proliferation. The dermal substitute does not cause any immune response incompatibility and allowed controlled vascularisation and fibroblastic colonization [196]. Thus, chitosan was considered as a potential biomaterial for fibroblast attachment, spreading and growth because of its benefits over collagen, and because it is not as thouroughly investigated as collagen.

2.2. Chitosan

The following sections summarize many important applications utilizing chitosan as a biomaterial. The interactions of chitosan with various cell types as well as chitosan's use as a biomaterial in various approaches to tissue engineering is discussed.

2.2.1. Applications of Chitosan as a Biomaterial

Studies indicate that chitosan has excellent potential as a structural base material for a variety of engineered tissue systems. Chitosan possesses both desirable tissue-specific properties and has a broad applicability, which can be tailored to several tissue systems [129]. Over the past 21 years, the biomedical applications of chitosan have been widely researched, but its application to tissue engineering has not been extensively investigated. Specific applications with chitosan as a biomaterial include its evaluation

as a wound healing agent [152], a substratum for skin replacement [40], a bandage material, and as a skin grafting template [196]. Chitosan has also been used as a cholesterol lowering agent, a hemostatic agent [116], and in the reconstruction of periodontal tissue [161]. Chitosan shows promise with applications in substituting or regenerating the blood-tissue interfaces, as biomedical membranes with application to artificial kidneys of both the filtration and portable type for improved dialysis, when modified with immobilized bioactive molecules, and as drug delivery vehicles [31].

Biodegradable chitosan wound dressings can be formed by complexing chitosan with ionic salts and proteins to form hydrogels. A specific example of the use of chitosan as a biomaterial suitable for biodegradable wound dressings involves a complex made of ammonium keratinate, chitosan acetate, and collagen acetate prepared in the form of hydrogel membranes. These membranes strongly adhered to wound tissues by virtue of their collagen content and consequent linkage to fibrin. They had a high degree of absorbency for fluid or cellular debris resulting from inflammation. The membranes also had a high vapor transport rate, which prevented fluid pooling beneath the dressing, and yet also low enough to maintain adequate moisture at the wound surface. These membranes were highly permeable to oxygen and stopped bacteria. The moist membrane was biodegraded by the skin cells, white cells and macrophages. In the latter stages of wound healing, the remaining membrane hardened and fell off without leaving any scarring [152]. These results indicate chitosan's non-toxic characteristics.

Anticoagulant membranes for blood ultra-filtration can be prepared by immobilizing important biological GAG molecules like heparin onto chitosan [30]. These membranes are effective in wound repair by using heparin to bind growth factors that can

modulate several phases of wound repair [114]. Antithrombotic agents (preventing blood clots within blood vessels) including hirudin, PGE1, antithrombin-III, and heparin were immobilized on albumin blended chitosan membranes modified with lipsomes for applications in blood purification through improved blood compatibility and permeability [30 218]. These membrane formation methods also illustrate the versatility of chitosan to undergo modification by the addition of biological molecules.

Chitosan has been utilized as a controlled release agent. Biodegradation of chitosan linked to bone morphogenetic protein (BMP) leads to the controlled release of BMP. Quantitative measurement of the surrounding tissue showed that bone tissue regeneration in a surgical bone defect was improved by using this special chitosan [160]. Another study used chitosan gels to model the controlled release of bovine serum albumin (BSA) [185]. Furthermore, controlled-release studies of BSA from chitosan-alginate membranes have shown chitosan's potential for the delayed release of a protein acid [175]. These studies indicate that chitosan's potential for stimulating wound healing can be further enhanced by modifying the polysaccharide with proteins.

2.2.1.1 Chitosan and Various Cell Types

Chitosan positively contributes to wound healing through interaction with various cell types. Chitosan macromolecules can strengthen and accelerate cell proliferation and tissue organization of connective tissue comprising the supportive framework of an animal organ (stromal tissue) [158 95]. Chitosan accelerates the growth of tissue in culture *in vitro* and encourages it to grow in a multi-level configuration, rather than in a monolayer [133]. The extent that chitosan accelerates the wound-healing process has been

determined in animal tests by measuring the bursting strength of the newly formed tissue of the wounds. The acceleration of healing was confirmed in human clinical tests [6].

2.2.1.1.1 Chitosan and Anchorage-Dependent Cells

Nerve cells are influenced by the presence of chitosan [76]. Studies indicate that neurons cultured on a chitosan membrane can grow well and that chitosan conduit can greatly promote the repair of the peripheral nervous system (PNS). Studies considered the attachment, spreading and growth of gliosarcoma cells as a model of affinity of nerve cells to chitosan membranes [48 102]. Chitosan coated with polylysine and a chitosan-polylysine mixture are even better materials than chitosan itself in nerve cell affinity, and are promising materials for nerve repair. Pre-coating materials with ECM molecules, especially laminin, can greatly improve their nerve cell affinity [76].

Chitosan is also viable as a 3-D matrix for cell encapsulation, which might be applied to implantable biomaterials. Because of its expanded structure, chitosan is suitable as a matrix for anchorage-dependent mammalian cell encapsulation. Chitosan supported the differentiation of encapsulated neuronal cells [232]. Mammalian cells were also successfully encapsulated in chitosan-alginate bi-polymer membranes. The concentration of the monoclonal antibody in the capsule was 20 times higher than that of the free cell culture [107]. Viable hybridoma (fused tumor and lymphocyte) cells were entrapped in chitosan-carboxymethylchitosan (CMC) capsules. These cells exhibited healthy morphology, and displayed a tenfold increase in cell density and a threefold higher product concentration in comparison to a suspended culture. For large-scale applications, however, the complexity of the encapsulation process and scale-up problems are still large hurdles to overcome [230].

2.2.1.1.2 Chitosan, Immune Cells, and Blood-Related Tissues

Chitosan exhibits a positive effect on wound healing through its interaction with macrophages and leukocytes. Moreover, chitosan enhances the immune response, which is desirable for the application of drug carriers to tumor-bearing hosts, whose immunities are depressed [158]. Chitosan exhibits promise for helping cells to participate in immunological defense against tumor cells and pathogens. Chitosan can accelerate wound healing through its interaction with leukocytes. Studies indicate that chitin and chitosan stimulate the migration of leukocytes and accelerate the reformation of connective tissue as well as formation and differentiation of blood vessels [143, 158]. Chitosan can be injected into tissue to close abnormal passages connecting arteries and veins and to stimulate necrosis in tumors by blocking circulation [153]. One study's findings support the notion that proliferation and differentiation of blood vessels is accelerated indirectly when chitosan is used *in vivo*. Chitosan stimulated the production of interleukin-8 (IL-8) from L929 fibroblasts, which activates and attracts phagocytes. This interleukin release stimulates the migration of white blood cells [147]. Furthermore, benefits of chitosan to wound repair are evident through vascular graft implantation and cell tissue cultures. Chitosan improves healing of surgical wounds by speeding up the process and supporting smoother scar formation [155]. These effects are the result of chitosan's ability to enhance tissue vascularization and supply chito-oligomers to the wound to stimulate the proper deposition, construction and orientation of collagen fibrils that are incorporated into ECM components [159].

Chitosan's positive effect on wound healing is also displayed through its interaction with macrophages. The activation of normal macrophages for the destruction

of tumor cells occurs when they interact with activating agents, such as microorganisms, and with substances secreted by T cells in response to antigen stimulation. Upon activation, these macrophages can lyse tumor cells either by direct contact or through the release of diffusible cytotoxic molecules. Nitric oxide, interleukin-1, tumor necrosis factor-α and reactive oxygen intermediates are among the major cytotoxic molecules produced by activated macrophages for the lysis of tumor cells [169]. Chitosan shows a biological aptitude for activating macrophages to destroy tumor cells and to produce interleukin-1 [165]. IL-1 is a compound that regulates cell-mediated immune responses and other biological functions [95]. Studies indicate that chitosan-activated macrophages, which destroy tumor cells, are probably related to nitric oxide (NO) production. Chitosan stimulates the activation of macrophages, which is attributed mainly to the N-acetylglucosamine (NAGA) unit of the chitosan molecule rather than the glucosamine residue [169].

Chitin and chitosan enhance the function of cells participating in immunological defense against tumor cell and pathogens. Chitin and chitosan were reported to be selectively collected into the tumor cells and to inhibit the growth of tumor cells [31]. One study showed chitosan to selectively aggregate leukemia tumor cells *in vitro*, resulting in a dense cell aggregate that inhibits cell growth [207]. Further evidence of chitin and chitosan's enhancement of the function of animal cells participating in immunological defense against tumor cells and pathogens has been obtained from measurements of enhanced enzymatic activity of lysozyme in the mouse macrophage *in vivo*. Both chitin and chitosan were effective in the survival of 80% of mice challenged with a bacterium.

Also, a significant increase in survival ratio of mice with Ehrlich or sarcoma 180 ascties tumor cells implanted in the abdomen was observed as a result of chitosan [47].

Although chitosan by itself is hemostatic (stops bleeding), some derivatives, such as sulfated chitosan, are blood anticoagulants. Chitosan tends to coagulate blood lacking fibrin, containing heparin, as well as purified red blood cells. The sulfation of *N*-carboxymethychitosan (*N*-CMC) results in a linear GAG with numerous functional groups similar to those in heparin. Results of studies with *N*-CMC as a blood anticoagulant were confirmed by the inhibition of thrombin by binding to antithrombin and through inhibition of the conversion of prothrombin to thrombin. Another benefit of *N*-CMC was the absence of adverse effects on white or red blood cells [153]. Chitosan bandages and sponges have been prepared for surgical treatment and wound protection that exploit its hemostatic effects [105 148]. Medical products were prepared by immobilizing partially sulfated chitosan oligomers on the surface of molded chitosan materials, such as artificial blood vessels and fibers. These materials inhibited the formation of blood clots within blood vessels [215].

2.2.1.1.3 Chitosan and Bone Tissues

Chitosan has been shown effective in the regeneration of bone tissue. Chitosan offers an alternative for the reconstruction of the periodontium (tooth supportive structures) by providing a less complicated, more tolerable treatment. A chitosan ascorbate gel was compatible with the periodontium and can rebuild its connective tissue with a normal functionality as demonstrated in clinical studies [161]. Methypyrrolidinone chitosan promoted bone regeneration in surgical wounds from wisdom tooth and tooth-root removal [154]. Chitosan also stimulates the differentiation of bone-producing cells and

thereby facilitates the formation of bone. It has been found that the number of bone-forming colonies is almost doubled in the presence of chitosan [110].

Chitosan can be fabricated into a practical scaffolding material that could function as an effective template in the repair of bone and cartilage defects. Chitosan supports viable and functioning human osteoblasts and chondrocytes. Studies showed chitosan-coated-coverslips supported viable human osteoblasts and non-fibrillated, articular chonrocytes that maintained a spherical morphology similar to that displayed by osteoblasts *in vivo*. Furthermore, these cells grew in higher densities than those on uncoated coverslips [116]. Also, modified chitosans can activate compounds responsible for the formation of bone-like tissue and promote mineralization. These modified chitosans include methylpyrrolidinone chitosan and a chitosan containing imidazolyl groups covalently linked to the glucosamine nitrogen via a methylene (IMIC). IMIC induced bone formation that filled osseous cavities which normal healing processes were unable to heal *in vivo*. IMIC appears to be much more effective in bone healing than chitosan itself or methylpyrrolidinone chitosan when used in an animal models and human models [156].

Chitosan-tricalcium phosphate (TCP) sponges are feasible as scaffolding materials for tissue-engineered bone formation *in vitro* and show promise as biodegradable matrices for growing osteoblasts in a three-dimensional structure for transplantation into a site for bone regeneration *in vivo*. Chitosan/TCP sponges supported the proliferation and differentiation of osteoblasts. This was confirmed through measurement of alkaline phosphatase (an enzymatic marker of osteoblasts) activity and through deposition of calcium in the cell-sponge construct [121]. Chitosan and TCP have

been combined to create a 3-D matrix to deliver platelet-derived growth factor (PDGF) to the site of small skull defects in rats. Histological findings indicate that the chitosan/TCP sponge alone had an affinity for osteoblasts and that the addition of PDGF further enhanced bone regeneration. *In vitro* examination of the PDGF-loaded sponge revealed that it consistently delivered a dose of PDGF for up to 21 days [122]. The ability of chitosan to deliver growth factors may be applied to the methods of chitosan film formation in this study and exploited to induce desirable effects on wound healing. These properties make chitosan an attractive candidate for future use in bone and cartilage tissue engineering. These studies further exemplify chitosan's versatility in the formation of gels, sponges and 3-D matrices for tissue engineering applications.

2.2.1.2 Other Important Applications

In conjuction with its wound healing capabilities and versatility with various tissues, chitosan can also be utilized with other related applications. Chitosan can be used to fabricate porous matrices with some degree of control of the pore size and morphology. These matrices may be used as scaffolds to build up tissues for space filling implants. Additionally, planar scaffolds may have applications in 2-D tissues such as skin or articular cartilage [129]. Chitosan has been successfully employed as a material for soft contact lenses, for the development of artificial skin, as a skin graft template, and for use with biopharmaceuticicals.

Several techniques for preparing contact lenses have been reported resulting in chitin *n*-butyrate lenses, chitosan lenses, and blue chitosan lenses. Chitosan is optically clear, wettable, gas permeable and non-toxic, which are all integral characteristics of soft contact lenses. Gas permeability is an important characteristic for soft contact lenses

because oxygen must be able to diffuse from the tear fluid to the eye surface, and carbon dioxide must be able to diffuse from the eye surface into the tear fluid [1].

Chitosan has also been extensively studied for use with biopharmaceuticals. Proteins such as BSA have been combined with degradable chitosan matrices. One study adsorbed BSA onto chitosan microspheres cross-linked with glutaraldehyde (GTA). This study demonstrated that a biological molecule which is very sensitive to organic solvents, pH, and temperature could be successfully combined with chitosan matrices while still preserving it's biological integrity [100]. Chitosan-alginate microcapsules with blue dextran as an affinity ligand for BSA showed great potential for the recovery of BSA from both saline medium and whole bovine plasma. These modified chitosans illustrate chitosan's potential affinity for proteins as well as its applications of protein recovery. [65]. Amino acids of methionine and lysine have been used with chitosan coating formulations. These coatings are pH sensitive and both *in vitro* and *in vivo* studies suggest that these coatings are a possible route for rumen-protected amino acids [178].

2.2.1.3 Chitosan and Fibroblasts

One very important tissue engineering approach was developing skin substitutes with chitosan-based materials. The success of these applications lies in part due to chitosan's favorable interactions with fibroblasts and bioactive molecules intimately related to fibroblasts and wound healing. The following section continues to describe various research studies conducted with chitosan and fibroblasts and the importance of these studies to the current study.

In vitro studies have confirmed chitosan's positive effects on wound healing are partially a result of the activation of fibrogenic mediators such as growth factors and

cytokines [165 167, 219 142 220]. These growth factors and cytokines enhance fibroblast activity and promote fibrous tissue synthesis, which are crucial to proper wound repair [116]. Chitosan's promotion of wound healing is also partially due to its ability to form poly-electrolyte complexes with heparin, which possesses anticoagulant as well as angiogenic (promoting vascularization) properties [213 28]. Heparin enhances cell mitosis by inducing and stabilizing fibroblast growth factor (FGF) [62 163 217 67]. Chitosan promotes tissue growth and wound healing by forming a complex with heparin and prolonging the half-life of growth factors [116]. This property of chitosan can be investigated and perhaps exploited with the materials developed from this project.

Chitosan was successfully utilized for the regeneration of skin tissue. Chitosan was inserted into a cut on the back of rats. A normal inflammatory reaction was observed after 2 days, followed by cell colonization after 7 days. A dermal equivalent with an average pore size of 100 μm provided an excellent environment for fibroblast growth and proliferation *in vitro*. This substrate was a mixture of bovine collagen types I and III, 85% weight per volume (w/v) chitosan extracted from shrimp shell, and GAGs of chondroitin-4 and chondroitin-6 sulfate, with a final composition of 72% (w/v) collagen, 20% (w/v) chitosan and 8% (w/v) GAGs. This study indicates that a minimum pore size is required as not to inhibit fibroblast migration, growth and metabolic activity, as well as the diffusion of nutrients in and out of the matrix[40].

Chitosan-collagen-GAG is beneficial for skin substitutes because it provides insolubility and increases the production of collagen and regulatory factors by fibroblasts. The addition of chitosan to skin substitutes provides better adhesion than collagen alone, and encourages fibroblast and keratinocyte proliferation. The dermal substitute does not

cause an immune response and allowed controlled vascularisation and fibroblast colonization. The final result of these skin substitutes was an organized matrix with little formation of granulation and excessive scar tissue. Fibroblasts play an important part in dermal-epidermal interactions [196]. A dermal substrate of collagen-GAG-chitosan colonized with fibroblasts for deep burn coverage, after 15 days, allowed formation of a continuous, adherent and differentiated epidermis with reconstruction of the dermal-epidermal junction. These observations were also found *in vivo*, where the dermal substrate is correctly colonized by fibroblasts within 15 days [45].

Foreskin fibroblasts were cultured in the matrix followed by a seeding of the surface of the lattice with normal human keratinocytes (NHK), which prevented penetration of the fibroblasts into this dermal equivalent. Keratinocytes proliferated and differentiated to form multilayered epithelium when seeded on the laminated surface of the dermal equivalent populated with fibroblasts. This observation was further confirmed by measuring markers of epidermal differentiation, which were expressed and distributed similar to expression *in vivo*. Fibroblasts induced involucrin (a marker for epidermal differentiation) expression in specific layers, whereas involucrin expression was observed throughout the multilayered, un-differentiated epidermal cell layers in the absence of fibroblasts. Filaggrin (another epidermal differentiation marker) expression appeared to depend completely on the presence of fibroblasts in the dermal equivalent. Fibroblasts showed no effect on the expression of protein in the dermal-epidermal junction including collagen VI, fibronectin, bullous pemphigoid antigen, laminin and collagen VII. The fibroblasts did, however increase the presence of hemidesmosomes along the dermal-

epidermal junction with basal lamina forming underneath. The fibroblasts also initiated a tight adherence between the dermal equivalent and the reconstructed epidermis. [196].

Clinical studies with a collagen-GAG-chitosan dermal substrate grafted onto burned tissues showed promising results. There was no observable rejection of this dermal substrate in rats or human subjects. This chitosan-containing substrate stimulated controlled vascularization and fibroblast colonization of burned tissue. Results from both *in vitro* and *in vivo* studies indicated the formation of a continuous, differentiated epidermis that adhered to the excised wound area after 15 days. Forty percent of the dermal substrate with cultured epidermis did not take to the subject, most likely from infection. These substrates did not achieve the 100% take-rate of a large-meshed autograft [23], which were free from infection [45]. These studies are among the most advanced applications utilizing chitosan as a structural base for wound and tissue repair.

Chitosan's affinity for fibroblasts was illustrated through the interaction of chitosan-poly vinyl alcohol (PVA) hydrogels and L-929 fibroblasts [37]. Chitosan-PVA blended hydrogels enhanced cell attachment and growth of L-929 fibroblasts *in vitro*. A 4-wt % chitosan-PVA hydrogel had a better quality of fibroblast attachment and growth than a collagen-coated film. Chitosan-PVA blended membranes exhibited better results for the culture of human fibroblasts than were exhibited by pure PVA membranes. After attachment, the fibroblasts on the chitosan-PVA membrane displayed considerable spreading, with cytoplasmic webbing attaching to the surface and long-filamentous pseudopods extending from the cell, whereas this same effect was not evident on the pure PVA membrane. These results indicate that chitosan-PVA blended membranes can promote fibroblast attachment and growth and may mediate cellular response. These

hydrogels may be investigated as starting materials for the development of 3-D matrices by freeze drying for further experimentation with fibroblasts.

In contrast to chitosan-PVA hydrogels, chitosan polyvinyl pyrrolidone (PVP) hydrogels have exhibited differential growth supportive properties for epithelial and fibroblast cells *in vitro*. These hydrogels inhibited fibroblast growth and proliferation by preventing their attachment on the surface, while supporting attachment and growth of epithelial (SiHa) cells in a number and quality similar to that shown with tissue-culture-grade polystyrene (TCPS). The properties of chitosan-PVP hydrogel imitate fetal wound healing as it selectively inhibits fibroblast growth and promotes epithelial cell growth that adult wounds lack. Thus, this hydrogel might be used in wound repair to limit excessive scar formation in wounds. This study, in conjuction with the previously mentioned studies, illustrates that through the incorporation of chemical additives, the attractive properties of chitosan gels for fibroblasts can be suppressed or enhanced depending on the chemical additive used [189].

Another study considered the effect of the degree of deacetylation (DDA) on the attachment and growth of L929 fibroblasts. L929 fibroblast cells and baby hamster kidney cells (BHK21(C13)) were shown to attach and grow on highly deacetylated chitosan-coated petri dishes. It was shown that as little as 10% difference in DDA of chitosan samples has a significant influence on the adhesion of cells to these substrates in culture, with highly DDA samples supporting the greatest fibroblast attachment and growth. Petri dishes coated with chitosan with a DDA of approximately 80% or less did not support significant cell attachment. Thus, the DDA is very important to the biocompatibility of chitosan [177].

One study illustrated the importance of the cross linking density of chitosan matrices for supporting fibroblast growth. This study used a precipitated chitosan as a matrix on the inside of a 60:40 acrylonitrile-vinylchloride (PAN/PVC) copolymer macrocapsule as a cell-immobilizing matrix that supported the spreading and growth of fibroblasts. Three cell lines (R208N.8 fibroblasts, R208F fibroblasts – the parent cell line, and PC12 – a phaeochromocytoma-derived cell line) were encapsulated in both micro and macrocapsules. The cells microencapsulated in chitosan were cross-linked with sodium chloride and TPP, and displayed evidence of necrosis. The microcapsules had a tightly cross-linked structure that may have mechanically inhibited cell attachment and spreading which are essential fibroblast functions. The viability of fibroblasts was significantly improved in macrocapsules containing precipitated chitosan. The microcapsules were washed with saline to precipitate the chitosan instead of cross-linking with TPP. These chitosan matrices supported both PC12 and fibroblast growth. Cells were evenly dispersed throughout the chitosan matrix. The chitosan prevented extensive fibroblast clumping and death. The PC12 cells appeared to attach successfully to the precipitated chitosan and responded to exposure to nerve growth factor (NGF) by extending neuritis. The precipitated chitosan inside the macrocapsule also enhanced the survival of PC12 cells and prevented extensive clumping. Cells were analyzed with epifluorescent microscopy by labeling cells with fluorescent molecules [232]. Thus, care must be taken when fabricating porous 3-D scaffolds for use with fibroblasts to improve on wound repair to ensure that the scaffolds allow for cell and nutrient migration throughout the matrix. Also, fibroblasts have been successfully encapsulated in chitosan. Chitosan-encapsulated fibroblasts did not display extensive cell clumping and death like

that displayed by other encapsulation materials such as alginate. Encapsulated cells implanted into the basal ganglia of monkeys were still viable up to 4 weeks post-implantation [151].

2.2.2 Film, Membrane and 3-D Matrix Formation Techniques for Chitosan

Chitosan can easily be prepared in many forms, including films and 3-D scaffolds. Rigby outlined the basic technique for the casting of films and fibers [187 188]. Two patents were granted to Rigby simultaneously in 1936, and the second of these describes the following procedure for making films and fibers. The chitosan was dissolved in a weak organic acid, which formed a suitably viscous solution in which the chitosan was in the form of a complex salt. This solution was then cast onto a smooth surface, followed by removal of the anion for the chitosan to exhibit a resistance to water. Two procedures for anion removal were given. In the first, the film was heated to remove the volatile acid component, and in the second, the film was first dried at a lower temperature and then immersed in a weak caustic solution and subsequently rinsed with water. The resultant films were described as flexible, tough, transparent and clear with a tensile strength of about 9000 pounds per square inch (psi). These procedures are the simplest and perhaps easiest methods to produce chitosan films.

The crystallinity of the chitosan film depends on the preparation procedure for the film and on the molecular weight of the chitosan, when using acetic, formic and hydrochloric acids as solvents [166]. The mechanical properties such as elasticity and relaxation response of chitosan films based on solvent and chitosan concentration were investigated in another study. Chitosan films were formed by a method similar to the Rigby technique, using acetic and propionic acids as solvents. Findings indicated that the wet-tested

apparent Young's modulus increases linearly with chitosan concentration. The relaxation time increased with increasing chitosan concentration, and was greater for acetic acid-cast films than for propionic acid-cast films [106]. Conversely, Mima and coworkers[142] characterized both the wet and dry tensile properties of chitosan films. They found an increase in wet tensile strength with increasing *N*-acetylation and no correlation in dry tensile strength and *N*-acetylation. The present investigation considers the Young's modulus of elasticity as an important physical parameter of the chitosan films as well as an indication of the reproducibility of the film-formation technique.

Chitosan and PVA membranes can be prepared by a technique similar to Rigby's method. Chitosan-PVA membranes were prepared by first dissolving a chitosan powder in an aqueous solution of acetic acid (chitosan:acetic acid = 5:4 by weight). Poly vinyl alcohol powder was added to the chitosan solution to prepare an aqueous solution of 10-wt % total polymer concentration. The clear solution obtained was cast on a glass plate, dried in air at room temperature and subsequently dried under vacuum. The membrane was then immersed in NaOH for to neutralize the acetic acid contained in the membrane. Finally, the membrane was washed thoroughly with deionized water. These hydrogels enhanced the attachment and growth of L-929 fibroblasts over that of PVA itself, when the chitosan content was greater than 15%. Additionally, the cell attachment and growth of a 40-wt % chitosan/PVA hydrogel exceeded the cell growth and attachment on collagen controls. These hydrogels had a water content of 65-75-wt %, and a peak chitosan concentration of 20 wt %. Hydrogels with greater than 15 wt% chitosan showed good affinity for L929 fibroblasts, whereas few cells attached or grew on hydrogels containing less than 10% chitosan [112]. Hydrogels can also be formed by immersing the

glass plate and casting solution into a coagulation bath to obtain a membrane. These membranes possessed a dense top layer lacking pores, supported by a porous sublayer with a spongy characteristic. The addition of PVA modified the structure of these membranes, but also indicated an incompatibility with chitosan. Chitosan and PVA were indicated to be immiscible, and the chitosan molecules were selectively present towards the surface of the membrane [37].

Cross-linked chitosan membranes were prepared by the addition of bifunctional reagents, such as aldehydes, carboxylic anhydrides, and glutaraldehyde to the chitosan solution. Two easily prepared examples are *N*-arylidene-chitosan and *N*-acyl-chitosan membranes. A chitosan-hydroacetate solution was first poured into a glass petri dish to give a thin liquid layer. After the addition of either an aldehyde or carboxylic anhydride, films formed within a few hours. These membranes are reported to be neither solubilized nor swollen by soaking for one week in water, NaOH, dimethyl sulfoxide, or formamide. It is suggested that the cross-linking mechanism involves formation of a Schiff's base structure [123]. These types of membranes might also be considered for freeze-drying and experimentation with NIH 3T3 fibroblasts.

Ionotropic gelation has been used to cross-link chitosan salts with counterions to form a gel. The gel forms as a result of interactions between the chitosan salt and counterions in solution. Ionotropic gelation for the formation of chitosan membrane is a very mild process. Chitosan membranes have been formed with a variety of counterions or polymers, such as pyrophosphate, octylsulfate, and alginate. Among the counterion polymers that gelate with chitosan, alginate is the most widely used. [15]. These gels can be dried by lyophilization.

Another effective method for modifying chitosan with functional molecular groups is with graft copolymerization. Graft copolymerization is a process using free radical polymerization to introduce a side chain or graft with a different chemical nature than the main polymer chain onto the chain. Of the various potential modifications to chitin and chitosan, graft copolymerization is one of the most attractive approaches for creating versatile molecular designs. Graft copolymerization can produce novel types of tailored hybrid materials composed of natural polysaccharides and synthetic polymers. The properties of the graft copolymers can be controlled by the characteristics of the introduced side chains, including the molecular structure, length, and number. Chitosan has been graft copolymerized with vinyl monomers and aniline. Graft copolymerization can be used to introduce peptide side chains onto chitosan, which can increase cell attachment, spreading, growth or expression of certain growth factors in cells [115]. This method has potential benefit in the development of effective biomaterials from chitosan for tissue engineering.

2.3. Cellular Function and the Wound Repair Process

2.3.1. The Wound Repair Process

Wound healing and regeneration are developmental processes involving different cellular functions, such as cell proliferation, cell migration, cell differentiation and interactions between the different tissue components [205]. Specific cellular phenomena studied in this project are the attachment and growth of NIH 3T3 fibroblasts on chitosan films relative to polystyrene controls. The attachment of fibroblasts to the site of wound repair is critical to the second stage of wound repair. Increasing the rate of cell attachment will increase the effectiveness and efficiency of the repair process.

Additionally, the rate of cell proliferation is essential to the proper function of the cell and the rate of protein synthesis. The rate of growth, proliferation, and differentiation of cells on a material rely upon the successful attachment and spreading of cells on the surface of the substratum [50].

The wound repair process is the series of actions in which unhealthy or damaged tissue is repaired. A thorough understanding of the processes involved in wound repair is necessary for the development of functional biomaterials for use in tissue engineering. Wound healing consists of three stages. First, inflammatory cells from the adjacent tissue move towards the damaged site. Second, fibroblasts migrate to the site and produce collagen fibers that provide tensile strength to the regenerated tissue. Simultaneously to the fibroblast migration, numerous capillaries begin to form to provide the site with nutrients and oxygen, while epithelial cells at the edge of the wound begin to fill in the area under the scab. Finally, the new epithelium forms and the wound is healed. Wound healing encompasses many biochemical processes regulated by hormonal factors and anti-inflammatory mediators, resulting in the repair of tissue and defense against infection. Regulating factors in wound repair include growth factors, immunologic mediators and biochemical substances [82]. As a result of inflammation, fluid, cells, or cellular debris escape from blood vessels and are deposited in tissues or on tissue surfaces. Enzymes present in this material may cause modification of the various parameters affecting cell contact [227]. Improving on the stages of wound repair can result in an accelerated, more efficient and complete wound closure and repair.

The inflammatory stage of wound repair is crucial to the function of implanted materials, as well as to natural processes of destruction, dilution or isolation of an

injurious agent. Normally, the implantation of a prosthesis is followed by an inflammatory reaction that can be moderate or severe depending on the properties of the prosthesis. A moderate inflammation response can illicit desirable effects, especially when resorption of materials is desired. As previously mentioned, the resorption of a material is the process of degradation and subsequent incorporation of by-products back into the surrounding tissue. A material should resorb without any significant toxic or immunological effects on the surrounding tissue [168 38]. During inflammation several cells (i.e. monocytes or macrophages) produce hydrolyzing agents (specific enzymes) and oxidizing agents (NO). The presence of these inflammatory agents can prompt polymer degradation, which allows normal growth of the tissue replacing the degraded prosthesis. Conversely, a severe inflammatory response to a foreign material can prompt massive destruction of the tissue at the site of implantation and restrict the healing process [184].

To understand the processes of wound repair, it is critical to know the responses of connective tissues to wounding. These responses are often mimicked in natural repair. This study utilizes the NIH 3T3 fibroblast as a model because of the intrinsic role fibroblasts play wound healing process. Fibroblasts are intimately associated with implanted biomaterials and wound repair. Fibroblasts produce collagen during the process of wound repair and participate in organization of new connective tissues [211]. Collagen is crucial to wound healing in all phases of the process. Initially, collagen (with input from fibronectin) sets the stage for the inflammatory response by initiating platelet adhesion to begin clot formation. Then, during inflammation, collagenase clears the wound area. Next, collagen is produced to provide an adequate matrix for wound repair,

while collagenase activity increases, permitting cell mobility. Finally, the tissue is remodeled as the collagen matures and collagenase removes excess collagen [205].

Fibroblasts produce many important molecules to wound repair including the glycoprotein fibronectin [193 229]. Fibronectin promotes a variety of reactions important to wound healing, including fibroblast migration, the adhesion and spreading of platelets on collagen bound to the fibrin clot and to collagen itself. During the inflammation stage, fibronectin promotes the formation of the fibrin clot by binding and cross-linking with transglutaminase to collagen, fibrin, and itself [51 72, 109]. Collagen also stimulates the treatment of cells with opsonin to make them more susceptible to inundation (opsonisation) by phagocytes (macrophages and neutrophils). The ability of fibronectin to promote opsonisation reactions in phagocytes could be important for removal of necrotic, infected or foreign material from the wound. Fibronectin contains the RGD domain, which is integral in the attachment of many cell types to surfaces. RGD is found in many adhesion proteins and binds to numerous integrin receptors [91]. Interactions between cell integrins like RGD and fibronectin of an ECM or adsorbed to a substrate result in cellular attachment and spreading. Fibronectin not only functions as an attachment protein, but also may play an important role in repair reactions. The multiple interactions and biological activities of plasma fibronectin (also known as cold insoluble globulin) are consistent with it having a role in wound repair. Fibronectin may also be one of the agents attracting fibroblasts into the wound, because it is highly chemotactic for fibroblasts, promoting the direction of movement through a gradient of diffusible fibronectin [59]. Furthermore, fibroblasts adhere to fibrin that has covalently bound fibronectin [72]. Once in the wound area, fibronectin can help maintain the fibroblasts by

promoting cell-matrix interactions and stimulating matrix production [53]. Another reason this investigation considers the NIH 3T3 fibroblast as a model cell type is due to its production of fibronectin.

Also, fibroblasts are a model cell type for wound repair due to their interaction with keratinocytes. *In vitro*, fibroblasts affect the proliferating and differentiation activity of keratinocytes [186 125 16]. *In vivo*, epithelial differentiation is controlled by the supporting mesenchyme. The effect of various components of the dermis on epidermal differentiation has been illustrated in embryonic development [204]. Thus, the fibroblast plays an integral role in the development of the dermis and epidermis through its effects on keratinocytes.

Growth factors are involved in the process of wound healing. *In vivo* studies have shown that growth factors stimulate and modify the different phases of wound healing, particularly in cases of impaired healing. These studies indicated that cells present in the healing area produced growth factors that stimulated wound healing. The wound fluid from surgical wounds was found to possess potent mitogenic and healing stimulatory properties, whereas fluid from chronic wounds did not have these effects. This implies that the growth factors secreted by acute wounds are not as susceptible to proteolysis as in chronic wounds. Several of these growth factors involved in the regulation of wound repair are protected from degradation by being bound to heparin [114 10].

Heparin is found in the granules of the mast cells and exerts its anticoagulant activity by binding and activating the plasma protein antithrombin. Heparin also binds with high specificity to a large number of different growth factors, which become activated and stabilized. For example, basic fibroblast growth factor's (bFGF) conformation changes

when bound to heparin and its activity increases over 20 fold *in vivo*, as well as a 100 fold increase in stability against proteolytic enzymatic degradation. Heparin stimulates proliferation in some cell types and inhibits growth in others. It also modulates several phases of wound healing [29 52 136 139]. In order to transmit its growth signal into a cell, FGF required heparin sulfate as a cofactor to bind the cell receptor [202]. Heparin tends to stabilize the interaction between fibronectin and collagen. Heparin sulfates, found in high concentration in a CHO cell line which detaches slower than it's normal counterpart from a substrate, indicate that the heparin sulfate GAG plays an essential role in cell attachment, *in vivo* [190].

The migration of cells is an integral aspect for the stimulation of tissue reconstruction [158]. Migration of cells and wound repair is encouraged by growth factors such as bFGF and PDGF. Wound repair is encouraged by bFGF's tendency to promote migration and proliferation of capillary endothelial cells, which are essential for the formation of new blood vessels in the damaged site. Glycosaminoglycans have the potential to bind different growth factors. Chitosan can bind growth factors such as FGF due to its similarity in structure to GAGs (the NAGA units). Chitosan can activate macrophages and monocytes, thereby inducing the production of FGF and PDGF, which stimulate the organization of bone tissue both *in vitro* and *in vivo*[150]. Fibroblast growth factor and PDGF can induce mitosis (mitogenic) in eukaryotes and through a gradient can induce a response towards the direction of migration of many cells involved in wound healing (chemotactic), including fibroblasts, epidermal cells and endothelial cells. Basic FGF can induce faster wound closure when introduced to the damaged site [11 81 20]. Platelet derived growth factor is mitogenic in eukaryotes and chemotactic to periodontal

ligament cells and osteoblasts [68]. Platelet derived growth factor has also been shown to enhance periodontal regeneration, and promote periodontal regeneration in beagles and non-human primates when combined with insulin-like growth factor [127 195 61]. Chitosan, in combination with FGF may have an increased stimulatory effect on tissue repair.

Chitosan shows biostimulating activities in the repair of various tissues [161]. Chitosan also assists wound healing and tissue growth by activating growth factors and cytokines *in vitro*. By increasing the expression of growth factors, chitosan enhances fibroblast activity and encourages the development of fibrous tissue. Additionally, chitosan exhibits wound healing properties by forming complexes with heparin, which promote tissue vascularization and has anticoagulant properties [116]. Chitosan *in vivo* seems to induce an attraction for stromal cells by exhibiting migratory and stimulatory effects on the stromal cells neighboring the polysaccharide [158].

2.3.2. Cellular Interactions

The following sections summarize important cellular processes of attachment, adhesion, spreading, growth and migration.

2.3.2.1. Cell Attachment and Adhesion

Cell adhesion is important to many cellular processes. Adhesive interactions play a critical role in the development of multicellular organisms by guiding cells to appropriate locations and securing them in place. Cell adhesion is thought to depend on intermediate adhesive molecules [192]. As previously mentioned, an important attachment protein is fibronectin, which is produced by fibroblasts and endothelial cells as well as some other cell types [128]. Fibronectin interacts with other molecules associated with the

ECM including collagens, GAGs, proteoglycans, fibrinogen, fibrin and actin, and promotes cell attachment and spreading [191]. Many adhesion molecules, including fibronectin, immunoglobulin (Ig) type proteins, and cadherins share similar structural features. Fibronectin contains multiple repeats of a 90-amino acid domain identified as fibronectin type III (FNIII) domains. Fibronectin type III contains the RGD sequence in the ligand protein, and is similar in structure to the Ig molecules [119 131 228]. The RGD sequence is also recognized by vitronectin, laminin and collagen types I, III, IV and VI [137]. Also, hydroxyl groups have been suggested to be important to initial adhesion of cells to substrates, whereas parts of carboxyl groups influence long-term cell growth [19].

Cell adhesion first involves non-specific forces, followed by specific adhesion interactions of the cell with the substrate or ECM. Non-specific forces influencing cell adhesion include electrostatic forces and van der Waals forces. Structural proteins involved in cell adhesion consist of extracellular and intracellular components, and cytoplasmic proteins. The extracellular proteins include collagen, fibronectin, vitronectin and laminin. Transmembrane proteins include α and β integrin subunits and cell-surface proteoglycans. Finally, cytoplasmic attachment proteins include actin, α-actin, fimbrin, vinculin, talin and tensin [170 42 7 118 60 24].

Serum or tissue proteins that support the cell adhesion process contain active sites, which bind to specific cell surface receptors, analogous to antigen-antibody or enzyme substrate binding [101]. Most adhesion receptors also function as signaling molecules. Phenomena such as anchorage dependence and contact inhibition of growth appear to be linked to integrin-mediated adhesion [202 210]. Fibroblasts, endothelial and

epithelial cells all cease growth when detached from the culture substrate *in vitro*. Cell-cell adhesion molecules may mediate contact inhibition [210].

One important step in cell-substrate interactions is the adsorption of proteins from the media onto the substrate. Additionally, the orientation and conformation of the adsorbed proteins can affect the cell-substrate interactions, such as cell attachment and spreading as well as specificity for certain cell lines. Fibronectin is known to enhance cell attachment and spreading to anchorage dependent cell lines. One study indicated an approximately linear correlation between 3T3 fibroblast spreading and the amount of fibronectin adsorbed onto the cell culture substrate. This was demonstrated for hydroxyethylmethacrylate (HEMA) and ethylmethacrylate, as well as for numerous polymeric substrates including polystyrene. However, if given enough time (up to 24 hours), 3T3 fibroblasts did spread onto a substrate, indicating that the cells secrete their own fibronectin. Furthermore, it was shown that glass surfaces pre-incubated with 10% serum for as little as 10 seconds showed similar enhancement in subsequent cell spreading to those pre-incubated for 90 minutes. This illustrates the rapidness of the adsorption process. [86].

Cell attachment will occur on most substrates coated with any protein, but spreading requires specific factors [101]. Cell attachment appears to be dependent on the surface free energy of the substrate. This has been illustrated with studies on the attachment of cells associated with collagen or adsorbed serum proteins, which indicate that in the absence of serum, attachment is primarily dependent on the surface free energy of the substrate [43]. Cells using glycoproteins such as fibronectin can adhere to specific collagens. Fibroblasts will adhere to all collagens, whereas other cell types including

chondrocytes, epithelial and endothelial cells will bind preferentially to specific collagens [109]. Fibroblast adhesion to collagen requires divalent cations (Ca^{2+}, Mg^{2+}) and is temperature dependent [108 180]

The ECM GAGs, hyaluronic acid and heparin sulfates, play an important role in cell adhesion. Heparin tends to stabilize the interaction between fibronectin and collagen whereas hyaluronic acid has a destabilizing effect. Heparin sulfates, found in high concentration in a CHO cell line which detaches slower than it's normal counterpart from a substrate, indicate that the heparin sulfate GAG plays an essential role in cell attachment, *in vivo* [190]. Another influential adhesion glycoprotein is laminin. Laminin is a high molecular weight glycoprotein that influences the adhesion and spreading of many cell types. Laminin mediates adhesion of epithelial cells and endothelial cells to basement membranes, thereby holding a significant role in cell development and differentiation [101].

Attachment of cells to substrates can depend on the surface topography. The alignment of baby hamster kidney cells, Madine-Darby canine kidney (MDCK) cells and chick cerebral neurons were significantly affected by groove depth over groove spacing in substrata when dimensions are comparable to a typical cell size. A cells susceptibility to substrate topography is cell-type dependent and depends on the availability of cell-cell interactions. Grooved substrate tends to stabilize shear sensitive cells subjected to a shear force. One proposed strategy to improve tissue attachment at implant surfaces with fibroblasts is to use parallel grooved substrata with subcellular dimensions. Fibroblasts will conform to these contours [22].

2.3.2.2. Cell Spreading

To achieve faster cell spreading and directed cell migration, one must first optimize the adhesion of the cell to the biomatrix [144]. Cell spreading is mediated by glycoproteins such as collagen, fibronectin, laminin, chondronectin and a spreading factor. Fibroblasts may exhibit different spreading behavior depending on the amount of adsorbed fibronectin on the substrate. The fibronectin affects the initial spread of cells onto the substrate, but subsequently, cells will spread due to their own production of fibronectin [88]. A major factor that regulates the mitogenic response of a given cell type to a given class of mitogenic agents is the cellular shape. Specific cell surface proteins control the cellular shape [66]. Cell adhesion to materials is mediated by cell-surface receptors, interacting with cell adhesion proteins bound to the material surface [4]. Many cultured cells including fibroblasts, myoblasts, hepatocytes, chondrocytes, and certain epithelial cells are suspected to utilize these adhesion glycoproteins bind the cells to the substrate [36 70]. Cells will attach to many surfaces in the absence of bulk phase or adsorbed proteins, but typically will not grow. The spreading of the cell is a characteristic of the cell functioning in a state more indicative of that found *in vivo* [86]. Cell attachment and subsequent shape can also effect the expression of genes and the translation of mRNA. Furthermore cellular attachment and shape change can affect differentiation as well as morphogenesis (spatial arrangement and tissue formation) [111 9 103]. One theory towards the maintenance of good cell growth in vitro and in vivo is to attach as many cells to the substrate as possible with the help of attachment proteins, as this will result in good spreading behavior as the cells produce the necessary products for this phase [101].

2.3.2.3. Cell Growth and Migration

The proliferation of cells is closely related to its cellular shape. The cellular shape is determined *in vivo* by the ECM, and *in vitro* by the substrate on which the cells are cultured. The ECM or substrate can induce the cells shape and growth. The substrate also controls cellular differentiation and can shift the pattern of genetic expression of an already differentiated fibroblast line. This was demonstrated by showing an inert matrix of demineralized bone capable of inducing fibroblasts to change their genetic expression to form cartilaginous bone and bone marrow [183]. Studies with porous substrata have indicated that surface morphology can affect cell growth and differentiated function. The effects on cell proliferation and function appear to be a result of a direct modulation of cellular shape due to substrate topography [54 94 98].

Cell migration is mediated by cell adhesion receptors and their ligands. Most cells in the body can use adhesion molecules for migration. Integrins mediate migration of anchorage dependent cells on the ECM. A weak or moderate strength of attachment favors cell migration, and a strong attachment tends to immobilize the cell. Also, similar to integrins, cell-cell adhesion molecules can control cell migration by promotion or inhibition [192]. Stress fibers composed of microfilaments are suspected to resist cell migration by anchoring cells to the substratum. During initial cell spreading, a radial stress-fiber pattern often develops. Subsequently, upon flattening, one side of the cell will display a fan-shaped array of stress fibers, and cell migration tends toward the side lacking these stress fibers [209]. Migrating fibroblasts exhibit contact inhibition by forming submembraneous actin filament bundles at contact areas. Cadherins subsequently interact with the actin filament system, negatively affecting cell migration [101].

2.3.3. Extracellular Matrix

With the exception of hemopoietic cells, gametes and tumor cells, most mammalian cells require a solid substrate or scaffold to attach to in order to proliferate and function, both *in vitro* and *in vivo* [5-9]. This substrate is tissue-specific *in vivo*, referred to as the extracellular matrix (ECM). The ECM is critical in directing tissue development and the cellular functions of adhesion, shape, growth, metabolism, differentiation and spontaneous mobility. In addition, the ECM provides necessary physical support for these functions. The natural ECM is the combination of many complex macromolecules that organizes cells to form complex tissues. The natural ECM is porous enough to allow for cellular migration and interaction, while not interfering with the diffusion of hormones, nutrients and metabolites into the matrix to provide nourishment and initiate cellular responses. The ECM is composed primarily of two kinds of macromolecules: proteoglycans and fibrous proteins. The proteoglycans are long unbranched chains of polysaccharides that can form 3-D matrices of hydrated gels in which cells can effectively function. These proteoglycans provide compressive strength to the ECM. The fibrous proteins, such as collagen, provide tensile strength to the ECM [2-12]. The ECM is rich in GAGs including hyaluronic acid, chondroitin sulfates, dermatan sulfate, heparin and heparin sulfate [17]. Many studies on the role of the ECM components in tissue functions have been carried out with cells cultured on matrix proteins deposited on plastic [35]. One method for increasing the biocompatibility of a material is by exploitation of the *in vivo* interactions of cells with their ECM molecules, which are often naturally occurring polymers [37].

The *in vitro* repair or replacement of damaged tissues has utilized strategies focused on manipulation of the cell environment by modification of cell-ECM interactions, cell-cell interactions, or soluble stimuli [12]. Every ECM compound plays a different role in cellular responses and processes, including cell shape, movement, proliferation and differentiation. The composition of the ECM influences the building up of tissue. ECM molecules including collagen, GAG and glycoproteins such as laminin and fibronectin are the keys to the development of new tissue. GAGs are widely distributed within tissues, and may be integral components of the cell membrane. GAGs may therefore participate in cell-matrix interactions as well as cell-cell interactions.

The ECM mediates cellular functions of growth, adhesion, migration and differentiation [216]. A major regulatory mechanism controlling cellular function is the adhesion of mammalian cells to surrounding ECM [101]. Cell matrix interactions are mediated by cell surface receptors known as integrins [93]. These interactions are regulated through the binding of cell receptors from the cell surface to molecules on adjacent cells or the ECM [19 124]. Examples of integrins are the fibronectin and vitronectin receptors of fibroblasts, which bind to the RGD sequence in the ligand protein. Though the context of the RGD seems important and there is also a divalent cation-dependence. Other integrins include the platelet IIb/IIIa surface glycoprotein (fibronectin and fibrinogen receptor), the LFA-1 class of leucocyte surface protein, together with the VLA surface protein. The requirement for the RGD sequence in the ligand does not seem to be invariable [25]. The development of chemically well-defined *in vitro* cell growth substrates, open to covalent addition of proteins, glycoproteins or other ligands acting as

extracellular molecules [174 13 73], will aid in better understanding the molecular basis of extracellular control of short and long-term cell behavior [19].

Further influence of the ECM on cellular functions relate to its ability to bind growth factors. Components of the ECM are capable of binding various growth factors, and can subsequently regulate the activity of the growth factors as well as their availability [194]. It is presently accepted that all cells in a multicellular organism are programmed to die unless externally stimulated otherwise [96 181]. These survival signals are provided by direct cell contact with the ECM as well as through soluble factors such as hormones or cytokines [58 179 182].

Fibroblasts produce collagen as a primary structural protein. Collagen shows evidence of directing cell differentiation. Similarly, proteoglycans and hyaluronic acid play a crucial role in movement of cells or groups of cells during development [79, 135 132]. Collagen also influences cell proliferation, migration and specific gene expression [109 120]. Collagen is frequently cross linked when used as an implantable biomaterial to increase the structural stability of the matrix and prolong its structural integrity during degradation. The addition of chitosan to collagen increases the structural integrity of collagen matrices. This may be advantageous for applications requiring long-term maintenance of 3-D cell-seeded matrices *in vivo* and *in vitro* [212].

Many vital processes of growth, development and tissue repair subsequent to injury depend greatly on the proper timing and rate of synthesis and breakdown of collagen molecules. Scar tissues are the end result of most healing processes in higher vertebrates and man, and are composed primarily of collagen. Also, collagen metabolism is an integral part of cellular processes including tissue regeneration and reshaping, and the

growth and development of hard tissues. Collagen has been utilized as an ECM for culturing cells *in vitro*. Collagen is not as versatile in the development of films, and 3-D matrices as chitosan. Additionally, collagen can be quickly broken down *in vivo* by collagenases, which is sometimes to fast for complete wound repair using an implantable substrate.

One of the primary factors that regulates the mitogenic response of a given cell type to a specific mitogenic agent is the cellular shape. The stimulation of cell to a mitogenic response can be guided *in vivo* by the ECM upon which the cells rest and *in vitro* by the substrate upon which the cells are maintained; the substrate itself may in turn induce the cells to manufacture their ECM and specific cell surface proteins which control the cellular shape [66]. Many cultured cells including fibroblasts, myoblasts, hepatocytes, chondrocytes, and certain epithelial cells are suspected to utilize adhesion glycoproteins to bind the cells to the substrate or ECM [36 71 83 85]. As previously mentioned, fibronectin, which is produced by fibroblasts and endothelial cells as well as some other cell types, is an important adhesion glycoprotein [109]. Fibronectin interacts with other molecules associated with the ECM including collagens, GAGs, proteoglycans, fibrinogen, fibrin and actin, and promotes cell attachment and spreading [191 80 173].

Hyaluronan is found in the ECM of various connective tissues and structurally resembles chitosan. Hyaluronan has been shown to promote cell motility, adhesion and proliferation, and to have an important role in processes of morphogenesis, inflammation, wound repair and secondary tumor development that require massive cell movement and tissue reorganization. Many of the effects of hyaluronan are controlled by cell surface receptors. These hyaluronan-mediated signals are conveyed partly through the activation

of protein phosphorylation cascades, cytokine release and stimulation of cell cycle proteins [155]. The ECM uses its proteoglycan components to regulate the activities of growth factors. For example, FGF requires heparin sulphate (a component of proteoglycans) as a cofactor to bind the receptor that transmits its growth signal into the cell [202].

2.4. Fibroblasts

This project utilizes fibroblasts as a model cell type for many reasons. Fibroblasts are acknowledged as critical components in the wound repair process. They follow the inflammatory cells to the damaged site and contribute to the repair through the production of structural proteins. The fibroblasts also encourage wound contraction and reorganization of the ECM [147]. Fibroblasts are intimately associated with implanted biomaterials. Fibroblasts in the metabolic state produce collagen during the process of wound repair and organization of new connective tissues [211]. Additionally, fibroblasts are among the easiest mammalian cells to cultivate. A predominance of the fibroblast and derivation of homogenous strains result from the serial cultivation of disaggregated cells from a piece of tissue from almost any location [69]. Furthermore, the fibroblast has differentiated functions that are easily maintained in culture [75]. Fibroblasts are often used as a model cell type for the evaluation of a biomaterial [112 37 77]. For these reasons, this project utilizes the NIH 3T3 fibroblast as the model cell type of investigation.

Fibroblasts are anchorage-dependent cells. Studies indicate that anchorage dependent cells have a preference for cationic surfaces [63 199]. Cations, including Ca^{2+} and Mg^{2+} in fetal calf serum (FCS) and Dulbecco's Modified Eagle Medium (DMEM) mediate fibroblast adhesion and may be bound to a chitosan membrane [177]. Also,

fibroblasts will attach and proliferate on many different substrates with varying chemistries. However, the fibroblast will not grow if detached from the substrate. Cell growth that is dependent on anchorage appears to be related to specific integrins, depending on the cell type. For example, CHO cells and human osteosarchoma cells were shown to attach (but not grow) through integrins in serum-free conditions, and only survived when attaching through the $\alpha 5\beta 1$ integrin [231].

Fibroblasts are model cells for assessing the cellular interaction with polymer substrates. Results of one study indicate that the polymer substrate influences initial attachment and spreading, but not subsequent growth rate of fibroblasts. Evidence indicates that fibroblasts produce enough of their own ECM proteins after 24 hours *in vitro* to render the surface chemistry of the attachment culture substrate unimportant at longer periods [75].

Fibroblasts are known to produce cytokines including interleukin (IL)-1, IL-6, IL-8 and tumor necrosis factor (TNF). These cytokines can alter the immune response during inflammatory and immunological reactions, and may be influential in attracting or restricting the build-up of connective tissue by altering the mobility and proliferation of fibroblasts in an inflammatory lesion. Furthermore, they can alter the immune response, as well as play an important role in promoting or restricting the accumulation of connective tissue by altering the migration and proliferation of fibroblasts in inflammatory lesions [147]. Fibroblasts synthesize the different macromolecules of the dermal ECM in an organized manner and limit formation of granulation tissues and hypertrophic (enlargement due to an increase in cell size) scars [45]. Cells known to depend on fibroblasts or products thereof include myoblasts, and keratinocytes. Thus, the

development of muscle fibers as well as the various differentiated layers of the dermis and epidermis depends on fibroblasts and their products. Epithelial cell types appear to be dependent on connective tissue for proliferation [69].

A collagen-GAG-chitosan sponge acts as an excellent 3-D matrix for human fibroblast culture, which can be used in the preparation of dermal or skin equivalents. Specific characteristics studied included cell proliferation, migration and metabolic activity. The spongy substrate was also studied for variations in weight and size with time. Human foreskin fibroblasts grew and displayed biosynthetic activities similar to those of cells cultured in collagen gel. A three-fold increase in cell growth was observed on chitosan-containing gels compared to collagen itself. Also, a two fold decrease in total protein and collagen synthesis was apparent in the pure type I collagen. This was the result of native collagen sponges quickly contracting and experiencing considerable weight loss because of enzymatic breakdown below 37 °C. The addition of chitosan and GAG acted to stabilize the collagen network and reduce this weight and size loss. These studies confirm previous studies that fibroblast growth is inhibited in a contracted collagen gel [221 34 8 49 162]. In another study, the attachment and growth of fibroblasts exceeded that of cells on a collagen-coated substrate [112]. Also, chitosan-cellulose-chitin polymers provide an ECM *in vitro* exhibiting greater cell differentiation and development of cell function for human periodontal ligament fibroblasts (HPLF) compared to a polystyrene tissue culture dish. This chitosan-polymer benefited the HPLF culture *in vitro*, mimicking the ECM of that *in vivo* [77].

2.5. Important Substrate Properties

One objective of this project is to develop a standard, reproducible chitosan film-formation technique. In order to establish that the films are similar in physical and chemical properties, it is necessary to characterize them. Therefore, the following measurements were performed on chitosan films for this characterization; the viscosity of the chitosan solutions in acetic acid, the physical dimensions of films including thickness, length, width, and roughness, Young's modulus of elasticity, yield stress, strain to failure, and the degree of deacetylation (DDA). A thorough characterization of these chitosan films will help confirm that they are produced with similar properties. It is also necessary to understand the properties of the chitosan films to explain their effects on the attachment and growth of NIH 3T3 fibroblasts.

2.5.1. Surface Free Energy

A vital characteristic of chitosan films and biomaterials in general is the surface free energy (SFE). The SFE of a substrate has been shown to affect cellular adhesion, spreading and migration. Cell adhesion appears to be maximized on moderately wettable surfaces with water-in-air contact angles in the range of 60 to 90 degrees [211 226 92 78]. The water-in-air contact angle of substrates is directly related to its surface free energy. Furthermore, fibroblast spreading has been correlated with surface free energy, with greatest spreading on substrates with SFE greater than 45 (mJ/m^2) [222 201]. Also, fibroblast synthesis of collagen has been shown to be highest on surfaces with surface free energies greater than 55 (mJ/m^2) [211 201]. Studies with human endothelial cells further suggest that moderately wettable surfaces increase the adsorption of serum proteins, which thereby increases cell attachment, spreading and adhesion [225].

2.5.2. Roughness. Relation to Attachment, Orientation and Adhesion

As previously mentioned, the roughness of a substrate can greatly affect the attachment, orientation, and adhesion of cells. One study demonstrates that rough surfaces develop higher adhesion than smooth ones[135]. Higher adhesion to rough surfaces may be expected because rough surfaces have a greater surface area than smooth ones, and a low viscosity adhesive could flow into all of the cavities available while a high viscosity adhesive could not [134]. Furthermore, cells cultured on substrates with textures, edges and grooves exhibit different behavior than those cultured on smooth surfaces. Studies confirmed that the extent of cell alignment on parallel grooved substrata mainly depends on groove depth, and is less dependent on groove spacing [39]. One example is the orientation and migration of neuron cell cultures along fibers or ridges in the substrate (termed contact guidance). Additionally, fibroblasts have been shown to orient along grooved surfaces, with optimum orientation occurring when groove dimensions were in the range of 1 to 8 μm. This orientation was shown to depend on the depth and pitch of the grooves [22]. Contact guidance has been suggested as a mechanism for tumor cell invasion. Many researchers have studied contact guidance using substrates with grooved or textured dimensions. Also, grooves tend to stabilize shear-sensitive cells subjected to shear forces [206].

Additionally, grooves can effect cell growth and function [33 84 214 140 203]. Fibroblasts showed improved growth when cultured on polydimethylsiloxane (PDMS) with uniformly distributed peaks of 4 to 25 μm^2 compared to larger dimensions. Also PDMS surfaces with 2 to 5 μm grooves maximized macrophage spreading [203]. The differentiated state of MDCK cells can be controlled with microporous membranes.

Epithelial cells, which are intimately associated with fibroblasts, when cultured on grooved titanium substrata showed an increase of proteinase secretion over that on smooth surfaces. Furthermore, bone cells showed increased protein synthesis on grooved polystyrene dishes. It has been hypothesized that differences in protein secretion are due to differences in cellular shape. As previously mentioned, cellular shape can affect cell growth, gene expression of ECM proteins, mRNA stability and differentiated function of cells [111 14 41 103].

2.5.3. Chitosan Degree of Deacetylation

An important chemical property of chitosan is the degree of deacetylation (DDA). The DDA is intrinsic and represents the amount of free amino groups in the polysaccharide [123]. The behavior of chitosan is partially dependent on the DDA [157]. The DDA, in turn, influences the overall charge density of chitosan solutions, films and 3-D matrices. The DDA of chitosan has been shown influential in supporting the attachment and growth of L929 fibroblasts and BHK21(C13) cell lines. As little as 10% difference in DDA had a significant effect on the attachment and growth of theses cell lines, with best performance on those polysaccharides with high DDA's [177]. The DDA also affects other properties of chitosan, including the molecular weight and therefore viscosity in solution. Chitosan with DDA's between 90 to 100% are considered fully deacetylated. The DDA can be determined by nuclear magnetic resonance (NMR), Fourier Transform infrared spectroscopy (FTIR), mass spectrometry, chemical or enzymatic titration, gas chromatography and dye adsorption [153 123].

2.5.4. Other Physical Properties

The viscosity is another important property of chitosan in solution. The viscosity is related to the molecular weight of the polysaccharide, and can be used to determine the molecular weight. Also, the shape and preparation of chitosan films and drug-containing chitosan beads was critically dependent on the viscosity of the chitosan solution. High viscosity chitosan solutions result in spherical and strong beads, whereas beads are not attainable with lower viscosity solutions [15].

Simple properties like the thickness of chitosan films are useful for determination of reproducibility of film-forming techniques. The thickness of films is also used for determination of other important mechanical parameters like the Young's modulus of elasticity, yield stress and strain to failure. These parameters give further measure of the reproducibility in the film formation technique, and variability in chitosan sample properties. One study considers the effect of solvent acid on elasticity and relaxation response of chitosan films. This study indicated that the wet-tested apparent Young's modulus of elasticity increases with increasing chitosan concentration [106]. Mima and coworkers[142] characterized both the wet and dry tensile properties of chitosan films. They found an increase in wet tensile strength with increasing *N*-acetylation and no correlation in dry tensile strength and *N*-acetylation.

2.6. Summary

This chapter describes previous work with chitosan as a biomaterial and with various cell types. The current research considered the attachment, spreading and growth of NIH 3T3 fibroblasts on 2-D chitosan films of varying concentrations. This appears to be the first study to consider the cell functions of attachment, spreading and growth of NIH 3T3

fibroblasts on chitosan films. A study similar to the current one by Prasitsilp and others [177] utilized L929 fibroblasts on 2-D chitosan-coated petri dishes to illustrate the importance of the DDA of chitosan on the attachment and growth of fibroblasts, with highly deacetylated chitosan supporting significant fibroblast attachment and growth. Examples of 2-D applications with chitosan as a biomaterial include its evaluation as a substratum for skin replacement [40], as a bandage material, and as a skin grafting template [196].

Previously established methods for the formation of 2-D chitosan films and 3-D matrices are reviewed in this chapter. One simple method for producing 2-D chitosan films was outlined by Rigby in 1936 [189]. Three-dimensional scaffolds were prepared by ionotropic gelation using tripolyphospate. Previous researchers have formed chitosan membranes with a variety of counterions or polymers, such as pyrophosphate, octylsulfate, and alginate. Among the counterion polymers that gelate with chitosan, alginate is the most widely used [15].

The importance of the cellular functions in wound repair as well how substrate properties affect these functions is reviewed in this chapter. Fibrblasts play a particularly important role in the wound repair process as one of the first tissues involved with the repair of damaged or diseased tissue. Substrate properties including the water-in-air contact angle [211], surface free energy [201], and roughness [22 111], as well as the degree of deacetylation of chitosan [157 177] can influence cellular processes of attachment, spreading and growth.

Chapter 3

CHITOSAN FILM FORMATION AND CHARACTERIZATION

3.1. Introduction

The goals of this part of the project were two fold: (1) to establish a standard, reproducible 2-dimensional chitosan film formation technique, and (2) to measure the properties of the films that can be related to its suitability as a biomaterial. It is essential that the film casting procedure produce films with similar physical and chemical characteristics, so that experiments performed on films cast at different times give similar results. Additionally, by establishing and executing a standard film formation method, one is able to familiarize oneself with the workability and properties of chitosan, as well as any limitations. To justify experimentation with cell culture and 3-D scaffolds, the viability of the material was first established through 2-D culture techniques. Furthermore, in order to establish a method for the fabrication of a porous 3-dimensional implantable scaffold, it is helpful to first establish a method for 2-D film formation.

Chitosan films were dissolved in 1.5% acetic acid at concentrations of 0.5%, 1.5% and 3.0% grams chitosan per ml of solution (w/v) using a technique similar to that outlined by Rigby [189]. By using different concentrations of chitosan films, the effect, if any, of chitosan concentration can be studied with respect to the physical and chemical properties of the films, as well as on the attachment and growth of NIH-3T3 fibroblasts. The physical and chemical properties used to characterize the chitosan films, as well as the reproducibility of the film-formation technique include SFE of the films, the DDA, surface roughness, film thickness, yield stress, Young's modulus of elasticity, strain to

failure and the viscosity of chitosan solutions. These properties give a good description of the chitosan films in both the physical and chemical aspects. In addition to characterization of the films, the surface free energy and roughness of cell culture substrate have been shown to have a significant affect on cell functions as described in Chapter 2 [211 201 5 22].

3.2. Materials and Methods

3.2.1. Two-Dimensional Film Formation

High molecular weight chitosan (Lot # 04919KU) was obtained from Aldrich Chemical Company (St. Louis, MO). The chitosan was prepared from crab shells has an approximate molecular weight of 600,000 g/mol, an 85% minimum DDA, and was in the form of white to tan powder and flakes. This supply was utilized to form all 2-D films for cell culture experiments. An acetic acid solution (20% (v/v)) was supplied by VWR Scientific (West Chester, PA). Sodium hydroxide (NaOH) pellets were supplied by Fisher Scientific (Pittsburgh, PA). Ultra-pure distilled water (UP dH_2O) was purified with a Barnstead EASYPure RO compact reverse osmosis water system. This water was used for all chitosan solutions and rinse treatments. Smooth glass plates (12 x 12 x 1/8 inches) were purchased from a local glass supplier. Pyrex dishes were utilized for soaking films. An Orion model 8000 pH meter was used for pH measurements. Finally, a drawdown coater was used for some film-forming applications (RK Print Coat Instruments, Model: Herts SG8 0QZ U.K.). Tinfoil, Kimwipes and clear tape were supplied through the University of Maine central supply.

The following protocol describes the general method for the formation of a 0.5% (w/v) chitosan film from 500 ml of solution. Amounts of each ingredient are modified

accordingly for the 1.5% and 3.0% chitosan solutions. First, 37.5 ml of 20% (v/v) acetic acid were added to 462.5 ml of UP dH_2O to make a 1.5% (v/v) acetic acid solvent. Next, 2.5 g of chitosan were dissolved in the solvent, resulting an a solution of 0.5% (w/v) chitosan in 1.5% (v/v) acetic acid. This solution was strained through cheesecloth to remove any undissolved particulates. Straining the chitosan through cheesecloth results in the loss of some solution and some chitosan.

All four edges of a clean, smooth, 12 x 12 inch rectangular glass plate were taped on top of sheet of tinfoil, resulting in an exposed glass surface of 11 x 11 inches (121 in^2). Glass was cleaned with a 70% ethanol solution and Kimwipes. The tinfoil was folded upward and taped together at the corners to create a containment wall. The tape also helped to detach the film from the glass support by creating a distinct edge in the film. Next, 100 ml of the chitosan solution was cast for each 60.5 square inch area. A cross-section schematic of the film casting set up at this point in the process is illustrated in Figure 4.

Figure 4. Cross section of the chitosan solution cast on a glass support

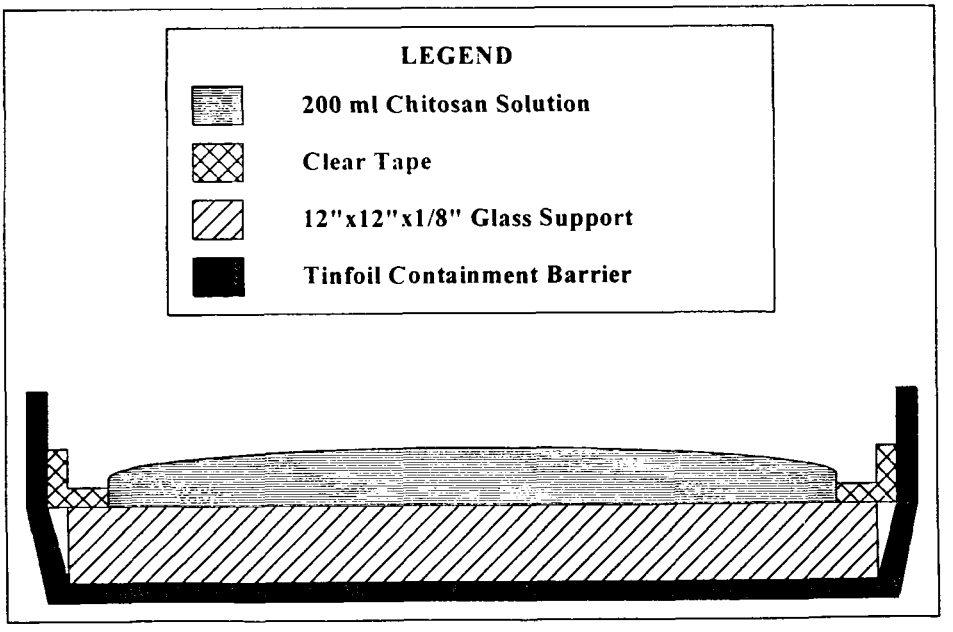

Once cast onto the glass support, the solution was dried at room temperature for 48 hours to ensure complete solvent evaporation. The humidity of the room was not controlled. The glass support was kept level during the drying process, resulting in an even film thickness. Once dried, the tape was removed from the glass, exposing distinct edges of the chitosan film. The edges of the chitosan film were carefully separated from the glass with a razor blade. Once the film edges were partially separated from the glass support, the film was peeled slowly away from the glass.

Once the film was dried and separated from the glass support, it was rinsed with 500 ml of 1 M of NaOH. The rinsing of films in a caustic solution gives the films water-resistance by neutralizing and removing any acetic acid anions present in the films. The caustic solution was placed in a Pyrex glass container with dimensions similar to or greater than that of the film. The film was immersed in the caustic, ensuring that the complete surface of the films were exposed, and soaked for 20 minutes. The films were then repeatedly soaked with distilled water for 30 minutes to wash away any soluble products. The pH of the film rinse-water was measured after each 30-minute soak, until a constant pH of the rinse water was obtained to ensure that no more soluble products were coming off of the film. Typically, four successive 30-minute dH_2O soaks were sufficient to obtain a stable pH near 7. Finally, the wet films were spread out and attached to the clean glass support with clamps and allowed to dry for 24 hours at room temperature. The resulting films were transparent and flexible.

Preparation of 0.5%, 1.5% and 3.0% (w/v) chitosan films varied slightly in method from that described above depending on the concentration of chitosan. For the

0.5% solution, the solution was stirred at 30% of the maximum stirring-speed for 3.0 hours. The 1.5% and 3.0% solutions were stirred at 70% of the maximum stirring-speed for 6 and 16 hours respectively. The increase in stirring speed and mixing time with increasing chitosan concentration was a result of a dramatic increase in solution viscosity, requiring longer times for the chitosan to become completely dissolved in the solution. Because the 0.5% chitosan solution contains a small amount of the polysaccharide, the solutions had very low viscosities and the resulting films were very thin and fragile. It was necessary to cast this chitosan concentration onto smaller areas, because the 0.5% concentration films showed difficulty during detachment. The 0.5% films were detachable when one of the length/width dimensions was less than 6 inches, so typical film dimensions were 5 x 11 inches (60.5 in^2). To reduce the dimensions of the film, an additional piece of 1-inch clear tape was placed in the center of the glass plate, separating it into two equal halves of just less than 6 x 12 inches. During detachment, the short edge of the 0.5% film was separated from the glass with a razor blade, and peeled away along the length of the film. The 1.5% and 3.0% films could be cast and easily detached from 121 in^2 areas.

Another method for casting 1.5% and 3.0% chitosan films was also employed using a RK Print Coat Instruments, Herts SG8 0QZ U.K. drawdown coater. The glass support attached to tinfoil was placed on the coater, and the smoothest rod (model #1) was placed in the apparatus. The rod was raised to a height of 2 mm above the glass support on the drawdown coater, and 200 ml of chitosan solution was placed on the glass support, just in front of the bar. The 3.0% chitosan solutions were spread at an approximate rate of 3 inches/second, and the 1.5% chitosan solutions were spread at an

approximate rate of 2 inches/second. The film was then placed on a level surface, and subsequently dried and treated as previously outlined for the above film-casting technique.

To create a chitosan film with grooved surfaces, chitosan was cast onto a grooved Lexan support. This support was made by machining grooves with a Bridgeport J-series variable speed drilling machine into an 8 x 8 x ¼ inch sheet of Lexan using a cutting tool with an approximate tip diameter of 1.0×10^{-3} inches. Grooves were spaced every 0.01 inch at a depth of 0.001 inches and cut at a rate of 20 inches per minute and RPM of 3000. The Lexan support was then cleaned with 70% ethanol solution. Finally, 200 ml of 3.0% chitosan solutions were cast onto the support and subsequently detached. The lower viscosity 0.5% and 1.5% chitosan solutions were not detachable from this support.

All films used in cell culture experiments were sterilized for 1 hour in a UV-IR oven. The UV bulbs are GE model RSM operating at 275 Watts and 110-120 volts, and emit light at 296 nm. The IR bulbs are GE model AJ IR reflectors, and are standard tungsten filament bulbs with a thin IR coating, emitting light over a broad spectrum at 250 Watts and 120 volts. Samples were placed in sterile, disposable 15 x 100 mm polystyrene petri dishes, and placed in the oven at 14.5 inches below the lamps. Films were characterized with no UV-IR treatment, as well as with UV-IR treatments of up to 24 hours.

The viscosities of the chitosan solutions were measured with a Bohlin CVO Rheometer. All chitosan solutions were measured over a shear range of 0.005 to 270 s^{-1}. The viscosity of the 0.5% chitosan solutions was measured using a double gap geometry. This geometry is used for fluids with very low viscosities. The viscosities of the 1.5% and 3.0% chitosan solutions were measured with a cone-and-plate geometry, which can

be applied to fluids with higher viscosities. The cone had a 4 degree angle and a 4 cm diameter. The intrinsic viscosity is reported as the viscosity of the respective chitosan solution over the Newtonian shear range. A cross section of the Bohlin CVO Rheometer is depicted in Figure 5.

Figure 5. Schematic of different Bohlin CVO geometries used for viscosity testing

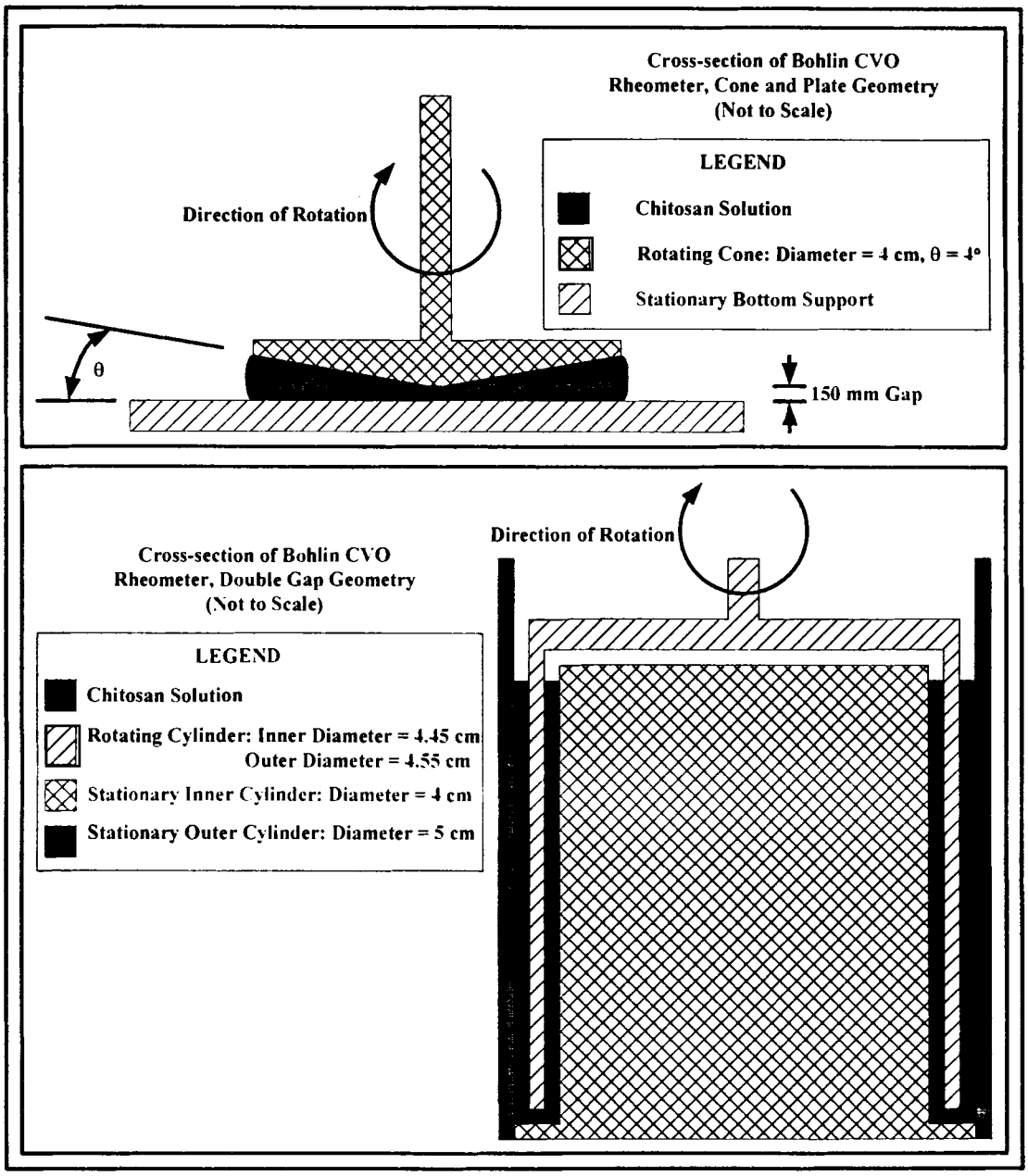

3.2.2. Film Tensile Properties

Specific physical properties were determined to characterize the chitosan films and to confirm reproducibility of the film-formation technique. These properties include the film thickness, Young's modulus of elasticity, yield stress and strain to failure. A method for testing the tensile properties of the films was adopted according to ASTM standards for testing the tensile properties of paper and paperboard using a constant-rate-of-elongation apparatus [2]. The instrument used to test these properties was an Instron Series 5500 tester. Film thickness measurements were obtained with a Mitutoyo digital micrometer with 1 μm accuracy (No. 293-705 7126095). Similar results for film thickness were also measured with a Starrett 0-1 inch micrometer (model no. 230), with a 12.7 μm accuracy.

Chitosan films were cut into strips of 25.4 mm x 254 mm and placed in the grips of the Instron tester so that distance between the grip clamping zones was 180 mm. An elongation rate of 7 mm/min for 0.5% and 1.5% films and 10 mm/min for 3.0% films resulted in specimen rupture 10-30 seconds following the initiation of the elongation force. An average of at least 9 tests per sample were used to determine the Young's modulus of elasticity, the yield stress and the strain to failure. All films were tested dry at room temperature.

3.2.3. Surface Roughness of Films

The surface roughness of a substrate used for tissue culture can greatly affect the attachment, adhesion and orientation of cells [134]. Cells cultured on rough surfaces exhibit different behavior than those cultured on smooth surfaces [197]. In addition, the roughness

can affect cell growth and function [206]. Therefore, it is very important to characterize the roughness of the chitosan films used for cell culture experiments.

Substrate average roughness was measured with a Tencor Instruments profilomter (Alpha 200), with a diamond-tipped stylus. Samples were mounted onto a glass slide with double-sided tape. Minimum sample dimensions were 25.4 mm x 25.4 mm. Samples were scanned by dragging the stylus along a 2000 μm line over the substrate at various points. The Tencor Alpha 200 uses internal software to calculate the average vertical variation in the substrate over the range of the scan. An average of at least 10 scans was obtained and used as the value for the average roughness (Ra). Scans were performed on both sides of the films. All concentrations of chitosan films cast on a glass support were tested for Ra. In addition, the 3.0%, grooved chitosan films that were cast on the Lexan support were also tested for Ra.

3.2.4. Surface Free Energy Estimation by Contact Angle Measurement

The SFE is an important property of a cell culture substrate. Another important property of a cell culture substrate, directly related to its SFE is the water-in-air (WIA) contact angle. The SFE of a substrate has been shown to be related to the function of tissue cultured on the substrate, including attachment, spreading and growth [211]. A substrate's SFE can be calculated by measuring contact angles of various fluids with different known surface tension characteristics and a generalized version of the Young-Dupre equation for the surface free energy components of a liquid on a solid.

Fluids utilized for SFE measurements were glycerol, ethylene glycol and distilled water. Molecular biology grade glycerol (Lot # 99H0099) was obtained from Sigma Chemical (St. Louis, MO) and analytical grade ethylene glycol (EG; Lot # 5001 T05753)

was obtained from VWR Scientific (West Chester, PA). Images were captured onto a standard 120 minute VHS tape with a Panasonic CCTV video camera (model no. WV-BD400) with a 2X adaptor fitted with a zoom lens (D.O. Industries model ZOOM 6000 II), connected to a Panasonic video monitor (model no. WV-5740), a video timer (FOR-A Video Timer, model no. VTG-55) and a Panasonic VHS VCR (model no. PV-S4167).

The contact angle of fluids on a solid support is directly related to the overall surface free energy of the film [64]. The contact angles of distilled water, ethylene glycol, and glycerol were measured on chitosan films and polystyrene controls according to the following procedure. A diagram of the experimental set up used to capture contact angle images is shown in Figure 6. Chitosan films were mounted onto a glass slide with double sticky-sided tape. 1.0 µl drops were placed onto films and substrates with a 1 µl Hamilton syringe accurate to 0.02 µl (model 7001). Images were captured onto a VHS tape at 60-125X magnification. Water and ethylene glycol contact angles were captured at 15 seconds after contact with substrate, which was the time required for the drop to stop spreading. Glycerol contact angles were captured at equilibrium 30 seconds after contact with the substrate. Fluid drops of 5 µl were also placed onto the sample with a Hamilton 10 µl syringe with an accuracy of 0.2 µl (model no. 1701) and captured according to the above protocol. These images were used to test the influence on fluid volume on contact angle. It was found that contact angles were equal for volumes of 1 and 5 µl. No significant adsorption of fluids by the chitosan films was observed, as evidenced by no visual change in drop shape or size over the time span of the experiments. The contact angle of all fluids was captured for chitosan films without UV-IR sterilization, as well as for films sterilized for 1, 12 and 24 hours respectively.

Figure 6. Experimental set up for contact angle measurement

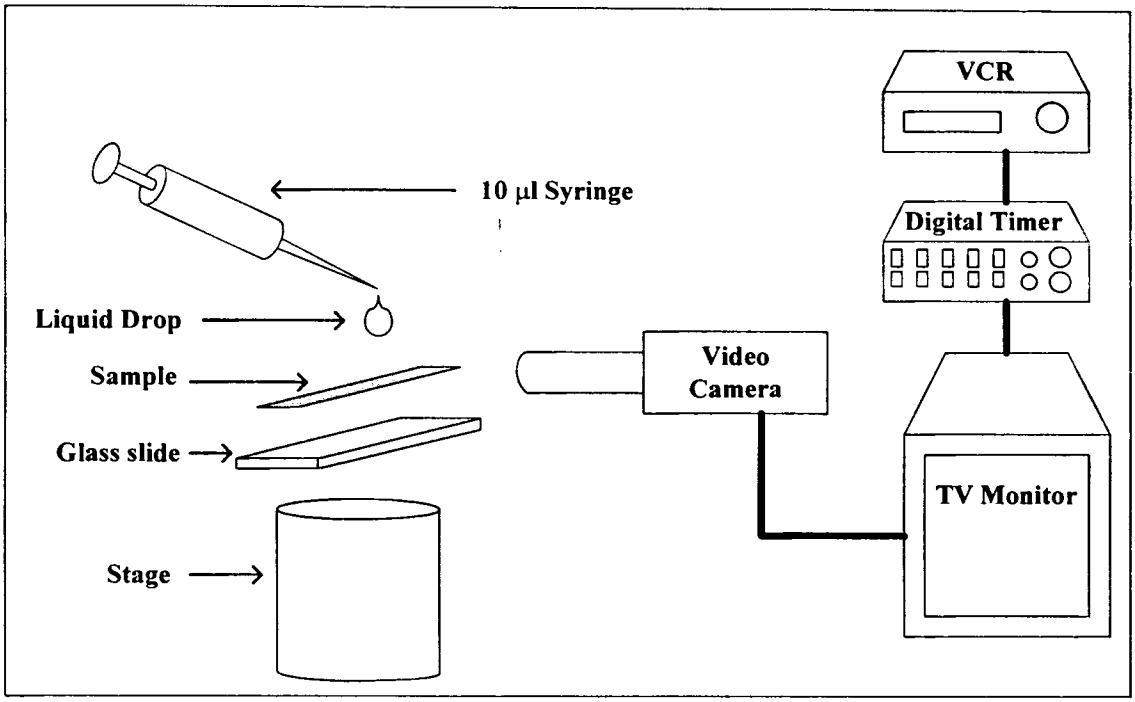

The contact angles were measured for both the left and right sides of the drop. and averaged. The average contact angle of a substrate reported is the average of a minimum of five different drop images on a substrate. Contact angles measured on either side of the film displayed similar results. The contact angle is experimentally measured as θ in Figure 7, and related to the solid and liquid surface free energies by the Young equation [64].

Equation 1. Young equation

$$\cos\theta = \frac{\gamma_{sv} - \gamma_{sl}}{\gamma_{lv}}$$

- γ_{sv} = the SFE of the solid in equilibrium with the saturated vapor of the liquid
- γ_{lv} = the surface tension of the liquid in equilibrium with the solid
- γ_{sl} = the solid-liquid interfacial free energy

Figure 7. Contact angle measurement

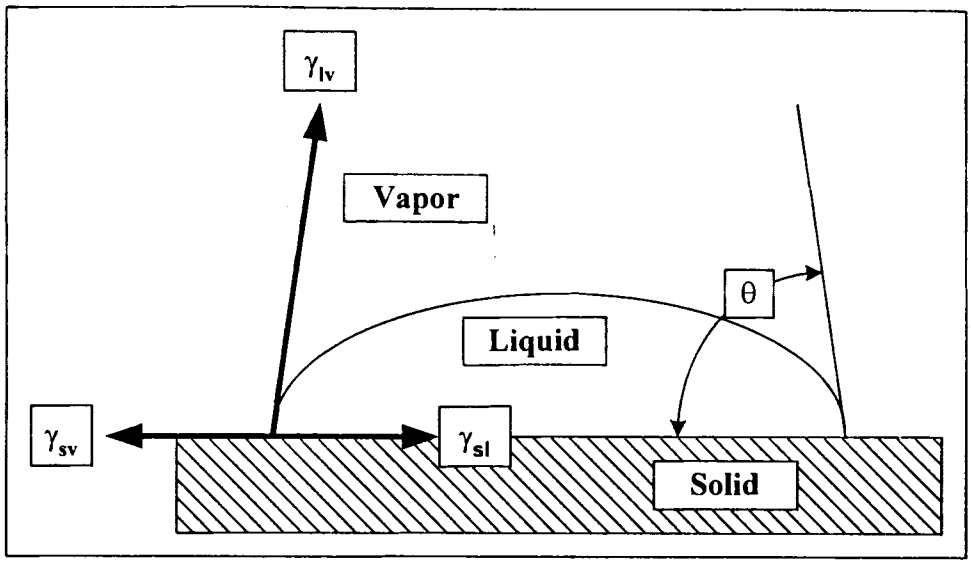

The parameters of the surface free energy of the substrate were obtained by rearranging the Young equation. The Fox-Zisman [55] principle, states that there exists a critical liquid surface tension γ_c (or γ_{lc}) for a solid s, such that for any liquid with $\gamma_l < \gamma_c$, $\theta = 0$. Good and Van Oss [64] apply this conclusion to the spreading of polar liquids on polar solids. The Young-Dupre equation, combined with Equations 3-5, yield Equation 6, a generalized equation for surface interaction of a solid and a liquid.

Equation 2. Young-Dupre equation

$$\Delta G^{a}_{sl} = -\gamma_l(1 + \cos\theta)$$

- ΔG^{a}_{sl} = free energy of adhesion between a solid s and liquid l
- γ_l = surface free energy of liquid phase in contact with its own vapor

Equation 3. Free energy of adhesion for the interface of two condensed phases

$$\Delta G^{a}_{sl} = \Delta G^{aLW}_{sl} + \Delta G^{aAB}_{sl}$$

- ΔG^{a}_{sl} = free energy of adhesion between a solid s and liquid l
- ΔG^{aLW}_{sl} = Lifshitz-van der Waals components of free energy of adhesion between a solid s and liquid l
- ΔG^{aAB}_{sl} = Acid-Base free energy of adhesion between a solid s and liquid l

Equation 4. Lifshitz-van der Waals components of free energy per unit area

$$\Delta G_{sl}^{aLW} = -2\sqrt{\gamma_s^{LW}\gamma_l^{LW}}$$

- γ_s^{LW} = Lifshitz-van der Waals components of surface interaction for solid
- γ_l^{LW} = Lifshitz-van der Waals components of surface interaction for liquid

Equation 5. Lewis acid and base components applied to the surface free energy of adhesion

$$\Delta G_{sl}^{aAB} = -2\sqrt{\gamma_s^{+}\gamma_l^{-}} - 2\sqrt{\gamma_s^{-}\gamma_l^{+}}$$

- γ_l^{+} = Lewis acid component of surface interaction of liquid
- γ_l^{-} = Lewis base component of surface interaction of liquid
- γ_s^{+} = Lewis acid component of surface interaction of solid
- γ_s^{-} = Lewis base component of surface interaction of solid

Equation 6. Generalized Young-Dupre equation for SFE components of a liquid on a solid

$$\gamma_l(1+\cos\theta) = 2\sqrt{\gamma_l^{LW}\gamma_s^{LW}} + 2\sqrt{\gamma_l^{+}\gamma_s^{-}} + 2\sqrt{\gamma_l^{-}\gamma_s^{+}}$$

All of the surface tension parameters for distilled water, ethylene glycol and glycerol have been characterized by Good and van Oss [64] and are included in Appendix C. The three liquids provide three equations with which the unknown surface interaction parameters for the chitosan films can be determined. Mathcad 2001 Professional software was used to solve the system of three equations for the chitosan film parameters.

The overall surface free energy of a solid (γ_s) is the combination of the Lifshitz-van der Waals component and the Lewis acid/base components of surface interaction and is shown in Equation 7 [64].

Equation 7. Surface free energy of a solid

$$\gamma_s = \gamma_s^{LW} + 2\sqrt{\gamma_s^{+}\gamma_s^{-}}$$

3.2.5. Degree of Deacetylation

The DDA is an important characteristic of chitosan. The DDA is a measure of the percentage of deacetylated amine groups on a polysaccharide. The behavior of chitosan is partially dependent on the DDA, and it influences the overall charge density of chitosan solutions, films, and 3-D matrixes. The DDA also defines the difference between chitin and chitosan, with chitosan generally having a DDA greater than 50% [177].

FTIR spectrometers record the interaction of IR radiation with a sample, measuring the frequencies at which the sample absorbs the radiation and the intensities of the absorptions. Determining these frequencies allows identification of the sample's chemical make-up, since chemical functional groups are known to absorb radiation at specific frequencies. The intensity of the absorption is related to the concentration of the component. Intensity and frequency of sample absorption are depicted in a two-dimensional plot called a spectrum. Intensity is generally reported in terms of absorbance, the amount of light adsorbed by a sample, or percent transmittance, the amount of light that passes through it. Frequency is usually reported in terms of wavenumbers. Samuels [198] indicated that the DDA of chitosan samples did not significantly influence changes in the FTIR spectrum of chitosan films. Conversely, the DDA does effect the relative intensity of adsorption bands for specific chemical groups present such as primary and secondary amides.

Three samples of ChitoClear chitosan with varying degrees of deacetylation were generously donated by Bjarte Langhelle of Primex Ingredients ASA (Norway). The samples had DDA's of 98.4% (batch no; TM 793), 97.6% (batch no: TD 012) and 96.1% (batch no: TM 761) and were characterized by a titration method, in house by Primex

Ingredients ASA. All samples were made from fresh shrimp shells. High molecular weight chitosan (Lot # 04919KU) was obtained from Aldrich Chemical Company (St. Louis, MO). The Aldrich chitosan has an approximate molecular weight of 600,000 g/mol, has an 85% minimum degree of deacetylation, and is in the form of white to tan powder and flakes, prepared from crab shells. The DDA of the Aldrich chitosan was determined from the calibration curve obtained with the ChitoClear samples.

The DDA of the chitosan used for film formation was characterized using FTIR. Chitosan films, cast according to previous methods, were cut into 15 x 15 mm pieces and loaded into a sample container. The testing equipment was a BOMEM MB Series FTIR machine. This machine utilized the BOMEM Grams/32 software for data analysis. Each test utilized 100 scans of the sample. Three ChitoClear chitosan samples (Primex Ingredients, ASA) with known DDA's were used to establish a calibration curve of absorbance versus degree of deacetylation. The % DDA of the Aldrich chitosan sample is estimated based on this curve.

Three methods were employed to estimate the DDA of the Aldrich, high molecular weigh chitosan. Method #1 was based on a technique described by Muzzarelli [157], and utilizes the ratio of the secondary amide stretch assigned at1540 cm^{-1} to the double-band C-H stretch assigned at 2880 cm^{-1} to create a calibration curve. Samuels assigned the adsorption band at 1540 cm^{-1} to the secondary amide [198]. The area of absorbance of the C-H stretch was determined by drawing a baseline from 2990-2785 cm^{-1} and the area of the secondary amide stretch was similarly estimated between 1740-1490 cm^{-1}. The % DDA of the Aldrich chitosan sample was then estimated using the linear fitted equation of the calibration curve.

Method #2 is the base-line method described by Moore and Roberts [146]. This method uses equation X to estimate the %DDA of chitosan samples.

Equation 8. Base-line method for the determination of degree of deacetylation of chitosan

$$\%N - deacetylation = \left(1 - \frac{A_{1655}}{A_{3340}} * \frac{1}{1.33}\right) * 100$$

- A_{1655} = maximum value of the absorbance peak at 1655 cm^{-1} assigned to the secondary amide stretch, representing the acetylated amines on chitosan
- A_{3340} = maximum value of the absorbance peak at 3340 cm^{-1} assigned to the primary amine stretch, representing the deacetylated amine groups on chitosan

Method #3 is a modified method of the base-line technique. The ratio of the maximum absorbance peaks of the A_{3340}:A_{1655} bands were plotted versus wavenumber to establish a calibration curve with the characterized chitosan samples. The % DDA of the Aldrich chitosan sample was then estimated using the linear fitted equation of the calibration curve.

3.3. Results and Discussion

3.3.1. Two-Dimensional Film Formation

The results of the characterization of physical and chemical properties of 2-D chitosan films are presented in the subsequent sections of this chapter. Viscosity appears to increase exponentially with increasing chitosan concentration. A common method for the determination of a polymers molecular weight is with the Mark-Houwink equation.

Equation 9. Mark Houwink equation

$$[\eta] = K_m \times M^a$$

- K_m = viscometric constant
- M = molecular weight
- A = viscometric constant

The viscometric constants are independent of the relative molecular mass over a wide range, but depend on the solvent, temperature, chemical structure of the polymer. When considering a polyelectrolyte such as chitosan, these constants also depend on the amount of chitosan present [130]. Thus, since the samples all had approximately equal molecular weights, we expect to see an exponential relationship between solution viscosity and concentration. The solution viscosity was an important characteristic, which related to the ease by which films were cast and subsequently detached from supports. The chitosan solution viscosities are presented in Figure 8. The 1.5% and 3.0% chitosan solutions with high viscosities were easily detached from supports, whereas the 0.5% chitosan solution resulted in a very delicate film, which was more difficult to completely detach from supports. Figure 8 represents a minimum of 4 viscosity tests for each sample.

Figure 8. Viscosity of chitosan solutions

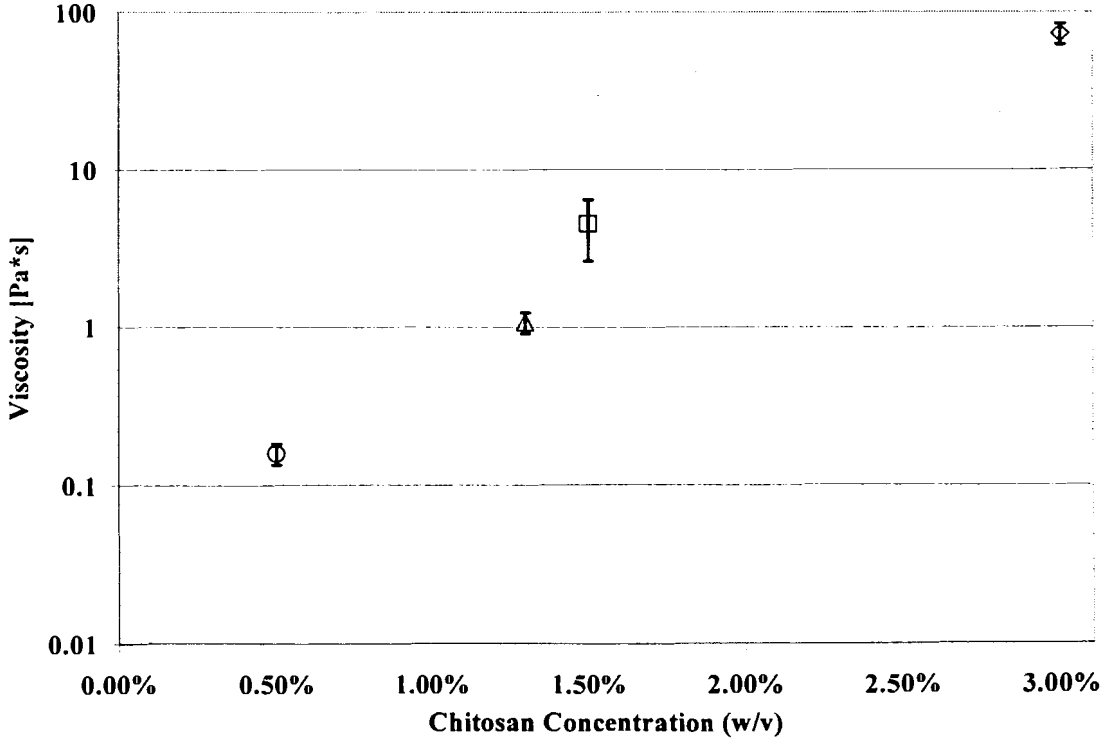

Chitosan films from 0.5% to 3.0% (w/v) were successfully cast onto glass supports to form thin, flexible, and transparent films. All films were mixed into a 1.5% (v/v) acetic acid solvent. The maximum concentration of chitosan dissolvable in a 1.5% solvent was approximately 3.0% (w/v). The 3.0% chitosan mixture was very viscous and more difficult to manipulate than the lower concentrations. The higher concentration chitosan films were stronger and easier to handle than the fragile 0.5% chitosan film, as indicated by the ease of detachment of the film from the support. Because of the thicker and stronger films at higher concentrations, the 3.0% chitosan films cast onto groove Lexan were the only films successfully detached intact from the grooved support.

3.3.2. Film Tensile Properties

The tensile properties of the chitosan films give an understanding to the mechanical properties of the films, as well as a measure of the reproducibility of the film-formation technique. The results of the tensile properties and standard errors of the varying concentration chitosan films are summarized in Table 1. Each result represents the average of two samples, each with a minimum of 10 measurments.

The thickness of the chitosan films increases with increasing concentration. This is to be expected, as films were cast with equal solution volumes over equal areas. Therefore, the amount of chitosan in each film increases with increasing concentration. Also, the thickness of the 0.5% and 3.0% chitosan films agreed with very low variability between samples as indicated by the standard error which is less than 5% of the mean for the 0.5% films and less than 2% of the mean for the 3.0% films. The 1.5% films varied slightly more in thickness than the other concentration chitosan films, with the standard error at about 15% of the average thickness. It is unclear why the 1.5% film displayed a higher

variability in thickness. One possible reason for the variability in the thickness of the 1.5% chitosan films may be because these films were produced earlier in the project, and the protocol was not as refined as for later film production. Also, the glass support on which the films were cast might not have been completely leveled, resulting in an uneven film. These results confirm that the 0.5% and 3.0% chitosan films were cast in a manner, that resulted in a reproducible film thickness.

Table 1. Summary of tensile properties of chitosan films

Tensile Property	0.5% (w/v) Chitosan Film	1.5% (w/v) Chitosan Film	3.0% (w/v) Chitosan Film
Thickness [mm]	0.012 ± 0.0005	0.02 ± 0.0031	0.038 ± 0.0005
Young's Modulus of Elasticity [Mpa]	4240 ± 80	5220 ± 160	4290 ± 110
Strain to Failure [mm/mm]	0.011 ± 0.001	0.020 ± 0.002	0.027 ± 0.002
Yield Stress [Mpa]	39.8 ± 0.3	56.5 ± 5.9	54.0 ± 1.0
Elongation [%]	1.74 ± 0.03	1.59 ± 0.02	3.11 ± 0.03

Yield stress and strain to failure also increase with increasing chitosan concentration. The standard error for the yield stress of the 1.5% chitosan film is very high. This implies that there were large variations in the physical properties of this film. The variation in the film thickness may be one of the causes for this variation. Also, some of the 1.5% film specimens broke near the grips of the Instron tester. The tension tests should only be considered valid if the sample breaks towards its center. The standard error for the yield stress of both the 0.5% and 3.0% chitosan films is acceptable and below 2%. The standard error of the strain to failure measurements is below 10% for

all chitosan concentrations. This indicates that the 1.5% chitosan films were quite different in terms of their tensile properties with respect films of higher or lower concentration.

The Young's modulus of elasticity of the 0.5% and 3.0% chitosan samples are very similar. The standard error in these measurements is below 3% of the mean value, which is an acceptable value. The Young's modulus of elasticity of the 1.5% chitosan films is indicated to be much higher than that of the 0.5% and 3.0% films. This further indicates that there was significant variance in the properties of the 1.5% chitosan samples. These data do not agree with that of Kienzle-Sterzer and others[106], who indicated that the Young's modulus of elasticity should increase with increasing chitosan concentration. However, the preparation and testing procedures of Kienzle-Sterzer differed somewhat from those utilized here. First, chitosan films were dried at a higher temperature. Second, tension experiments were performed on chitosan samples that were immersed in deionized water at room temperature. Therefore, the results presented here are not directly comparable to those published by Kienzle-Sterzer. Conversely, Mima and coworkers[142] characterized both the wet and dry tensile properties of chitosan films. They found an increase in wet tensile strength with increasing *N*-acetylation and no correlation in dry tensile strength and *N*-acetylation. Although this study did not consider the relation to chitosan concentration, there was still no observable trend in the dry tensile strength with various degrees of *N*-acetylation, partially confirming our observations.

Finally, disregarding the 1.5% film due to the high variability in other tensile properties, the percent elongation of the chitosan films increases from 0.5% to 3.0%. This might be explained by the greater thickness of the 3.0% chitosan films compared to

the 0.5% films. These results illustrate that the 0.5% and 3.0% chitosan films were formed with reproducible tensile properties. The 1.5% film exhibited high variability in most of the tensile parameters investigated.

3.3.3. Surface Roughness of Films

The roughness of the chitosan films cast on the glass support are summarized in Figure 9. The films cast on the glass support have similar values of roughness regardless of chitosan concentration. The Ra of the 0.5% and 1.5% films are about 250 nm, with very low variation between samples. This low error is indicative of good reproducibility of Ra between samples of equal concentrations, as well as reproducibility in film-formation technique.

Figure 9. Roughness of chitosan films versus chitosan concentration

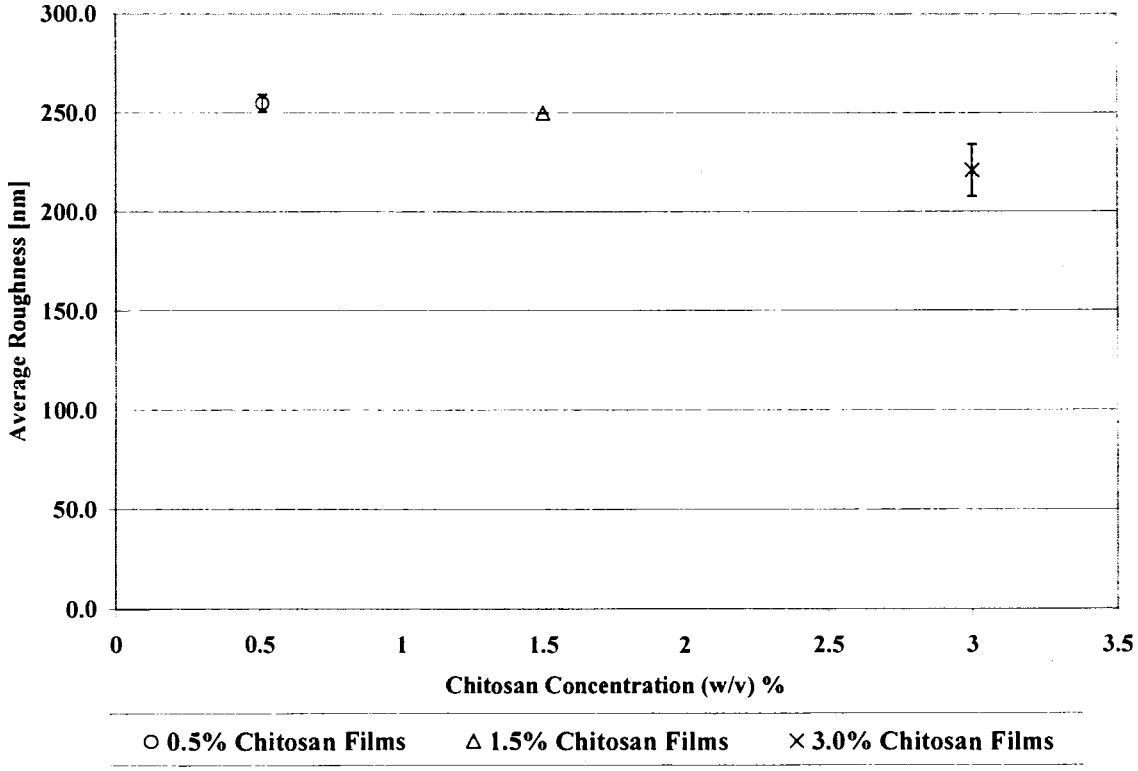

The Ra of the 3.0% film is slightly lower than that of the lower concentration films, at 220 nm. The roughness values of all concentration films increased approximately 200 nm due to the testing procedure with double-sided tape. The films were not easily tested when not securely attached to a substrate such as tape, but the few films tested which were directly attached to a completely smooth surface exhibited Ra values on the order of 10-40 nm. Because to the thicker nature of the 3.0% films, the effect of the tape may not be as pronounced as on lower concentration films. However, the increase in Ra appears relatively constant for all film concentrations. The error in the roughness of the 3.0% films is also much greater than that for the lower concentration films, although still acceptable at less than 6% of the mean roughness for this film. The higher error in this value is most likely because the higher concentration chitosan film contained more entrapped air than the lower concentration films. When air was removed from the solution under a vacuum before casting, the casting process introduced air into the 3.0% solution. A larger vacuum container might be employed to remove any entrapped air from samples after casting onto the glass support. The polystyrene controls were completely smooth, as indicated by Ra values of 0.

The Ra of all of the chitosan films cast onto glass supports is much lower than the dimensions shown to affect cellular function (1-10 μm), as discussed in Chapter 2. Therefore, the Ra of these films was assumed to have little or no effect on cell culture experiments and the films were considered smooth. The smooth support also afforded an easy detachment of cast films from the support.

Of the three film concentrations studied, only the high-viscosity 3.0% (w/v) chitosan films were successfully detached from the Lexan support with machined grooves.

Horizontal grooves were spaced approximately every 250 μm. The film side in contact with the lexan had an average Ra of 11.8 ± 0.4 μm, with vertical grooves averaging 40 ● 2.2 μm . The film exposed to air had a smoother average Ra of 3.1 ± 0.4 μm with vertical grooves averaging 7.5 ± 0.3 μm. The lower limit on horizontal groove spacing dimensions using the machining method described in section 3.2.1 was 250 μm. Using a more precise cutting tool and a support material with better machinablility can further reduce this dimensional spacing. The vertical groove dimensions are on the scale of those suspected to influence cellular processes of attachment, spreading and growth. The Lexan is a poor polymer to use for this application. It was utilized for its availability and as a test material to determine the magnitude of grooves machinable into a support. Lexan cannot be autoclaved for sterilization. Also, the cutting tool chipped the Lexan during machining, resulting a rougher surface with higher variability. The cutting debris remained attached to the Lexan in many places, and inhibited the detachment of 0.5% and 1.5% chitosan films. It appeared that the films were retaining some of these debris after detachment. The lower concentration films were constantly tearing, and remained attached to the Lexan. A metal such as aluminum or stainless steel has better machinability, and may result in a support with little to no debris attached remaining after machining. It is important that the microscopic properties of the support are smooth to aid in the detachment of the film from the substrate.

3.3.4. Surface Free Energy Estimation by Contact Angle Measurement

Images of contact angles for each liquid used to estimate the SFE of substrates on a 0.5% chitosan film are depicted in Figure 10. The WIA contact angles on all substrates and films were lowest for ethylene glycol, and highest for water. The numbers present in

the upper left hand corner of each image represent the elapsed time in seconds that the drops have been in contact with the chitosan film.

Figure 10. Contact angles of various fluids on 0.5% chitosan film

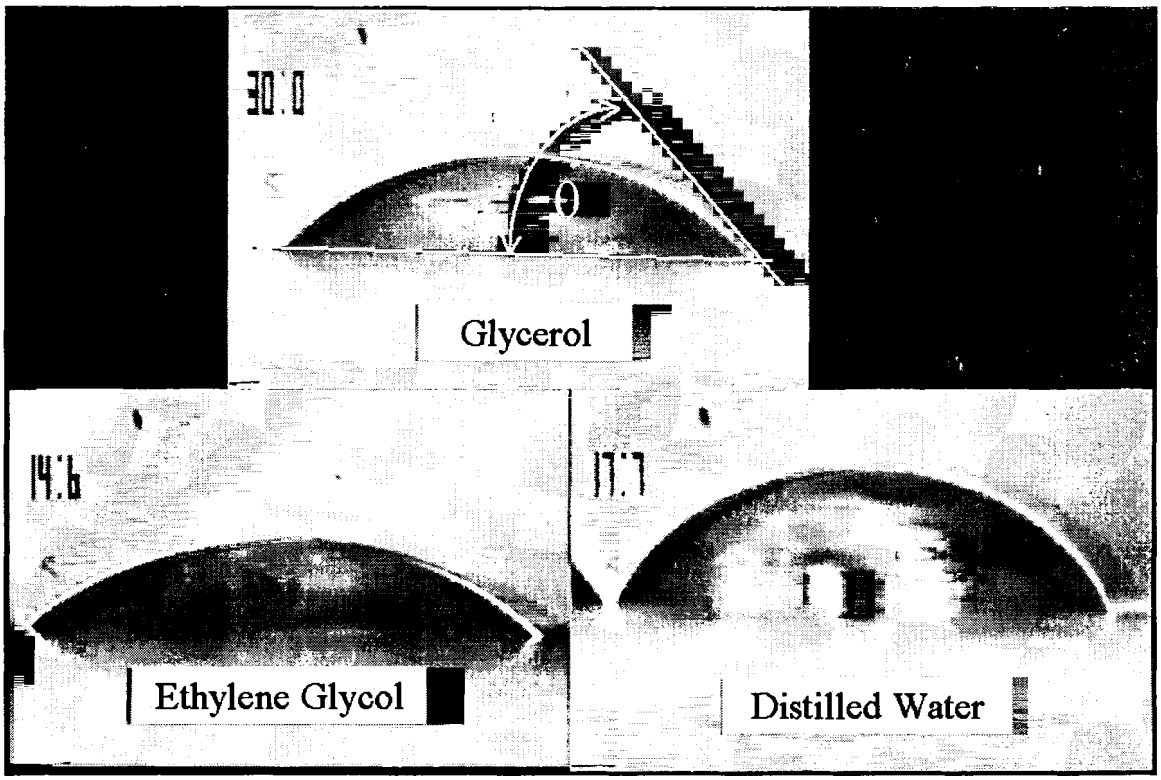

Summaries for WIA contact angles and surface free energies of chitosan films before UV-IR sterilization and polystyrene controls are depicted in Table 2. Each data point is the average of four tests on two films cast at different times, with each test representing a minimum of 5 contact angle measurements at various points on the substrate.

The polystyrene controls have moderate wettabilities, as illustrated by the WIA contact angles of 75.6 and 73.2 degrees for the tissue-culture-grade polystyrene and untreated polystyrene, respectively. These values agree with the data of previous studies [211] [197]. These studies indicated that cell culture substrates with WIA contact angles

between 60 and 90 degrees displayed improved cell adhesion compared to substrates with other WIA contact angles. Furthermore, all of the chitosan films also have WIA contact angles in this optimum range. This indicates that our chitosan films should support cell attachment. Each result is the average of two tests, with 20 test points per test.

Table 2. Summary of WIA contact angle and SFE of substrates

Sample	Water-in-Air Contact Angle (Degrees)	Surface Energy γ_s (mJ m^{-2})
Treated polystyrene multiwell tissue-culture dish	**75.6 ± 0.4**	**37.4 ± 1.7**
Untreated polystyrene petri dish	**73.2 ± 0.3**	**48.4 ± 0.9**
0.5% (w/v) chitosan in 1.5% (v/v) acetic acid (No UV-IR treatment)	**73.2 ± 2.7**	**41.5 ± 4.2**
1.5% (w/v) chitosan in 1.5% (v/v) acetic acid (No UV-IR treatment)	**80.3 ± 5.2**	**36.4 ± 11.2**
3.0% (w/v) chitosan in 1.5% (v/v) acetic acid (No UV-IR treatment)	**76.0 ± 1.8**	**36.5 ± 4.7**

Studies have also shown that cell culture substrates with SFEs greater than 55 mJ/m^2 will support better fibroblast spreading than those with SFEs below 30 (mJ/m^2) [211] [197]. The SFE of the chitosan films and polystyrene controls are in a range shown to support fibroblast attachment by Tamada and Ikada[214] and Saltzman[199] indicating that these substrates should support fibroblast spreading to a lesser extent than substrates with SFE's greater than 55 mJ/m^2. All concentration chitosan films have WIA and SFE values in a range shown to promote fibroblast attachment and spreading[211] [197]. The WIA contact angle of chitosan films indicates these films should support fibroblast attachment to a similar extent as the polystyene controls. The SFE data indicates that the fibroblasts should spread to a lesser extent than polystyrene controls. Interestingly, the SFE of the

tissue-culture grade polystyrene is lower than that of the untreated polystyrene and the 0.5% chitosan film. The untreated polystyrene dish has the highest SFE at 48.4 mJ/m^2. This suggests that the untreated polystyrene may exhibit better cell spreading than the tissue-culture grade polystyrene.

The untreated chitosan films (no UV-IR sterilization) all had SFEs between 36 and 42 mJ/m^2. The errors in Table 2 represent the 95% confidence intervals for the data points. The 1.5% chitosan film has the highest error with respect to the average SFE and WIA contact angle values, which suggests that there was a higher variation in the surface properties of the 1.5% chitosan films cast at different times. Conversely, the error associated with the polystyrene controls and the 0.5% and 3.0% chitosan films is acceptably low. These results indicate that the 0.5% and 3.0% films were cast in a reproducible manner with similar properties.

The overall SFE of the chitosan films appears to be affected by the length of time for which the films were subjected to UV-IR sterilization, as indicated by Figure 11. This may be due to crosslinking induced by the UV radiation, or possibly a change in the degree of deacetylation of the chitosan films. All three concentrations of films exhibit similar trends during 24 hours of exposure to the UV-IR lamps. Each data point for all SFE/UV-IR plots represents the average of a minimum of 4 tests on two samples.

Figure 11. Surface free energy versus UV-IR sterilization for all chitosan films

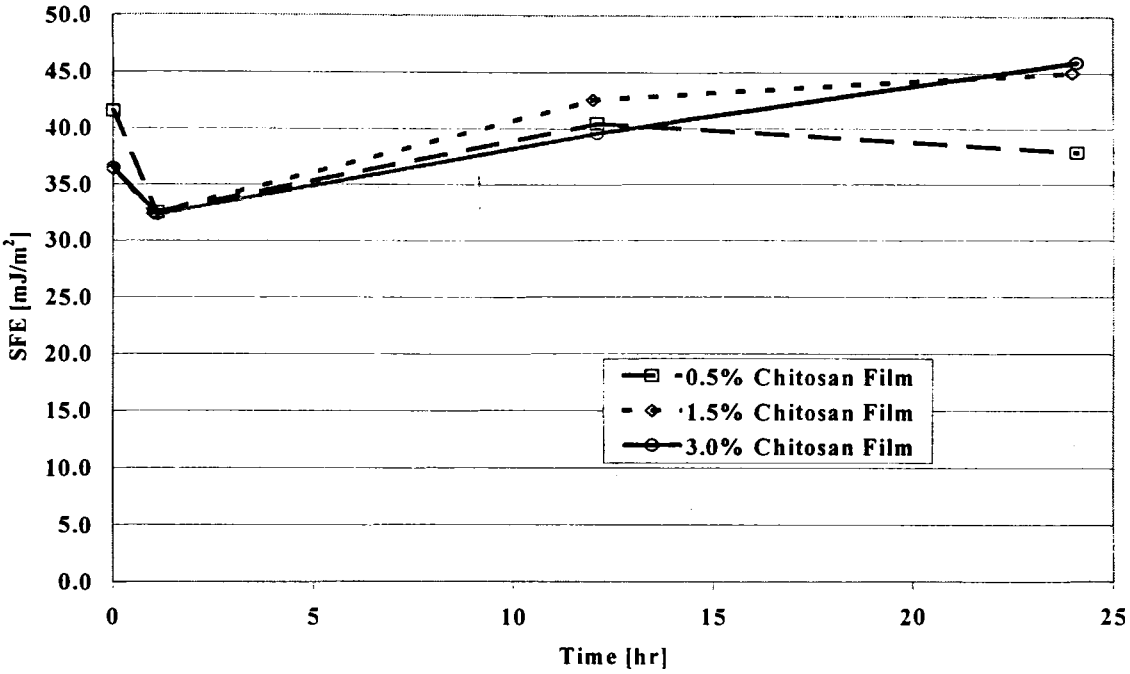

Figure 12. Surface free energy versus UV-IR sterilization for 0.5% chitosan films

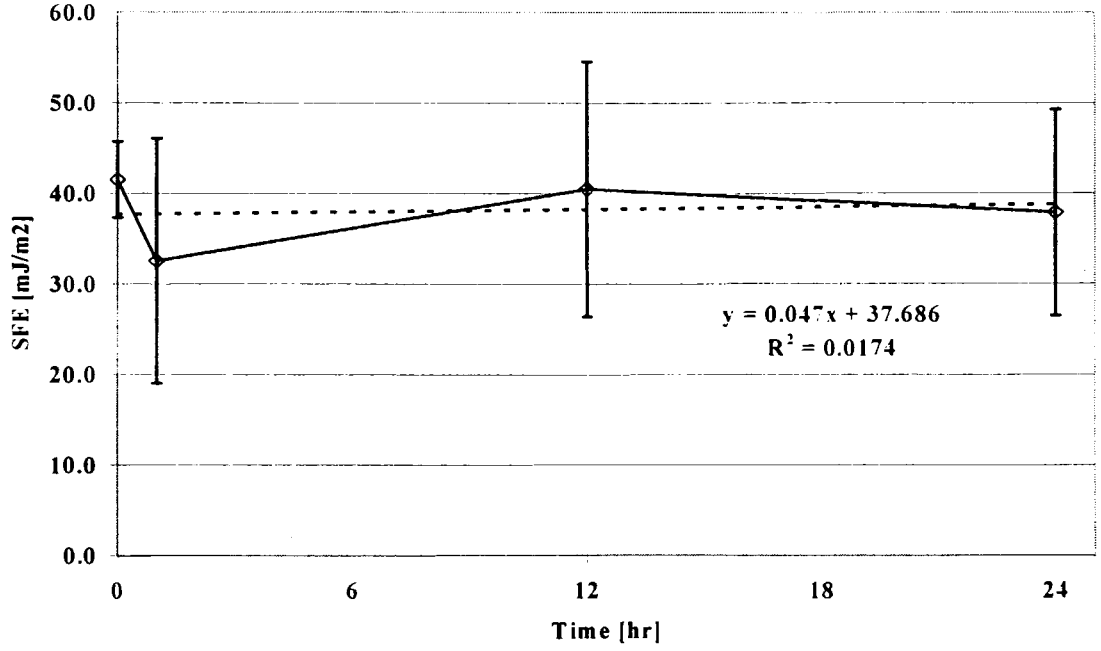

The 0.5% film SFE versus UV-IR sterilization times is depicted in Figure 12 The error bars on Figure 12 represent the the 95% confidence intervals for the mean values. There is a very slight increasing trend in the SFE over time as indicated by the linear fit in Figure 12. However, because of the confidence in the mean values of Figure 12, the effect of UV-IR sterilization on this film is considered negligible. Thus, the treatment of the 0.5% chitosan films with UV-IR doesn't appear to effect the overall SFE of the substrate. The estimation of SFE of the 0.5% chitosan films had a larger variability in average value than the 1.5% and 3.0% films and will be discussed shortly.

The SFE of the 1.5% chitosan film with UV-IR sterilization is depicted in Figure 13. The error bars represent the 95% confidence interval for each sample time. There is a clear increase in overall SFE over time for the 1.5% chitosan film. This may be due to crosslinking of the films by the UV radiation. Also, the sterilization process may be changing the DDA of the chitosan films. The increase in SFE with sterilization is indicated by the line fit in Figure 13. The confidence in the untreated SFE data point is lower than other data points, and may be increased with further testing.

Figure 13. Surface free energy versus UV-IR sterilization for 1.5% chitosan film

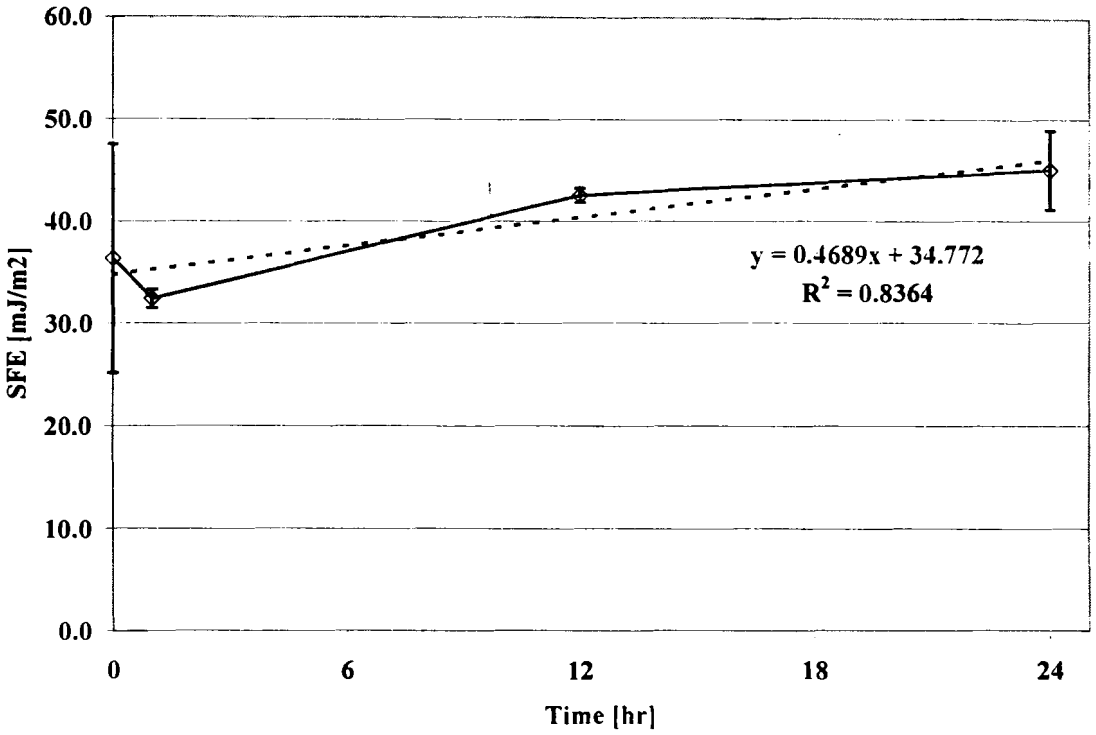

The average SFE of the 3.0% chitosan film with UV-IR sterilization and 95% confidence is depicted in Figure 14. Similar to the 1.5% film, there is a clear increase in overall SFE over time for the 3.0% chitosan film. The line fit in Figure 14 indicates the increase in SFE with sterilization. This increase may be due to crosslinking of the films by the UV radiation, or a change in the DDA of the chitosan films. Further testing on the zero and one hour time points should further reduce the error associated with these results.

Figure 14. Surface free energy versus UV-IR sterilization for 3.0% chitosan film

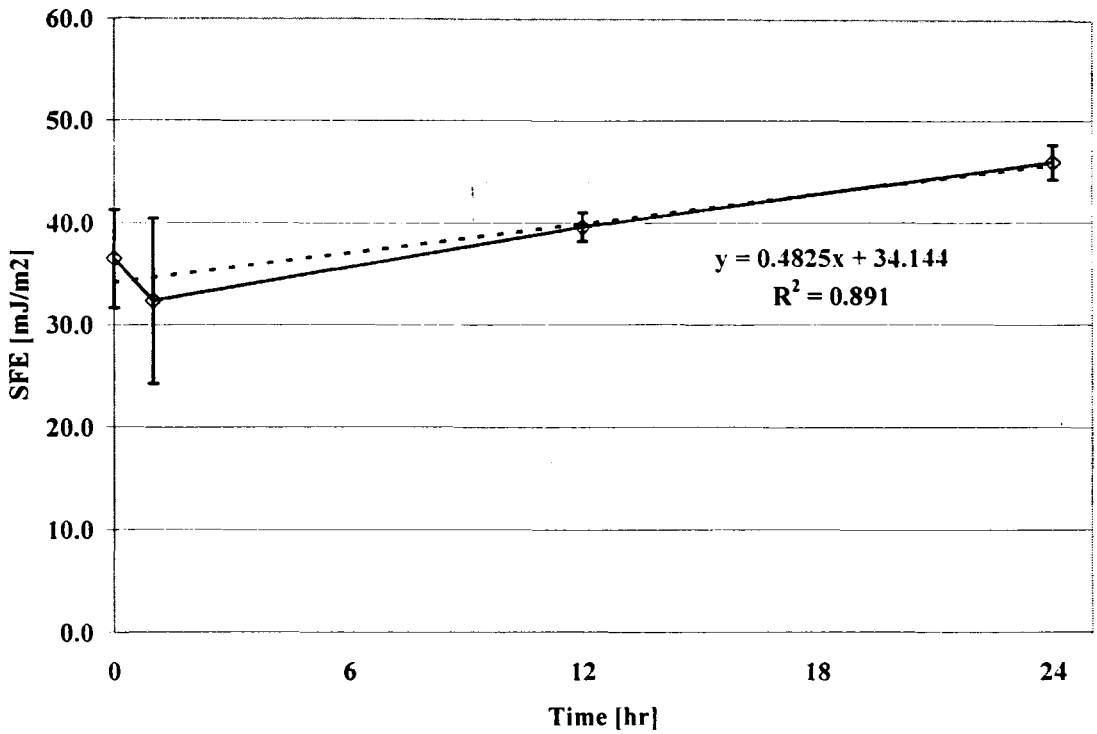

3.3.5. Degree of Deacetyaltion

The DDA of the Aldrich, high molecular weight chitosan was determined using FTIR spectroscopy. The absorption spectrum of a 0.5% chitosan film from 4000 to 600 cm^{-1} is depicted in Figure 15. The complete FTIR spectrum of the 0.5% chitosan film in Figure 15 shows characteristic adsorption bands and their respective frequency. This FTIR spectrum closely resembles that given by Pouchert for 99% *N*-acetyl-D-glucosamine [176].

Figure 15. Complete FTIR spectrum of 0.5% chitosan film

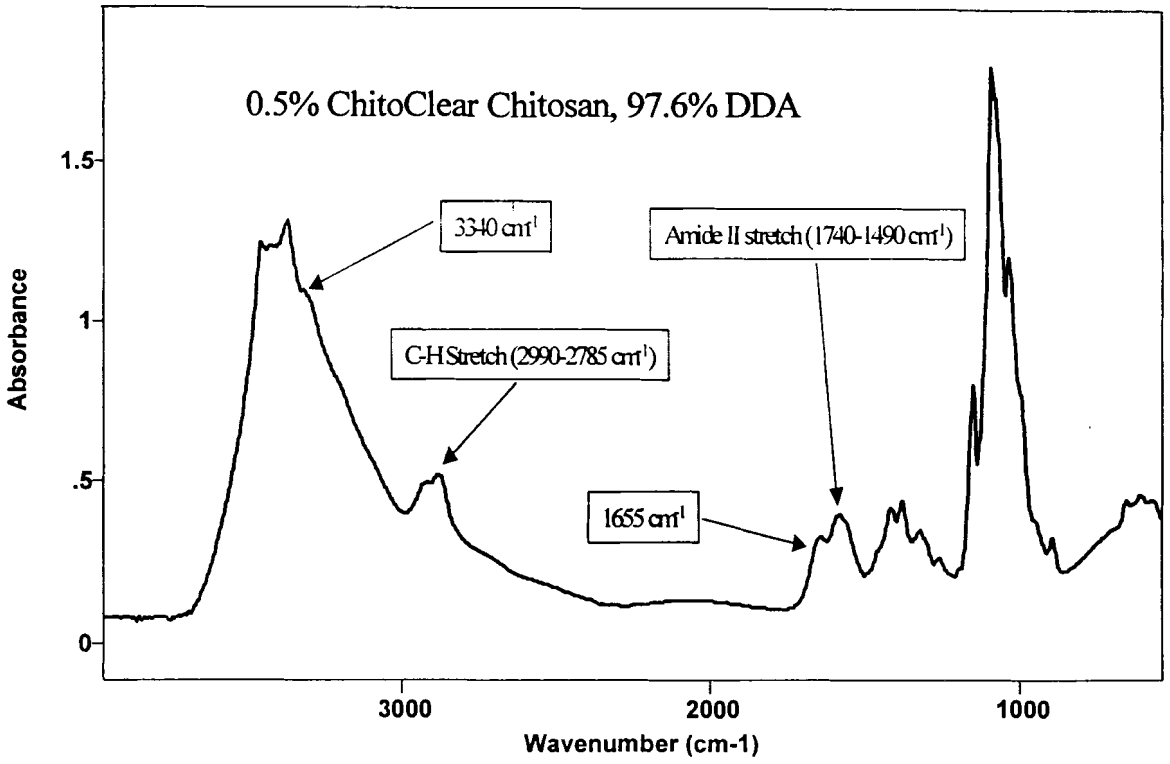

The FTIR adsorption bands used to establish the calibration curve for Method #1 are depicted in Figure 16. The C-H stretch at 2880 cm^{-1} and the amide II stretch at 1540 cm^{-1} are depicted. A noticeable difference in the size and shape of these peaks can be observed, especially with the amide stretch at 1540 cm^{-1}.

Method #2 utilizes the baseline technique used by Moore and Roberts [147], which gave very low estimates for the DDA of the known samples characterized by conductimetric titration by Primex Ingredients, ASA. Method #2 does not require the establishment of a calibration curve like methods #1 and #3, rather, it uses an intrinsic formula to estimate the DDA of a sample. This method gave a low estimate for the DDA of the 96.1% DDA sample to be 72.3%. Similarly, the 97.6% and 98.4% DDA samples

were estimated to be 77.0% and 81.1% respectively. Finally, the Aldrich chitosan, with a minimum DDA of 85% was estimated to have a DDA of 72.5% by this method. This may be due to the intrinsic constant in the formula utilized in this method. This constant may reflect chitosans prepared by a different method than the ones used in this project. Therefore, this technique was not considered accurate for the estimation of the Aldrich chitosan's DDA.

Figure 16. Partial FTIR spectrum. C-H and amide II stretches.

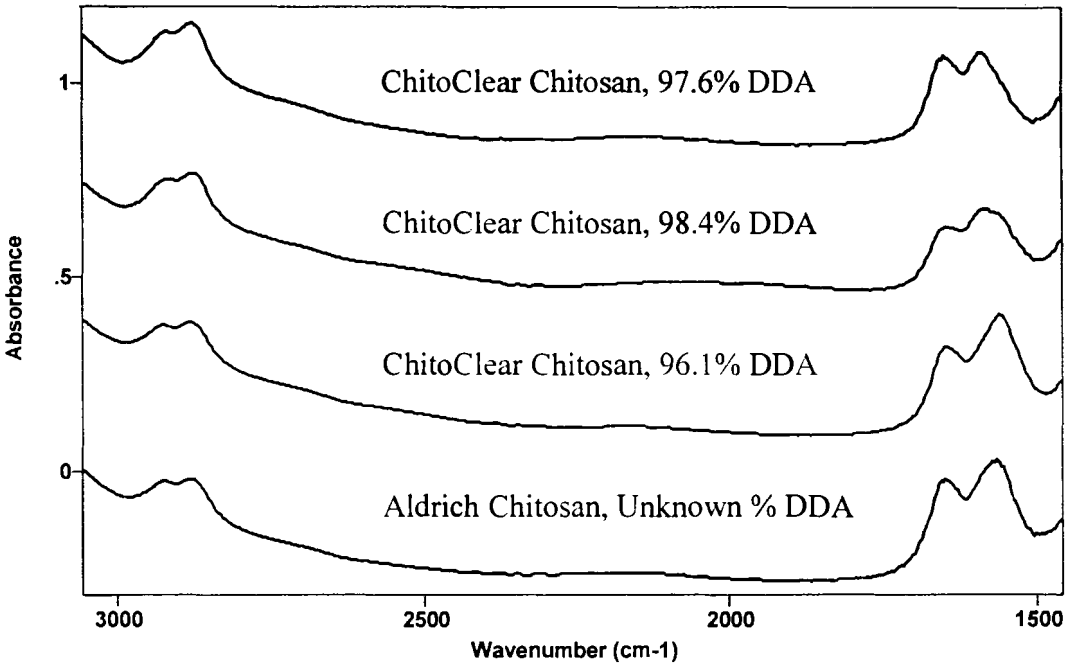

The calibration curves, established using methods #1 and #3 are depicted in Figure 17. The calibration curve established with method #3, using a modified base-line technique, gave a better linear correlation than the calibration curve established by Method #1, as indicated by the R^2 value in Figure 17. Therefore, the calibration curve for method #3 was used to estimate the % DDA of the Aldrich chitosan sample. Method

#3 closely estimates the known 96.1%, 97.6% and 98.4% DDA chitosan samples to be 96.3%, 97.3% and 98.5% respectively.

Figure 17. Calibration curves for % DDA using FTIR

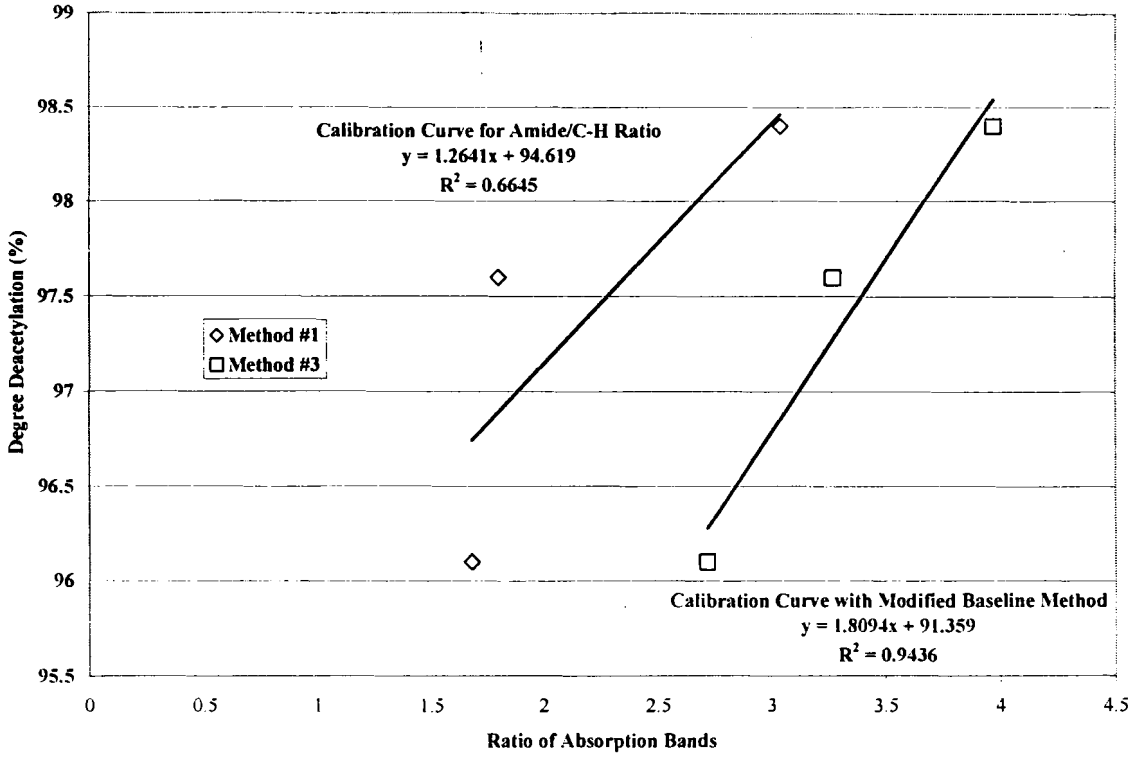

According to method #3, Aldrich chitosan is 96.3% deacetylated. This seems to be a reasonable value for the DDA of this sample, and it agrees with the in-house Aldrich testing which reports the DDA to be at least 85% as well as the determination of ChitoClear chitosan samples by Primex Ingredients, ASA. Also, the IR spectra depicted in Figure 16 are very similar for the Aldrich sample and the 96.1% DDA sample.

3.4. Conclusions

3.4.1. Two-Dimensional Film Formation

The method described for the formation of chitosan films of varying concentration is a simple and effective technique for developing 2-D chitosan films. The viscosity of the

chitosan solution increases exponentially with increasing chitosan concentration, as expected for a polyelectrolyte according to Equation 9. When casting a film onto a rough surface, a higher concentration chitosan solution gives a thicker film. A thicker films was required for the successful detachment of the intact film from the grooved surface. The Lexan was a poor support for casting films. Debris attached to the Lexan surface were taken up by chitosan films during detachment or inhibited the detachment of films by remaining attached to the Lexan surface. Although the chitosan films were desired to be pure, their characteristic of curing around support debris and subsequently retaining these debris may be employed to incorporate desired substances, such as attachment proteins into films, by casting films onto supports containing these attachment proteins. There is no visually observable change in chitosan films subjected to sterilization by UV-IR treatment.

3.4.2. Film Tensile Properties

The 0.5% and 3.0% chitosan films were cast with reproducible tensile properties as indicated by the low standard errors of the mean values in Table 1. The 1.5% chitosan film had very high standard errors for most of the film properties, and was not considered for observation of trends in tensile properties with varying chitosan concentration. One possible reason for the variability in the thickness of the 1.5% chitosan films may be because these films were produced earlier in the project, and the protocol was not as refined as for later film production. Also, the glass support on which the films were cast might not have been completely leveled, resulting in an uneven film. The dry-tested Young's modulus of elasticity of chitosan films does not show an increase with increasing chitosan concentration as previous researchers have suggested with wet films.

Another study partially confirms our observation of no trend in Young's modulus of elasticity with the dry tensile strength through testing of the degree of polymer *N*-acetylation and dry tensile strength [141]. Because of the variable tensile properties of the 1.5% chitosan films, a trend still might exist between chitosan concentration and the dry-tested Young's modulus of elasticity. The wet tensile properties of the films should also be investigated.

3.4.3. Surface Roughness of Films

The chitosan films cast on the glass support all displayed similar average roughness values. The Ra values were greater when mounted on tape for testing compared to when tested on a completely smooth surface. These Ra values were approximately one order of magnitude lower than texture dimensions shown to affect attachment, orientation and spreading. All concentration films were considered to be smooth. The solution concentration doesn't appear to affect the surface roughness of films cast on glass supports. The 3.0% chitosan films cast on lexan had parallel groove dimensions similar to those machined into the support for casting. These dimensions were on the μm scale suspected to influence cellular behavior. The average Ra values were very similar for equal concentration films with very low standard error in mean value, indicating that the films were cast in a reproducible manner.

3.4.4. Surface Free Energy Estimation by Contact Angle Measurement

The WIA contact angles of the three concentration chitosan films are in the reported optimum range of 60-90 degrees to support maximum cell adhesion[214]. All concentration chitosan films as well as polystyrene controls should support cell attachment and

adhesion based on the reported WIA contact angles. The estimated SFE of the untreated chitosan films is in a range shown to promote fibroblast spreading[203]. Thus, all of these substrates should support the adhesion and spreading of 3T3 fibroblasts.

Exposing the 1.5% and 3.0% chitosan films to UV-IR radiation for varying times can change the increase SFE of the films. This may be due to crosslinking of the chitosan films due from the UV radiation. Also, the sterilization process may be changing the degree of deacetylation of the chitosan films, which may result in an increase in the overall film SFE. These results suggest the possibility for optimizing cell spreading and growth of 3T3 fibroblasts on these chitosan films by changing the increasing SFE. Fibroblast spreading is greatest on substrates with surface energies greater than 55 (mJ/m^2)[203]. Further study of this behavior with SFE and UV-IR sterilization should include more time points between 0 and 12 hours of UV-IR treatment, as well as longer sterilization times. Experiments should be performed on films exposed to UV-IR radiation for times longer than 24 hours to determine whether the SFE of the chitosan films will continue to increase or approach an asymptotic value. Also, the effects of the UV and IR radiation should be studied separately. The treatment of films with IR radiation is not expected to significantly effect the films, because it is a low energy treatment.

3.4.5. Degree of Deacetylation

The degree of deacetylation for chitosan was characterized with FTIR measurements. The DDA of the Aldrich chitosan was best characterized using a modified baseline technique that was modeled after that outlined by Gupta and Kumar[74]. This technique gives accurate estimations of the DDA of chitosan samples. The DDA of chitosan

samples sterilized with UV-IR should be estimated with this technique to determine whether the sterilization process is affecting the DDA of the films.

Chapter 4

CELL CULTURE EXPERIMENTS

4.1. Introduction

A fundamental objective of this project is to study the interactions of NIH-3T3 fibroblasts with the 2-D chitosan films. Good interaction of fibroblast cells with a matrix biomaterial is crucial in developing tissue engineering substrates. This part of the project considered the attachment, spreading and growth of the NIH-3T3 fibroblasts on 2-D chitosan films.

4.2 Materials and Methods

4.2.1. Cell Culture

The 490N3T strain of 3T3 fibroblasts were obtained from Don Blair of the National Institute of Health (NIH) and generously donated by Dr. Rebecca van Beneden of the University of Maine. Fibroblasts were routinely cultured with Dulbecco's Modified Eagle Medium (DMEM, lot # 1084121) supplemented with 10% calf serum (CS, lot # 1060198), 100 U/100 μg penicillin/streptomycin (100 U/100 μg Pen-strep lot # 1079370), all obtained from Life Technologies (Grand Island, NY). Sterile, tissue-culture-grade, Falcon T-25 (25 cm^2) flasks were obtained from VWR Scientific (Bridgeport, NJ). These polystyrene flasks are plasma-treated by surface activation, which introduces oxygen or nitrogen gas to the polystyrene to increase its hydrophobicity [3]. Fifteen-ml centrifuge tubes, 50-ml centrifuge tubes, and 1-ml freezer vials were obtained from VWR Scientific (Bridgeport, NJ). Dimethylsulfoxide (DMSO) used for freezing cells was obtained from Sigma (St. Louis, MO). Cells were observed with a

Hund-Wetzlar Wilovert AS phase contrast microscope. Cells were incubated in a Forma Scientific CO_2 water jacketed incubator (model no. 3110). Manual cell counts were performed with a hemacytometer (Leavy Counting Chamber manufactured by Hausser Scientific) supplied by VWR Scientific (Bridgeport, NJ).

All work with cell culture was performed in a sterile, biological hood (Forma Scientific Class IIA/3B Biological Safety Cabinet, model no. 1284). The NIH-3T3 fibroblasts were used for experiments between passages 10-30. Fibroblasts were maintained at 37 °C in an incubator, equilibrated with 5% carbon dioxide (CO_2) and kept at approximately 95% humidity. Culture flasks allowed open-air exchange in the incubator. The CO_2 acts as a buffer, to keep the culture medium near a pH of 7.

Stock cultures were frozen according to the following procedure. Freezing medium of DMEM with 20% CS and 100 U/100 μg pen-strep was prepared. The NIH-3T3 fibroblasts were aspirated of DMEM towards the end of the exponential growth phase, while the majority of the cells were still dividing. The flasks were rinsed twice with 5 ml of sterile phosphate buffered saline (D-PBS). Cells were loosened with trypsin-EDTA and dislodged. Five ml of freezing medium was added to cell suspension and pipetted up and down two times to loosen cell clumps. Cell suspension was pipetted into a 15-ml centrifuge tube and centrifuged in a Fischer Scientific centrifuge (model MARATHON 10K) at 1000 RPM at room temperature for 3 minutes. After aspirating the supernatant, cells were resuspended in freezing medium (1 ml per flask used). Ten percent DMSO was added to cell suspension, and 1 ml of suspension was pipetted into freezing vials. Freezing vials were frozen at –30 °C and transferred to liquid nitrogen after 24 hours. Stock cultures were stored in liquid nitrogen.

Cells were thawed by rapidly by warming the freezer vial in a 37 °C water bath. A T-25 flask was supplied with 10 ml of culture medium (DMEM with 10% CS and 100 U/100 μg pen-strep). The freezer vial was then quickly pipetted into the T-25 flask with the DMEM, and cells were placed in a 37 °C incubator with 5.0% CO_2 and approximately 95% humidity.

Cells were subcultured every 4-6 days. Cell confluency was confirmed visually by observation of the culture flask with a phase contrast microscope. The old DMEM was aspirated from the culture flask. The flask was then rinsed twice with 5 ml of sterile phosphate buffered saline (D-PBS). Two ml of trypsin-EDTA was applied to the confluent layer and aspirated from the flask. After 30 to 120 seconds of addition of the trypsin-EDTA, cells were observed to begin detaching from the flask by rounding up under the microscope. Cells were detached d by gently tapping the sides of the culture flask. Immediately following the detachment, 10 ml of DMEM + 10% CS + 100 U/100 μg pen-strep is added to the cell suspension. The CS deactivates the enzymatic action of the trypsin-EDTA. The cells were then placed in an incubator as previously described.

4.2.2. Growth Cycle

The cell growth cycle is an important process in which the cell divides. The growth cycle in a batch culture consists primarily of four phases: lag phase, logarithmic or exponential growth phase, deceleration phase, and death phase. The lag phase occurs immediately following inoculation of cells to culture, and represents the time for cells to attach and spread in culture. During the exponential growth phase, the cells multiply rapidly, and cell mass and number increase exponentially. A short deceleration phase follows the exponential growth phase and is indicative of a depletion of nutrients or

slowed cellular growth due to contact inhibition at cell confluency. The stationary phase represents when cell growth is equal to cell death, and the death phase is self-explanatory.

Some important parameters to the growth of cells include the saturation density and population doubling time (PDT). The saturation density (SD) is the maximum number of cells per unit area that a given cell line can attain. The absence of a stable saturation density in a given cell line indicates that the cells have transformed from the normal cells possessing a stable saturation density. The NIH-3T3 fibroblast growth slows considerably upon reaching a confluent layer of cells while in culture due to contact inhibition. Phenomena such as anchorage dependence and contact inhibition of growth appear to be linked to integrin-mediated adhesion [202 210]. Fibroblasts, endothelial and epithelial cells all cease growth when detached from the culture substrate *in vitro*. Cell-cell adhesion molecules may mediate contact inhibition [210]. The PDT is the time required for an entire cell culture to double its number. Assuming that all cells are participating in cell division, then the PDT is a good measure of the overall metabolic efficiency of the cells. The PDT and SD are important indicators of baseline NIH-3T3 cell behavior. The growth curve of the NIH-3T3 fibroblasts was characterized from culture on tissue-culture-grade polystyrene T-25 flasks. This curve was used for the determination of the important growth characteristics of SD and PDT of the fibroblasts. These parameters were used to determine the seeding densities and sampling times of subsequent experiments on the attachment and growth of NIH-3T3 fibroblasts on chitosan films compared to polystyrene controls.

A cell growth curve was determined by counting the fibroblast density in T-25 flasks over the course of 5 days in culture, using passages 25 through 27. A growth

experiment was set up as follows. The number of cells in a confluent flask of NIH-3T3 fibroblasts was determined by trypsinizing the cells, suspending them in 10 ml medium as described earlier, and then counting them with a hemacytometer. This suspension was diluted to 4.0×10^5 cells/ml with cell culture medium as previously described. One ml of this suspension was added to each of eight T-25 flasks, and diluted to 10 ml total volume. This procedure ensured a known starting number of cells. The cells were incubated as described previously. Cell concentration was determined at 12 hours and every 24-hour interval up to 6 days after inoculation by counting cells in duplicate with a hemacytometer, as described earlier in this section.

4.2.3. Attachment Experiments

The attachment of cells to the ECM is an integral part of cell function. The faster cells attach to an ECM in culture, the more likely the cells will remain viable and proliferate. Biomaterials that can promote rapid cell attachment are desirable for cell culture applications and tissue matrices where growth is intended. To determine the suitability of solvent-cast chitosan films for cell culture, the attachment of NIH-3T3 fibroblasts onto chitosan films of three different concentrations (0.5%, 1.5% and 3.0% (w/v)) was measured using the Bradford assay and compared to polystyrene controls. A detailed procedure for the Bradford assay can be found in Appendix B. Additionally, the attachment of 3T3 fibroblasts onto 3.0% grooved chitosan films cast on Lexan was investigated.

A punch-like cutting tool was machined from a stainless steel cylinder (ID = 1-1/4 inches, OD = 1-5/16 inches). The inner diameter of the cylinder was machined to create a sharp edge. Corning six-well tissue culture plates were obtained from VWR Scientific

(Bridgeport, NJ). Untreated, sterile polystyrene dishes were Silicone O-rings were obtained from McMaster-Carr (ID = 1-1/16 inches, OD = 1-5/16 inches). Images were captured with a Minolta 35 mm SLR camera, attached to a Hund-Wetzlar Wilovert AS phase contrast microscope. Disposable untreated polystyrene petri dishes used as controls (15 x 100 mm standard) were obtained from VWR Scientific (Bridgeport, NJ).

Bradford reagent was prepared with Coomassie Brilliant Blue G (Lot # 1838A17), supplied by EM Science (Gibbstown, NJ), certified A.C.S. 85% o-phosporic acid (Lot # 001815) and certified A.C.S. methanol (Lot # 001009), both supplied by Fisher Chemical (Fair Lawn, NJ). Bovine serum albumin (Lot # 78H0696) was obtained from Sigma Chemical (St. Louis, MO) for protein standards. Sodium hydroxide pellets were obtained from Fisher Chemical (Fair Lawn, NJ).

Chitosan films were prepared according to methods given in Chapter 3. Films were sterilized by UV-IR radiation for one hour. Films made from chitosan solutions of 0.5%, 1.5% and 3.0% (w/v) concentrations were cut into 7.9 cm^2 discs using a stainless steel cutting tool. The cutting tool was autoclaved, and then wiped with 70% ethanol solution prior to use. Films were placed on a sterile Teflon support, the cutting tool was placed on top of the film, and a 2"x2"x1" stainless steel plate was placed on top of the cutting tool. Films were cut by hitting the plate with a hammer, and punching out the resulting chitosan discs.

The attachment experiment used two polystyrene controls. The first was the Corning six well tissue culture plate. This polystyrene was plasma treated to ensure hydrophobicity, and was expected to perform best with for cell attachment compared to the other control and chitosan films. The second control was an untreated polystyrene

petri dish. The set up of the attachment experiment was as follows. Sterilized chitosan films were placed into 4 of the 6 wells and held stationary with silicone O-rings. Silicone O-rings were also placed in the remaining empty wells, which were used as the tissue-culture grade polystyrene control. Finally, silicone O-rings were placed into untreated polystyrene petri dishes used as a second control. The O-rings kept the chitosan films stationary when exposed to cell culture and medium, as well as provided an experimental control for a standard area to which fibroblasts were exposed during experimentation. Experiments were assembled in six-well tissue culture polystyrene dishes according to Figure 18. The untreated polystyrene controls are not depicted. Three plates were set up for each film concentration and cell concentration was measured at 15, 30 and 60 minutes after inoculation with the Bradford assay (nine multi-well tissue-culture-grade plates per attachment experiment as well as three untreated polystyrene petri dish controls were used). In all multiwell plates, four wells of each plate were supplied with one concentration chitosan film as illustrated in Figure 18. Silicone O-rings were sterilized in an autoclave at 250 ^{o}F for 30 minutes before use with experiments. Silicon O-rings were also used as experimental controls by placing them in untreated polystyrene dishes to confine the cell growth and ensure that the experimental test areas were 5.72 cm^2 for all samples. This experimental set up was also applied to attachment experiments on grooved 3.0% chitosan films cast on Lexan.

Figure 18. Attachment experiment set up

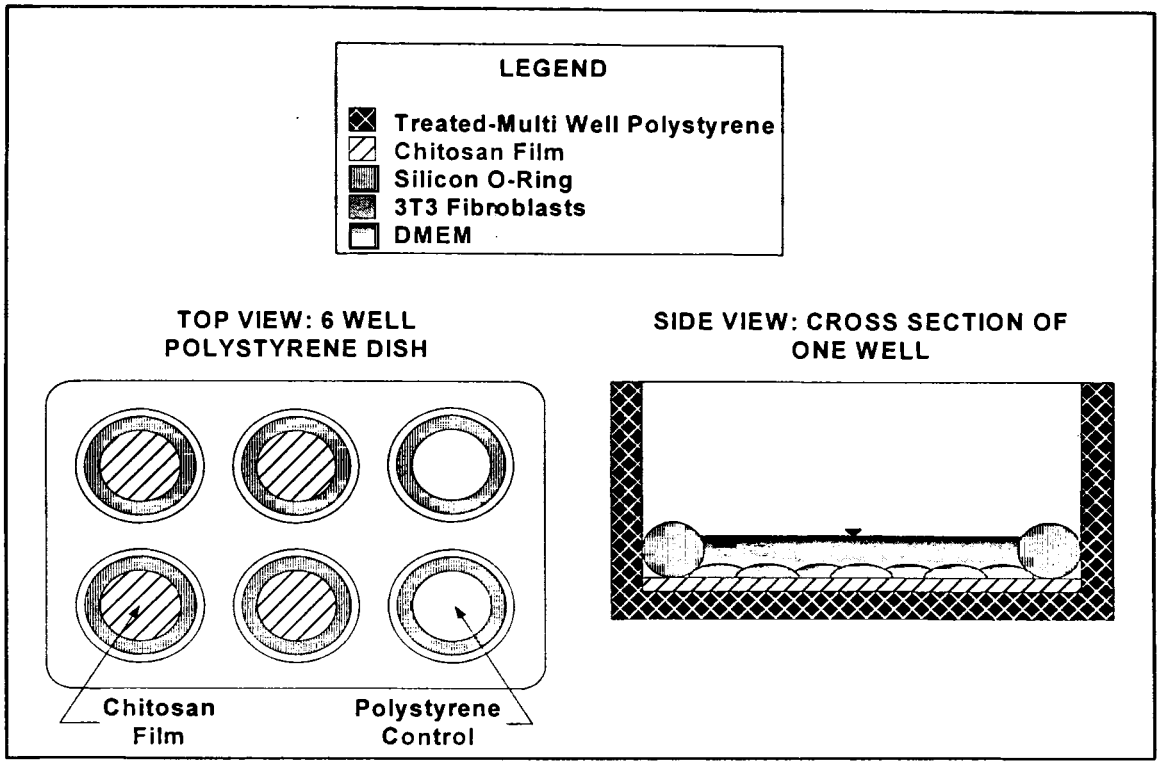

All samples were inoculated with 8.8 x 10^5 cells per dish (1.1 x 10^5 cells/cm^2) and supplemented with 2 ml total volume of DMEM with 10% CS and 100 U/100 μg pen-strep, then placed in a 37 °C incubator with 5.0% CO_2 and approximately 95% humidity. This cell density is near the saturation density of the NIH 3T3 fibroblasts on a tissue culture grade polystyrene and is easily detected with the Bradford assay. At sample times of 15, 30 and 60 minutes after inoculation, samples were removed from the incubator. The DMEM was aspirated and the silicon O-rings removed from the samples, and the number of cells that remained attached to the chitosan films or controls was counted according to the following procedure. The samples were rinsed twice with 2 ml of sterile D-PBS to remove any unattached cells and media. Cells were loosened from the surface by adding 1 ml of trypsin-EDTA and gently tapping the sides of the sample dishes or

plates. Cells were then suspended in 1 ml DMEM with 10% CS and 100 U/100 μg pen-strep.

Cells were recovered and quantified by a total protein determination. The total protein concentration is proportional to cell concentration and is a commonly used method to determine cell number with a standard plot of cell number versus protein content. Each sample was transferred to a 15-ml centrifuge tube, and samples were centrifuged at 1000 RPM for 3 minutes. The supernatant was aspirated and the cells resuspended in 2 ml sterile D-PBS. The cells were again centrifuged at 1000 RPM for 3 minutes and the supernatant aspirated to remove proteins present in the calf serum in which the cells were originally suspended. The cell pellet was dissolved in 0.5 ml of 0.3 N NaOH solution, to lyse the cells and create a protein suspension. The total protein concentration of each sample was measured in duplicate using the Bradford assay by spectrophotometry. A calibration curve was established using BSA standard solutions from 0 to 2000 μg/ml. The absorbance of the standards and samples was measured at 595 nm.

The total cell concentration of samples was correlated to the total protein content of the solubilized cell pellets with the Bradford assay, which is currently one of the most widely used protein assays [57]. Protein content is widely used to estimate total cell concentration and can be used in cell growth experiments. Protein content can also be used to determine the expression of specific enzyme activities, ligand receptor content, or intracellular metabolite concentrations. The majority of the cellular proteins come from nucleic acids, and other protein sources are negligible. Colorimetric assays use a chemical reaction that produces color to identify molecules. The Bradford assay uses a

reaction with Coomassie Blue, which binds to proteins. Coomassie Blue undergoes a spectral change on binding with proteins in an acidic solution, which can be measured with spectophotometry at 595 nm. The Bradford assay was used because it is more sensitive than the commonly used Lowry assay, and is independent of aromatic amino acid frequency in the protein. A calibration curve was established by solubilizing various known cell concentrations (determined by a hemacytometer count) and determining the total protein content of these lysed cell suspenstions. These protein concentrations were then correlated to a standard BSA protein concentration to establish the calibration curve. The calibration curve is depicted in Appendix B. For attachment experiments, cell pellets were dissolved in 0.3 N NaOH at room temperature for 1 hour. Standard BSA solutions were prepared from 0 to 2000 μg/ml and used to establish a standard curve. Then 2 ml of Bradford assay reagent was added to a 10 ml glass test tube. Solubilized cell solutions were vortexed at 70% maximum speed for 1 minute, and then 40 μl of this solution was added to the Bradford assay reagent. The contents of the test tube were then emptied into a 4 ml disposable cuvette. This act of pouring the solution from the glass tube to the cuvette mixed the reagent and the protein solution. The absorbance of the samples was recorded at 595 nm in a spectrophotometer at room temperature. The cell concentration was estimated from the calibration curve of cell concentration versus total protein concentration.

4.2.4. Growth and Spreading Experiments

For tissue regeneration to be guided by implanted materials, the matrix material must support cell growth. It is possible for cells to attach to surfaces, but not grow. The growth experiments conducted as part of this study aimed to determine how well chitosan

films support the growth of NIH-3T3 fibroblasts. The rate of NIH-3T3 fibroblast growth on two controls and three concentration chitosan films was measured with the Bradford Assay. The controls included untreated polystyrene and tissue-culture-grade polystyrene. Additionally, the extent to which the fibroblasts will spread on chitosan films of varying concentration was observed and photographed.

Chitosan films, polystyrene tissue culture flasks and petri dishes utilized for the NIH-3T3 growth experiments were the same as those described in the attachment studies. The experimental set-up for the growth experiment was similar to that for the attachment experiment with the following exceptions. First, the cells were inoculated at a lower density of 6.0×10^4 cells/dish compared to the 8.8×10^5 cells/dish for attachment experiments. This initial inoculation density was chosen because it was towards the detection limit of the Bradford assay used to determine the total protein content of cell suspensions. At this lower cell density the cells have room to grow without contact inhibition. Second, more multi-well dishes and untreated polystyrene controls were set up for each concentration chitosan film with the growth experiments than for the attachment experiments, because more time-point measurements were made. Measurements were taken at 12 hours, 1, 2, 3, and 4 days in culture. Based on the population doubling time of 21.4 hours, the fibroblasts should achieve the saturation density of 1.17×10^5 cells/cm^2 within 4 days. Two time-point measurements were performed within the first 24 hours of inoculation to study the initial attachment and growth of the fibroblasts. Culture media was changed every other day.

For fibroblast spreading characterization, images were captured with a Minolta 35 mm SLR camera, attached to a Hund-Wetzlar Wilovert AS phase contrast microscope.

Pictures were taken of the fibroblasts on the polystyrene controls and chitosan films at 12, 24, and 48 hours of the growth experiments. The microscope was set at 20X magnification, and the shutter speed of the camera was automatically set, usually between 1/60-1/125 seconds depending on the external lighting. Each picture presents a unique film and area of growth. In other words, the exact area of growth on the same films was not photographed. Rather, pictures were taken to convey an overall idea of how the cells were spreading over time on the various samples.

4.3. Results and Discussion

4.3.1. Growth Cycle

The NIH-3T3 fibroblast growth cycle, cultured in T-25 flasks is depicted in Figure 19. The phases of cell growth described in section 4.1.1., PDT and SD of the NIH-3T3 fibroblasts are displayed in Figure 19. The PDT was estimated from the slope of the growth curve during the exponential phase of growth. The SD was simply the asymptote of the highest cell concentration attained. These values were used to design the experimental parameters for the cell attachment and growth experiments. Additionally, these values are used as a baseline for the cell behavior, which can be compared to subsequent experiments.

The SD of 1.2×10^5 cells/cm^2 and PDT of 21.4 hours are typical for a healthy line of NIH-3T3 fibroblast cells supplemented with 10% calf serum. Cells cultured from passage number 25 to 27 all showed similar growth behavior, and cells below this passage number range were used for subsequent experiments. The results of Figure 19 indicate that the fibroblast SD and PDT were reproducibily measured. These parameters were also confirmed periodically throughout the study by measuring the SD and PDT of

cells between passage number 10 and 30, at confluency and during the exponential phase of growth.

Figure 19. NIH-3T3 fibroblast cell growth cycle

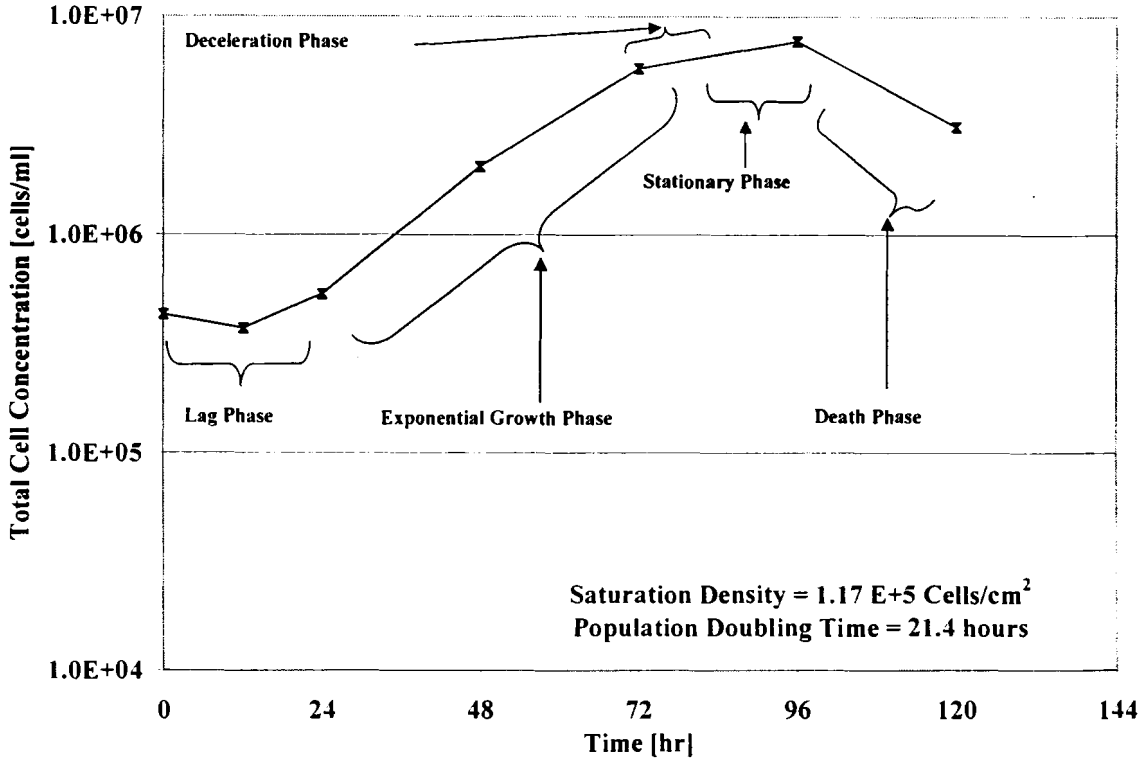

Saturation density and PDT were used to establish initial cell concentrations for the attachment and growth studies. For the attachment experiments, a concentration near the SD was used. As discussed in chapter 2, the initial attachment of cells in critical for subsequent cellular processes of spreading, growth, migration as well as for the production of important products including fibronectin and various growth factors. The Bradford assay [18] used to estimate cell concentration in subsequent experiments gave more accurate results when applied to higher cell concentrations. Thus, an initial seeding density near that of the SD was utilized for attachment experiments. In contrast, a much

lower initial cell concentration was used for the growth experiments, so that the cells could be observed in the different phases of the growth cycle.

Although fibroblasts are anchorage dependent and usually cease growth upon attaining confluency, the NIH-3T3 fibroblasts utilized in this study behaved slightly different. This line of fibroblasts continued growth in multi-layers after reaching confluency at a decreased growth rate. The death phase indicated in Figure 19 was the result of nutrient depravation upon reaching confluency.

4.3.2. Attachment Experiments

The attachment experiment results are depicted in Figure 20. The cell concentrations depicted in Figure 20 were estimated with the Bradford assay. The Y-axis of the plot represents the percentage of the total number of cells attached compared to the original 8.8×10^5 cells per dish inoculated. The results of Figure 20 indicate that 3T3 cells will attach to chitosan films. The error bars of Figure 20 represent the 95% confidence interval for this data. The polystyrene controls definitely support greater NIH-3T3 attachment than the 1.5% or 3.0% chitosan films. The data is not significantly different for the 0.5% chitosan films and the polystyrene controls. The rate of attachment for the 0.5% chitosan film and controls within the first 20 minutes is much greater than that for the next 40 minutes. The controls and the 0.5% film achieved greater than 50% attachment after 20 minutes in culture. This implies that the attachment step for the 3T3 fibroblasts is very fast. The polystyrene controls and the 0.5% chitosan films approach an asymptotic value at 60 minutes in culture of about 65-80 % attachment, and display similar trends. This implies that the majority of the cells that will attach do so within the first 60 minutes of inoculation.

Figure 20. Cell attachment on chitosan films and polystyrene controls

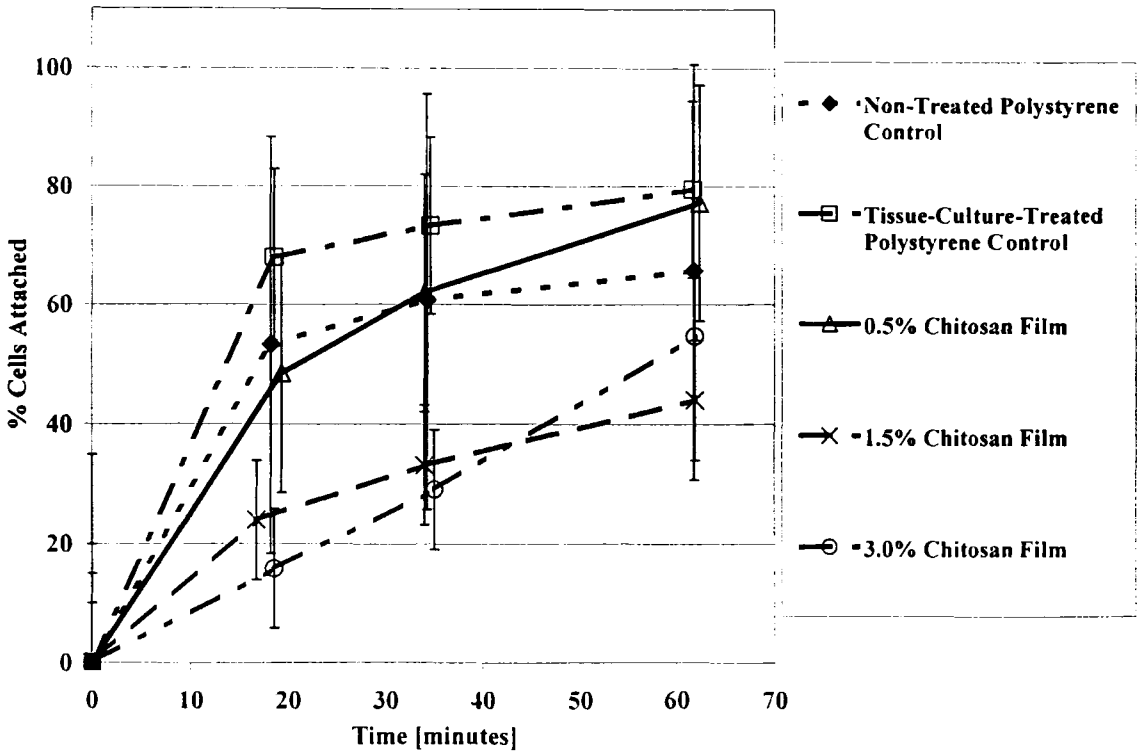

The tissue culture grade polystyrene control supports the greatest cell attachment, which was expected as this substrate is designed for cell culture applications. This control showed nearly 70% of cells attaching after 20 minutes in culture and approximately 80% of the original cells inoculated attaching at 60 minutes in culture. The untreated polystyrene control exhibits lower attachment than its counterpart, with about 55% of cells attaching after approximately 20 minutes in culture and almost 70% of cells attaching after 60 minutes in culture.

The results of these attachment experiments confirm our data from Chapter 3 on the WIA contact angles, which indicated that all concentrations of chitosan films should support cell attachment. The 0.5% chitosan film exhibited the apparent greatest NIH-3T3

fibroblast attachment. The 0.5% film exhibited nearly 50% cell attachment by 20 minutes in culture, and approached 80% attachment of cells inoculated after 60 minutes. The 0.5% film appears to out-perform the untreated polystyrene control after 60 minutes in culture, surpassing the attachment of this control at just after 30 minutes in culture. However, because of the higher variability shown as the 95% confidence intervals in Figure 20 in the mean attachment values of the 0.5% chitosan films and the untreated polystyrene controls, this improved attachment should not be considered statistically different. The 1.5% and 3.0% films supported cell attachment, at lower rates than the 0.5% film or controls. The 1.5% films and 3.0% films exhibit similar attachment characteristics from 0 to 60 minutes after inoculation. These films display an almost linear trend with cell attachment over the first 60 minutes in culture, approaching 45-55% cell attachment at 60 minutes. It should be noted that a larger variability in the 1.5% chitosan film with respect to cell attachment is not observed compared to other films and controls, as was with its tensile properties, water-in-air contact angle and surface free energy reported in Chapter 3. Thus, the variability noticed in the physical parameters of the films doesn't appear to affect their biological function.

The observation that the NIH-3T3 fibroblasts attach to the chitosan films confirms that these films are suitable for cellular attachment. Good attachment indicates that the chitosan films will promote other cell functions including cell growth. The 0.5% film displays the fastest apparent initial attachment and highest apparent percentage attached of the three film concentrations studied. Additionally, the 0.5% film possesses the lowest WIA contact angle of the three films at 73.2 degrees as indicated in Chapter 3. The 1.5% and 3.0% films had higher WIA contact angles than the 0.5% film and displayed lower

cell attachment than that of the 0.5% film. This implies that chitosan films with lower WIA contact angles will support improved fibroblast attachment compared to films with higher WIA contact angles. There is little difference in the absolute values for the WIA between the three film concentrations. The attachment of NIH-3T3 fibroblasts is likely enhanced by the adsorption of serum proteins onto the polystyrene controls as well as onto the chitosan films. As mentioned in Chapter 2, many polymers will adsorb proteins present in serum to their surface, with maximum adsorption occurring on polymers with intermediate wettabilities.

Fibroblasts will not attach to the grooved 3.0% chitosan film cast on Lexan. Attachment experiments with this film were unsuccessful. Hardly any fibroblasts attached to these films, and those that did attach did not grow. Reasons for this are probably related to the Lexan support on which films were cast. This support showed evidence of chipping, and contained debris resulting from the machining process. The films were observed to retain some of this debris after detachment from the Lexan support. Because the Lexan could not be autoclaved for sterilization, the resulting films cast on this support most likely contained contaminants from the support, which were toxic to cells. Unsuccessful attempts were made to sterilize the Lexan surface with a 70% ethanol solution. Future experimentation with a grooved film should utilize a support that can be autoclaved for sterilization. Also, a better material should be used to ensure that machined grooves are smooth so that films will easily detach from the support.

4.3.3. Growth and Spreading Experiments

The growth of the NIH-3T3 fibroblasts is depicted in Figures 21 and 22. The polystyrene controls support the better cell growth than the chitosan films. The tissue culture grade polystyrene control displays the fastest growth of 3T3 fibroblasts with a PDT of 21 hours. The fibroblast growth on the untreated polystyrene control displayed a PDT of 22 hours. These results agree with the parameters previously determined on polystyrene. The controls also approach the saturation density of 1.2×10^5 cells/cm^2 after 4 days in culture as expected based on the PDT and the initial inoculation density. The fibroblasts on controls appear to enter into the exponential growth phase around 12 hours after inoculation. Figure 21 displays the total cell concentration on the Y-axis on a normal scale, whereas Figure 22 displays this information on a logarithmic scale. Both figures display the 95% confidence interval for the mean cell concentrations. Each point represents three separate tests, sampled in duplicate.

Figure 21. Cell growth on chitosan films and polystyrene controls

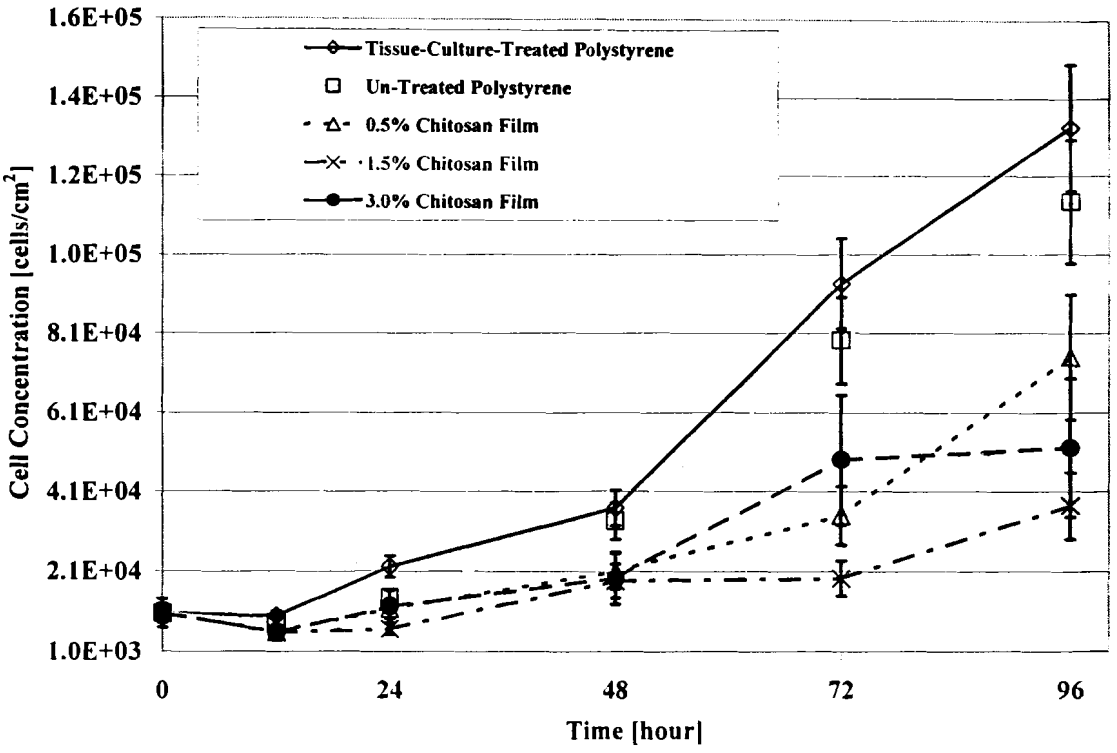

Figure 22. Logarithmic cell growth on chitosan films and polystyrene controls

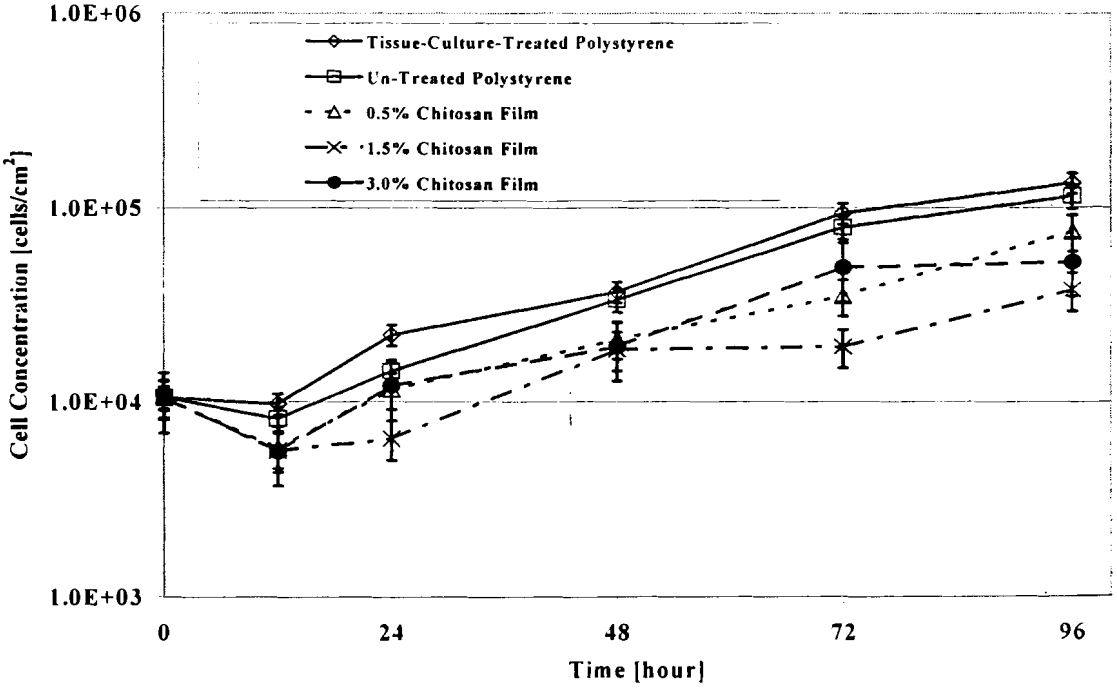

All concentrations of chitosan films support NIH-3T3 fibroblast growth to a similar extent. The initial attachment and subsequent growth of NIH-3T3 fibroblasts on chitosan films appears to take longer than for the controls. Less than 20% of the initial cells inoculated onto chitosan films attach and subsequently grow. This is evidenced by the cell concentrations at 12 hours in culture. This is an interesting result indicating that even though the chitosan films were shown to support over 50% cell attachment within the first 60 minutes of inoculation, only a fraction of those cells attached actually continue to proliferate.

For the polystyrene controls, the cells display a lag phase for about 12 hours. This is most likely representing the time it takes for the fibroblasts to attach, spread, and begin secreting ECM proteins. Once the cells have established a sufficient ECM, then the proliferation proceeds to the exponential growth phase on all substrates. The fibroblasts cultured on chitosan films appeared to begin the exponential phase of growth around 24 hours after inoculation. This is 12 hours later than the time for fibroblasts cultured on controls to begin this phase of growth. This may be because the viable attached cells were secreting ECM proteins so that they could continue to proliferate. These results partially agree with previous studies which indicated that after 24 hours in culture, fibroblasts will have produced enough of their own ECM proteins to continue growth at rates comparable to other substrates [75]. The cells were observed to begin exponential growth at 24 hours in culture, but at slightly slower rates than controls.

The 0.5% chitosan film and 3.0% chitosan films exhibited similar cell growth characteristics over 4 days. The 0.5% film had the highest cell density after 4 days at 7.5 x 10^4 cells/cm^2, followed by the 3.0% film with 5.2 x 10^4 cells/cm^2. The 1.5% chitosan

film had the lowest cell concentration after 4 days in culture at 3.7×10^4 cells/cm^2. All concentration chitosan films exhibit longer PDT's than the controls. The PDT's were determined by assuming the NIH-3T3 fibroblasts in the exponential phase of growth from day 1 to day 4 of the growth experiment. Although the 3.0% chitosan film had a lower cell density at 4 days than the 0.5% film, its PDT of 24.5 hours indicates that this concentration film supported the fastest fibroblast growth. The 0.5% film supported the next fastest fibroblast growth with a PDT of 27.2 hours, followed by the 1.5% film with a PDT of 31.5 hours. Future experiments with these concentration films should include later time points at 5 and 6 days to determine whether the fibroblasts will achieve the same SD on the chitosan films as on controls. The confidence in the average values for cell denities in the growth experiments is much higher than that obtained in the attachment experiments. One reason for a difference could be due to a weaker initial attachment of fibroblasts during the first 60 minutes in culture compared to 12 hours post inoculation. The cells should be completely attached after 12 hours in culture, whereas they may be more susceptible to shear forces during initial attachment stages.

The NIH-3T3 fibroblast cells also spread onto the chitosan films in a similar manner as on polystyrene controls. The photographs of the fibroblast spreading show that the number of fibroblasts spreading on the varying concentration chitosan films increases with time. After subculturing fibroblasts, cells exhibit a rounded shape when suspended in culture medium as well as after initial attachment to a substrate. After some time, the cells would spread onto the substrate and begin proliferation until reaching confluency. The cell morphology, after subculturing without significant spreading, and

the after growing to a confluent layer is depicted in Figure 23. The dark spot in the top portion of Figure 23 represents external debris on the outside of the tissue culture flask.

Figure 23. Cell morphology after subculture and at confluency

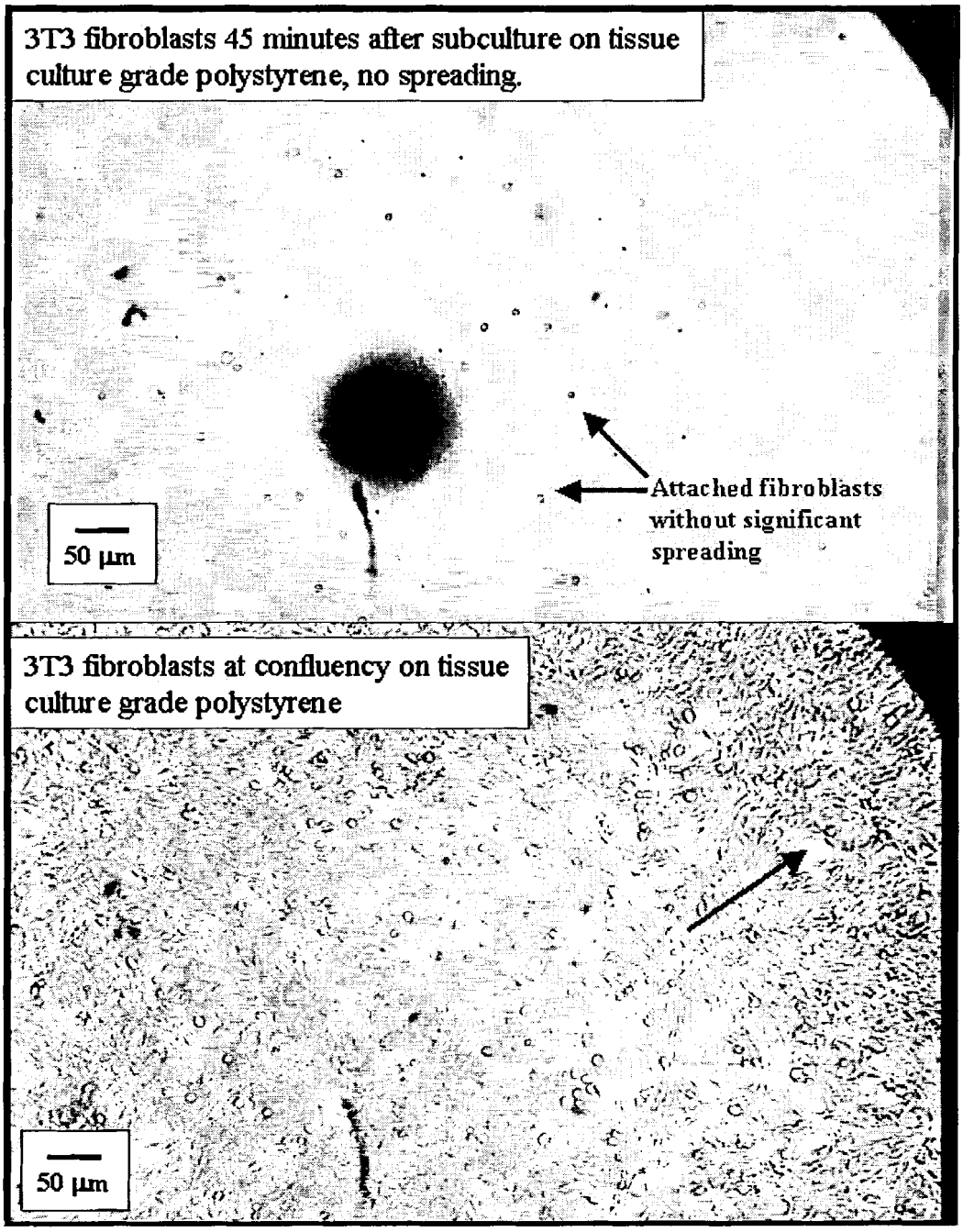

The confluent layer of cells in Figure 23 displays a generally random orientation of fibroblasts on the substrate. This is probably due to the smooth nature of this substrate.

One area indicated by the arrow in the confluent layer shows cells growing radially around an empty space on the polystyrene. This may be due to some factory-caused irregularity in the polystyrene during manufacturing. Cells with rounded morphologies in the confluent layer indicate mitosis. The time required for the cells to attach and reach confluency in Figure 24 was 5 days at 37 °C, 95% humidity and 10% calf serum in DMEM.

The NIH-3T3 fibroblasts may exhibit different spreading behavior depending on the amount of adsorbed fibronectin on the substrate. Fibronectin affects the initial spread of cells onto the substrate, but subsequently, cells will spread due to their own production of fibronectin [88]. One theory towards the maintenance of good cell growth *in vitro* and *in vivo* is to attach as many cells to the substrate as possible with the help of attachment proteins, as this will result in good spreading behavior as the cells produce the necessary products for this phase [101].

The spreading and growth of cells on the untreated polystyrene control is depicted in Figure 24. The NIH-3T3 fibroblasts have attached and begun spreading in seemingly random orientation at 12 and 24 hours in culture. The spread cells usually take on either an elongated shape or a triangular form. There is no visibly noticable increase in cell density from 12 to 24 hours. Similar cell morphologies were observed on the tissue culture grade polystyrene control as on the untreated polystyrene control (results not shown). The results of the growth experiments indicate the fibroblasts enter into the logarithmic phase of growth after 12 hours. One explanation for no observable cell density change between 12 and 24 hours is that separate areas of polystyrene control were photographed. As previously mentioned, these pictures do not depict the same place on

Figure 24. Cell morphology on untreated polystyrene control over time

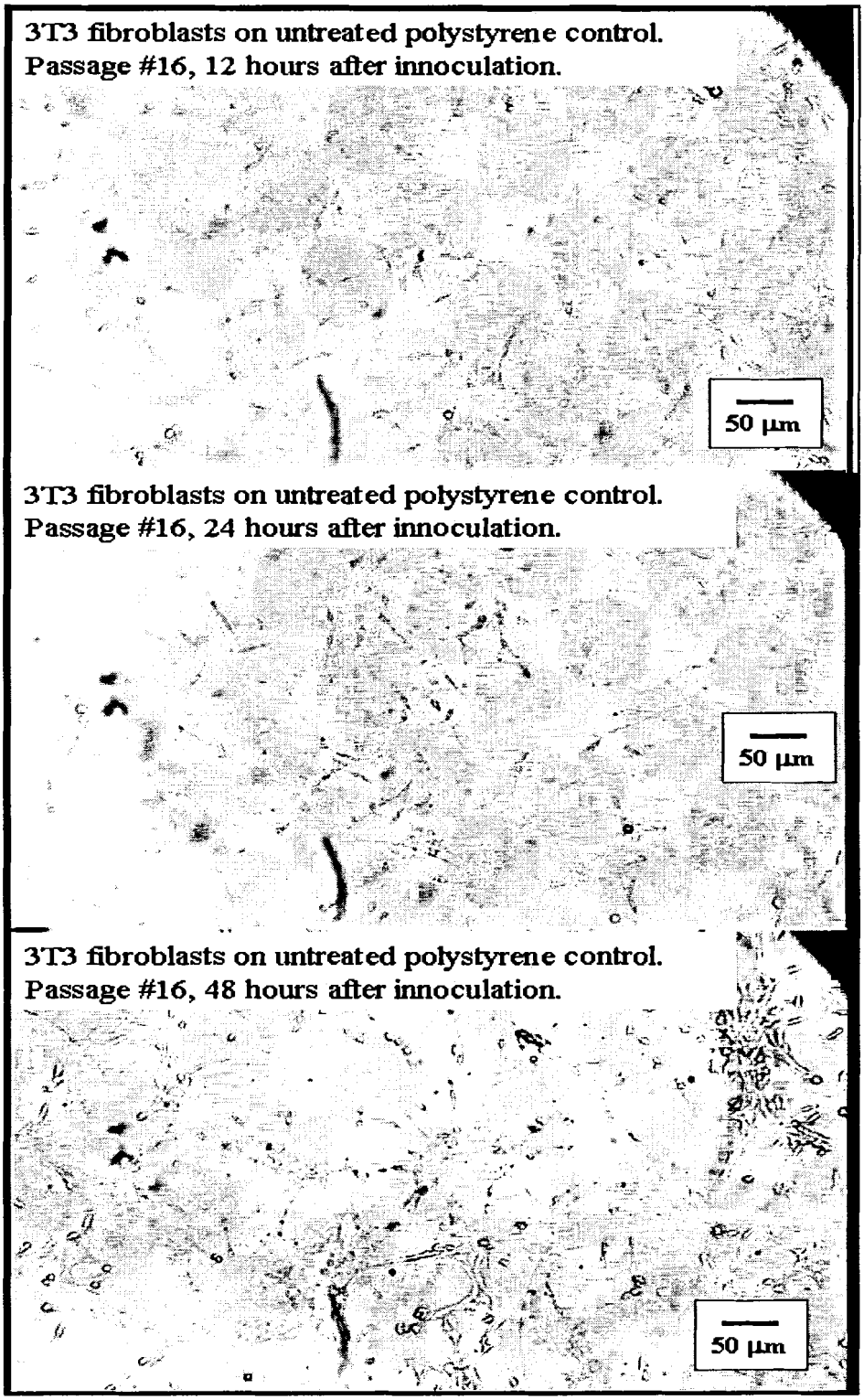

the sample. The cells remain in a random orientation at 24 hours. The cell density noticeably increases from 24 hours to 48 hours in culture. At 48 hours in culture, the fibroblasts appeared to be aggregating and growing at higher densities near these aggregations then where single cells were growing. This may be the result of an increased production of collagen or fibronectin by the colonies of cells, enabling faster spreading, growth and migration.

The spreading and growth of fibroblasts on 1.5% and 3.0% chitosan films is depicted in Figure 25. The spreading of fibroblast cells on the 0.5% chitosan film is not shown. The reason for the smaller image of the fibroblasts on the 1.5% film at 48 hours was the film in the camera ran out on this exposure. Both the 1.5% and 3.0% chitosan films supported the attachment and spreading of fibroblasts at 12 hours in a seemingly random orientation. This confirms our assumption that these films are relatively smooth, because a higher Ra of the films should affect the orientation of cells during attachment. There was a noticeable increase in cell density for both the 1.5% and 3.0% chitosan films from12 to 48 hours. The fibroblasts appeared to aggregate on the 1.5% chitosan films at 24 and 48 hours to a greater extent than that observed in Figure 24 on the untreated polystyrene control. There was no apparent aggregation of the cells on the 3.0% chitosan films at any of the times depicted in Figure 25. However, some cell aggregation was observed during experimentation that is not shown. There was an air bubble in Figure 25 on the 3.0% chitosan films at 12 hours. The ability of the chitosan films to support the attachment, spreading and growth of 3T3 fibroblasts is confirmed by Figure 25. The 0.5% films (not shown) displayed fibroblast spreading and growth characteristics very similar to the 1.5% chitosan films at all times of the growth experiment.

Figure 25. Cell morphology over time for 1.5% and 3.0% chitosan films

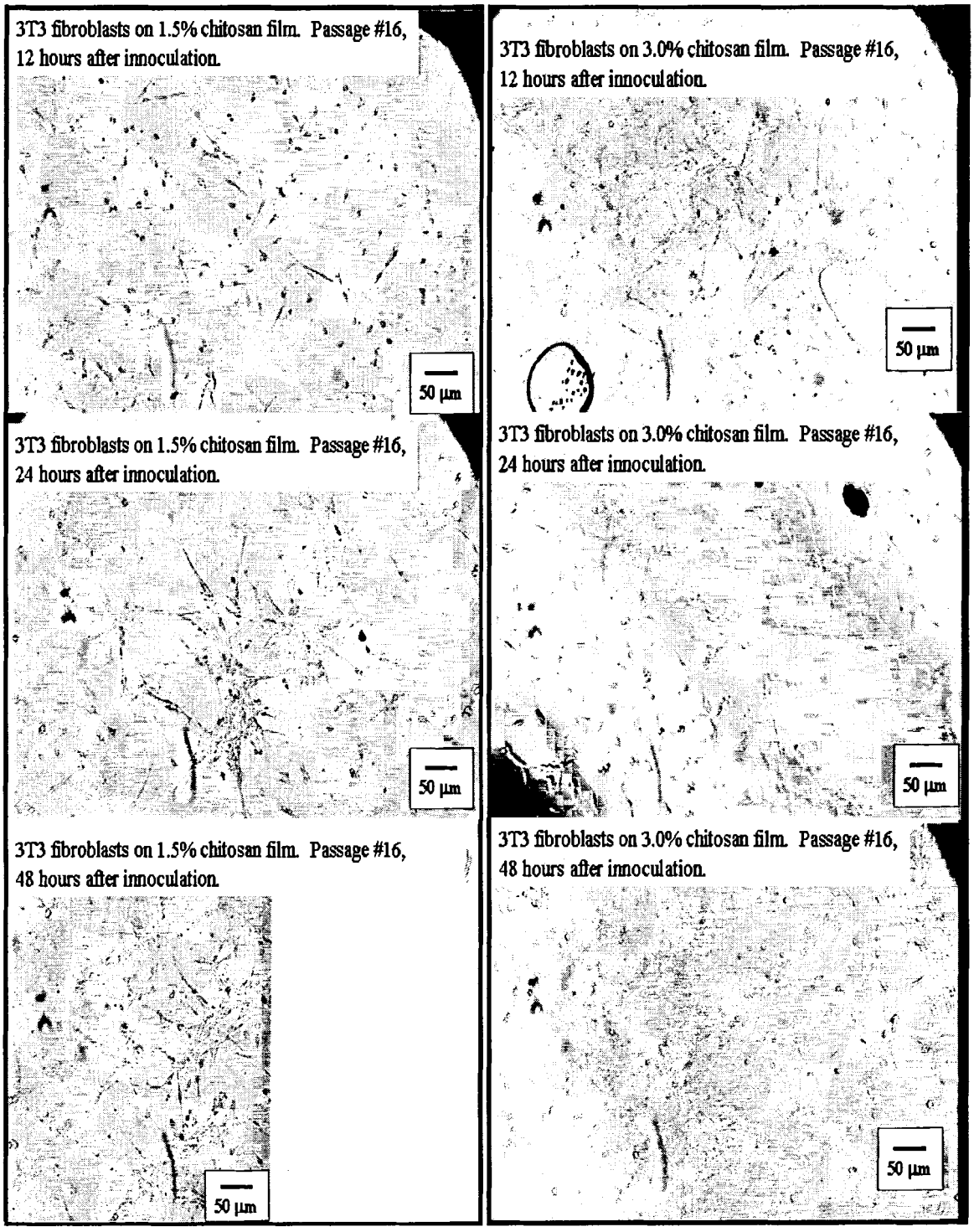

A comparison of the fibroblast cell morphology on the tissue culture grade polystyrene control (MWPS) and the different concentration chitosan films at 48 hours after the start of a growth experiment is depicted in Figure 26. The 0.5% and 3.0% films exhibit better cellular spreading than the 1.5% film as evidenced by the larger individual cells. This agrees with our previous assumption that a lower WIA contact angle might

Figure 26. Cell morphology at 48 hours of growth experiment

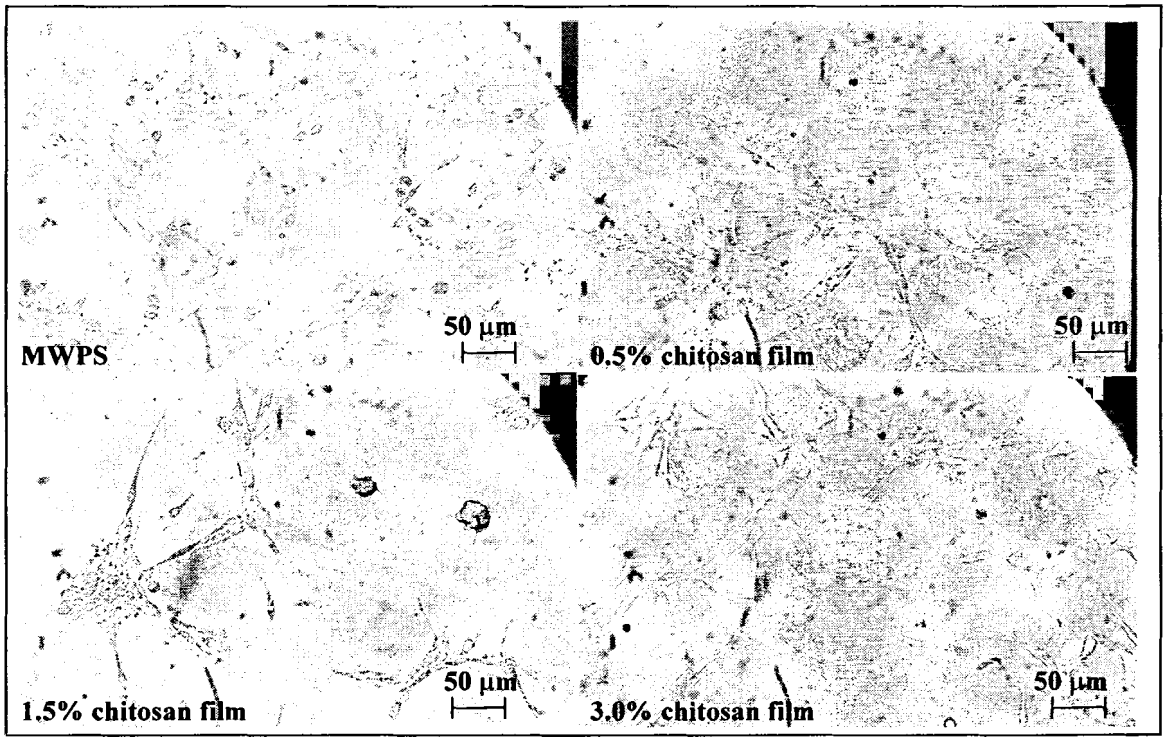

imply greater fibroblast spreading. The NIH-3T3 fibroblasts had a greater tendency to proliferate in clumps on the chitosan films compared to the polystyrene controls as indicated in Figures 24-26. This may be due to a higher density of amine or hydroxyl groups at specific points on the films. Hydroxyl groups have been suggested to be important to initial adhesion of cells to substrates, whereas parts of carboxyl groups influence long-term cell growth [19]. Another reason for the aggregation of the fibroblasts

may be that an aggregate will produce more collagen and fibronectin than single cells and promote faster cell spreading, growth and migration on its own extracellular matrix proteins.

The observation of cells aggregating and growing is very important. These aggregates can be correlated to cell-cell interactions, cell differentiation, viability, migration and subsequent tissue formation. The aggregation of cells resembles the cell-cell interactions typically found in tissues, and cell function and survival can be improved in aggregate cultures. Also, chitosan films promoting these aggregates may be beneficial to the tissue engineering aspects of these films, as they may act to enhance tissue function [197].

4.4. Conclusions

4.4.1 Growth Cycle

The NIH-3T3 fibroblasts display the standard phases of cell growth, as depicted in Figure 19. The PDT and SD are important indicators of baseline NIH-3T3 cell behavior. These parameters can be used to determine the seeding densities and sampling times of experiments on the attachment and growth of NIH-3T3 fibroblasts on chitosan films and controls. The SD and PDT should be used as a baseline for comparison to subsequent experiments of NIH-3T3 attachment and growth.

4.4.2 Attachment Experiments

All substrates support the attachment of NIH-3T3 fibroblasts. The polystyrene controls support greater fibroblast attachment than the 1.5% or 3.0% chitosan films. The 0.5% chitosan films and the polystyrene controls exhibit very similar attachment

behavior. The rate of attachment for the 0.5% chitosan film and controls within the first 20 minutes is much greater than that for the next 40 minutes, indicating the attachment process to be very fast. The majority of fibroblasts that will attach do so within the first 60 minutes of inoculation. These results in conjunction with the WIA contact angle data from chapter 3 indicate that the WIA contact angle of chitosan films may be an indicator for the degree at which they will support fibroblast attachment, with lower WIA's implying better fibroblast attachment.

Based on the 95% confidence intervals of attachment data, the 0.5% chitosan films and the untreated polystyrene controls exhibit similar attachment and should not be considered statistically different. The 1.5% and 3.0% films supported similar cell attachment, at lower rates than the 0.5% film or controls. A higher variability in the 1.5% films compared to other concentrations or controls was not observed, as was reported for this films tensile properties, water-in-air contact angle and surface free energy in Chapter 3. Thus, the variability noticed in the physical parameters of the films doesn't appear to affect their biological function. Fibroblasts did not attach to grooved 3.0% chitosan films cast on Lexan. Reasons for this are probably related to the Lexan support on which films were cast. Because the Lexan could not be autoclaved for sterilization, the resulting films cast on this support most likely contained contaminants from the support, which were toxic to cells. Future experimentation with a grooved film should utilize a support that can be autoclaved for sterilization. Lexan is not a suitable material for casting chitosan films.

4.4.3 Growth and Spreading Experiments

The chitosan films cast on glass support the growth of NIH-3T3 fibroblasts. The number of cells that will attach and grow during the first 12 hours in culture was lower than the number of cells that will attach to the films in the first 60 minutes. This may be due to cells initially attaching to the chitosan films but not subsequently spreading or growing. This is an interesting result indicating that even though the chitosan films were shown to support over 50% cell attachment within the first 60 minutes of inoculation, only a fraction of those cells attached actually continued to proliferate. This indicates that many initially attached cells did not grow and detached from the films.

The fibroblasts begin exponential growth on polystyrene controls after 12 hours in culture and on chitosan films after 24 hours in culture. This may represent the time required for viable attached fibroblasts to secrete ECM proteins which encourage subsequent proliferation. These results agree with previous studies which indicated that after 24 hours in culture, fibroblasts will have produced enough of their own ECM proteins to continue growth at rates comparable to other substrates [75]. Once in the exponential growth phase, fibroblasts cultured on chitosan films displayed slightly longer PDT's than ones cultured on polystyrene controls.

The chitosan films support the attachment, subsequent spreading and growth of NIH-3T3 fibroblasts. This data confirms the WIA and SFE data of Chapter 3 which indicated that all films and controls should support cell functions of attachment, spreading and growth. The NIH-3T3 fibroblasts initially attach to the films and controls in a random orientation, confirming the hypothesis that the Ra of the films would not affect the orientation of cells during attachment. The fibroblasts appear to prefer growth

in colonies on all concentration chitosan films, which may be a result of increased collagen and fibronectin production by fibroblast colonies. This observation is very important, because these aggregates can be correlated to cell-cell interactions, cell differentiation, viability, migration and subsequent tissue formation. The aggregation of cells resembles the cell-cell interactions typically found in tissues, and cell function and survival can be improved in aggregate cultures. Also, chitosan films promoting these aggregates indicate potential tissue engineering aspects of these films, as they may act to enhance tissue function [197].

Chapter 5

3-D SCAFFOLD FORMATION AND CHARACTERIZATION

5.1. Introduction

The results of Chapter 4 confirmed that 2-D chitosan films support the attachment and growth of NIH 3T3 fibroblast cells. Many tissue engineering applications require 3-D cell supports. The next step in this study was to develop and characterize a 3-D chitosan scaffold for cell culture applications. This chapter describes the formation of a 3-D chitosan matrix, and the subsequent testing of the matrix physical properties.

5.2. Materials and Methods

Aldrich high-molecular weight chitosan was used for all applications. Pentasodium tripolyphosphate (TPP) was supplied by Aldrich Chemical (St. Louis, MO). A LABCONCO freeze dryer (model LYPH-LOCK 6) was used to lyophilize samples. Porosity and surface area tests were performed using a Micrometrics Gemini 2360 Surface Area Analyzer. Corning, six-well tissue culture plates were supplied by VWR Scientific (Bridgeport, NJ). The wells of the tissue culture plates have a 9.4 cm^2 area and a working volume of 16.8 ml. Samples were weighed using an OHAUS 110 g scale (Explorer model) with an accuracy of 0.1 mg.

The following procedure outlines a method for the formation of a 1.5% chitosan 3-D matrix by ionotropic gelation with TPP and subsequent lyophilization. A solution of 1.5% chitosan (w/v) in 1.5% acetic acid was prepared similar to methods described in Chapter 3. The 1.5% solution was used because it was viscous enough to retain the shape of the mold without significant disruption during the addition of the TPP for gelation.

Lower concentrations were prone to mixing upon addition of the TPP, which changed the final shape of the gel from a cylinder to one with irregularity. Five ml of the chitosan solution was added to each of 6 wells of a tissue-culture-grade polystyrene plate. Each chitosan solution was gently covered with 5 ml of 10% TPP (v/v) to cause ionotropic gelation, with care taken not to disrupt the chitosan solution through shear forces. The TPP was gently added by slowly decanting along the side of the multiple-well in which the chitosan was placed. The TPP-chitosan remained at room temperature for 24 hours to ensure complete dissolution of the TPP into the chitosan solutions. Visual inspection of the gel indicated the TPP slowly diffused downward into the chitosan solution, identified by the interface between the gel and the clear chitosan solution. The TPP was aspirated after 24 hours, and the resulting gelled matrices of chitosan conformed to the cylindrical shape of the polystyrene dish (34.8 mm diameter). These chitosan gels were milky-white in appearance and swollen.

The gelled chitosan matrices were gently covered with 5 ml of 0.3 N NaOH, and let stand for 24 hours at room temperature. This caustic treatment was performed to neutralize any residual acetic acid that may be present in the gel. The caustic was aspirated 24 hours after addition and the gel was rinsed by gently adding 5 ml distilled H_2O (dH_2O) in the same manner as previously outlined for the TPP. After 24 hours, the dH_2O rinse was aspirated and repeated for another 24 hours. The long rinse times were employed to ensure that the caustic and dH_2O could completely penetrate the gelled chitosan matrix. The dH2O was aspirated and the chitosan samples placed in a –20 °C freezer for 12 hours. The frozen chitosan gels were then placed in a freeze dryer at a maximum temperature of –40 °C and pressure of 33×10^{-3} mBar for 40 hours. The

resulting 3-D matrices were white, flaky and cylindrical. Thin disc shaped layers could be peeled from the cylinder-shaped matrices. A schematic for the experimental procedure is depicted in Figure 27.

Figure 27. Steps for forming 3-D chitosan matrix

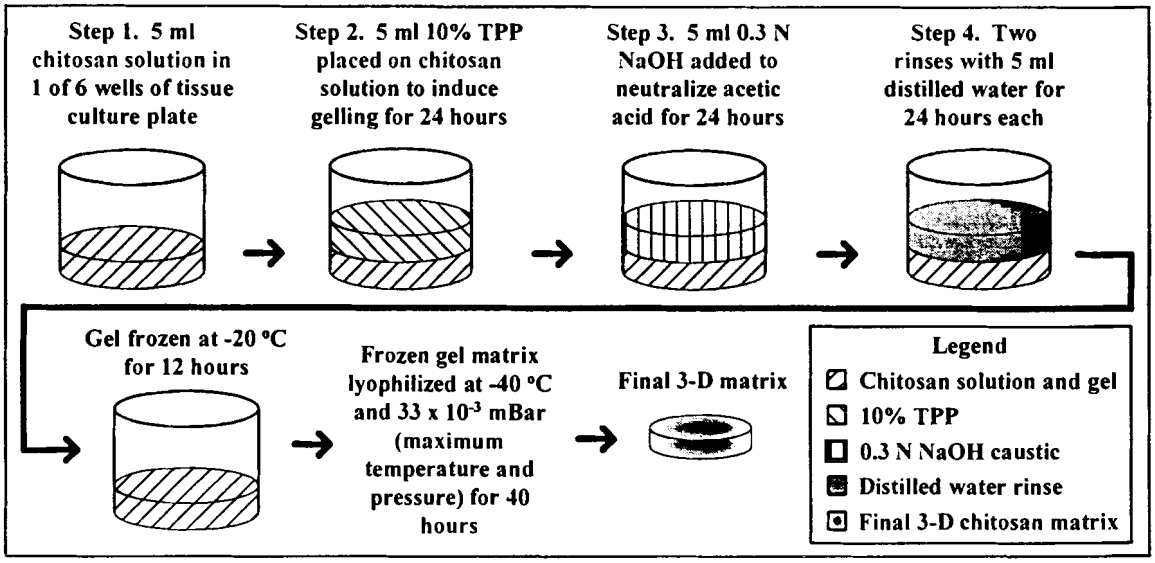

The physical properties of surface area and the porosity of the 3-D matrices were measured to characterize the samples and used to confirm the reproducibility of the matrix forming procedure. For surface area and porosity measurements, approximately 0.1 grams of cross-linked sample was obtained by breaking off small pieces of the matrix. The testing apparatus utilized a glass tube requiring small sample pieces. The 0.1 grams of sample were tared, and degassed with nitrogen for 1 hour at 100 °C to remove any moisture or gases from the sample with a Micrometrics Gemini 2360 Surface Area Analyzer. The weight of the sample was measured after degassing and used for the calculations. Surface area and porosity tests were performed in duplicate. The first test was a five-point surface area test. The analyzer measured the amount of nitrogen adsorbed by the samples at five partial pressures (P/Po) from 0.1 to 0.5, and used this

data to estimate the total pore volume and surface area by BET method [21]. The second test measured a complete adsorption isotherm over the partial pressure range of 0.0001 to 0.7. The adsorption isotherm was used to estimate the pore size distribution within the sample using the Horvath-Kowazoe method which estimates pore radius as a function of partial pressure [89]. An effective pore diameter was estimated based on the volume of nitrogen gas absorbed at each partial pressure of the isotherm. The pore size distribution was estimated by correlating the change in volume and rate of nitrogen gas adsorbed by the sample at each partial pressure point of the adsorption isotherm to the effective pore size diameter of the chitosan matrices.

A preliminary cell-culture compatibility study was performed. Thin discs were separated from the 3-D chitosan matrix and placed in sterile Corning six-well tissue culture plates. The chitosan samples were approximately 0.5 mm thick, which enabled viewing of through the sample with a phase contrast microscope. Samples were conditioned in five ml DMEM +10%CS + 100U/ml pen-strep for 24 hours at 37 °C in an incubator with 95% relative humidity and 5% CO_2. The medium was aspirated, and 5 ml of 2.0×10^4 cells/ml were added to each 3-D chitosan-containing well. The cell concentration added was 1.0×10^5 cells per well. The subsequent attachment and growth of NIH 3T3 fibroblasts on the 1.5% chitosan matrices was visually observed.

The surface free energy of the 3-D matrices was not estimated. Because of the 3-D nature of these samples, the method for determining the surface free energy of the samples with contact angle measurements is not applicable, as the fluids applied will adsorb into the sample and are not measurable according to techniques outlined in Section 3.2.4. Another method is available to estimate the surface free energy of

substrates, which correlates the spreading of fibroblasts to the substrate SFE. Fibroblasts have been shown to spread to different extents based on the SFE of the substrate on which they attach [201] [222]. The SFE of fibroblasts can be estimated indirectly by experiments characterizing the spreading of fibroblasts on substrates with various SFEs [201]. The SFE of the fibroblasts are estimated assuming an analogy between liquid-solid and cell-solid interactions [222]. Thus, an indirect correlation between the extent of fibroblast spreading on the 3-D matrices and the 3-D matrix SFE could provide estimation for the SFE of these materials.

Another important characteristic of a 3-D implantable biomaterial is its degree of cross-linking. A high degree of cross-linking can reduce a material's conformational mobility [171] as well as inhibit fibroblast attachment, spreading and growth [232]. Additionally, the degradation rate of 3-D chitosan matrices depends on the degree of crosslinking as well as the pH of the culture medium [74]. One indicative property of the degree of cross-linking of a matrix is the denaturation temperature (Td) [171]. An increase in degree of cross-linking corresponds to an increase in Td. The denaturation temperature can be determined with differential scanning calorimetry [172].

5.3. Results and Discussion

The resulting chitosan matrices were very light and fluffy, white and cylindrical in shape. After freeze-drying, the gels had decreased approximately 37% in volume from the original cast dimensions, to an approximate 30 mm diameter and 4.5 mm height, weighing approximately one gram. The average surface area of the 1.5% cross-linked chitosan samples was 0.67 ± 0.3 m^2/g. No data was available from literature on the surface area of 3-D chitosan matrices. The standard error associated with this parameter

is very high, at about 45% of the mean value. This is too high to consider this result accurate with high confidence. The high standard error of the sample surface areas is a result of testing only two samples. The two samples were tested in duplicate for the determination of the surface area. Performing more measurements on various samples should decrease the standard error associated with this value.

The average porosity of the samples was $4.8 \times 10^{-3} \pm 2 \times 10^{-5}$ cm^3/g. The standard error of the average porosity is below 1% of the mean porosity. This average value and low error indicate that the 1.5% chitosan matrices have similar porosities and were cast in a reproducible manner. The error is reduced from that of surface area measurements because 40 pressure measurements were taken over the partial pressure range of 0.0001 to 0.7 for the determination of the adsorption isotherm, and the sample porosity was estimated at all partial pressures. The samples were tested in duplicate, further reducing the standard error associated with the porosity. A study by Bodmeier [15] characterized chitosan beads formed by a similar technique as that described above. A 1% chitosan solution (w/w) dissolved in 1% acetic acid (v/v), containing 1% drug (w/w) was gelled by adding the solution drop wise to TPP solutions of concentrations ranging between 0.5 and 10% (v/v). Scanning electron micrograph (SEM) images indicated these matrices to possess pores approximately 5-20 μm in diameter. The gelling process was almost instantaneous with the Bodmeier study, whereas the gelling process took several hours with the process presented here. Another study reported chitosan ascorbate gels to possess a honeycomb structure with pores between 1-15 μm by SEM analysis [161]. Also, chitosan-PVA membranes, prepared by immersing a film of chitosan-PVA into a coagulation bath had 5-15 μm pores, as indicated by SEM imaging [37].

The porosity of the 3-D samples is very low at $4.8 \times 10^{-3} \pm 2 \times 10^{-5}$ cm^3/g. The test matrices occupying an approximate 0.7 cm^3 volume weighed approximately one gram. Based on the porosity estimation by the Micrometrics Gemini 2360 Surface Area Analyzer, the resulting volume occupied by the pores is less than 1% of the total volume of the sample. This data indicates that these matrices are not porous. These matrices may exist in a "sponge" like form. The matrix has an expanded structure, but there are negligible pores within this structure. This is also indicated by the large amount of the 1.5% chitosan sample required to achieve the 0.1 grams of sample used for the surface area and porosity tests. The estimated pore size distribution of the 1.5% chitosan matrix is depicted in Figure 28.

Figure 28. Pore size distribution of 3-D chitosan matrix

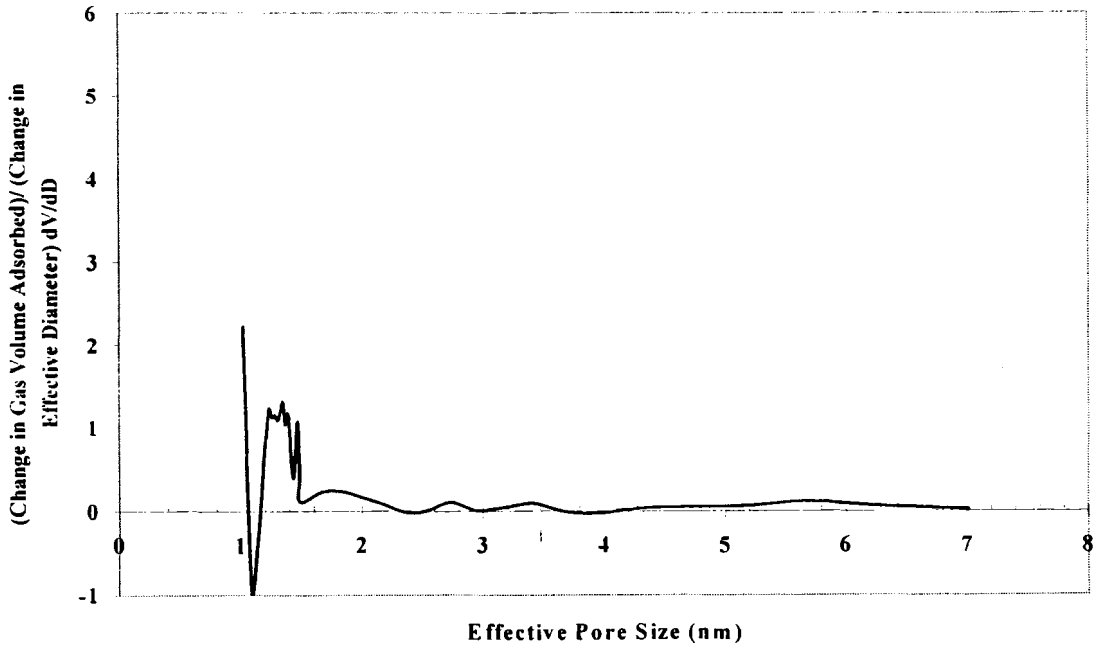

The respective peaks indicated at 1.3, 1.8, 2.7, 3.4 and 5.7 nm indicate pores with these effective diameters. These results should not be considered accurate estimates of

the pore size distribution of the 1.5% cross-linked chitosan matrix because they are at and below the limits of the testing apparatus, which is approximately 5-10 nm. Also, these results support the low estimated porosity estimation and visual observations indicating that there was little or no pores structure in these matrices. The magnitude of the pore sizes indicated is much too small to allow NIH 3T3 fibroblasts or essential nutrients to migrate within this matrix [161 15 37]. To further confirm the microstructure of these 3-D matrices, SEM imaging should be employed.

Other methods for forming 3-D chitosan scaffolds with mean pore diameters ranging between 1 to 250 μm were described by Madihally and Matthew [129]. These methods are discussed in detail in Chapter 7. Scaffolds should have pores with cellular dimensions (greater than 10 μm) to allow for cellular migration and interaction, while not interfering with the diffusion of hormones, nutrients and metabolites into the matrix to provide nourishment and initiate cellular responses [212]. The porosity of a matrix also depends on the intended replacement tissue. The freezing conditions for the development of 3-D sponges described in section 5.2 can be varied to study the effect on the pore structure of these sponges. Another technique for forming porous 3-D matrices is porogen leaching. This process involves developing a chitosan gel structure containing small particles such as salts. These particles are subsequently removed from the matrix by leaching, resulting in the formation of pores in place of the particles.

A preliminary experiment showed that NIH 3T3 fibroblasts were attaching and growing on the outer surfaces of 1.5% 3-D chitosan matrices. The NIH 3T3 fibroblasts were observed to attach, spread and proliferate on the surface of these thin chitosan discs with a phase contrast microscope. The fibroblasts were not observed to migrate into

these matrices, and only attached to the external surface of the matrices. This is probably a result of the small or non-existent pore size distribution of the 1.5% chitosan matrices.

5.4. Conclusions

The 1.5% chitosan matrices were formed with very similar porosities. The low error with this parameter indicates that 3-D matrices were formed in a reproducible manner. The surfaces of thin discs of the 3-D matrices supported NIH 3T3 cell attachment, spreading and proliferation as indicated by visual observation of cells on these samples. This method for 3-D matrix formation results in sponge-like matrices with very low porosities.

Future attempts to develop porous scaffolds from the gels described by the procedure in Section 5.2 might utilize some of the freezing methods described by Madihally and Matthew[130], which are discussed in detail in Chapter7. In brief, a modification of the freezing conditions may introduce pores into a non-porous material, resulting in a structure with pores that possess a non-porous outer membrane. A 3-D matrix with controlled porous and non-porous components may have greater structural integrity than a completely porous matrix. Further characterization of porosity of samples should include SEM imaging. These tests provide a clear picture of the pore size and structure of porous matrices. Also, future experiments should attempt to characterize the SFE of 3-D matrices through cell spreading experiments. This will be discussed in further detail in Chapter 7.

Chapter 6

CONCLUSIONS

6.1. Chitosan Film Formation and Characterization

6.1.1. 2-D Film Formation

The 0.5% and 3.0% chitosan films were cast with reproducible tensile properties as indicated by the low standard errors of the mean values in Table 1. The 1.5% chitosan film had very high standard errors for most of the film properties, and was not considered for observation of trends in tensile properties with varying chitosan concentration. One possible reason for the variability in the thickness of the 1.5% chitosan films may be because these films were produced earlier in the project, and the protocol was not as refined as for later film production. Also, the glass support on which the films were cast might not have been completely leveled, resulting in an uneven film. The dry-tested Young's modulus of elasticity of chitosan films does not show an increase with increasing chitosan concentration as previous researchers have suggested with wet films. Another study partially confirms our observation of no trend in Young's modulus of elasticity with the dry tensile strength through testing of the degree of polymer *N*-acetylation and dry tensile strength [141]. Because of the variable tensile properties of the 1.5% chitosan films, a trend still might exist between chitosan concentration and the dry-tested Young's modulus of elasticity. The wet tensile properties of the films should also be investigated.

6.1.2. Surface Roughness of Films

The chitosan films cast on the glass support all displayed similar average roughness values. The Ra values were greater when mounted on tape for testing compared to when tested on a completely smooth surface. These Ra values were approximately one order of magnitude lower than texture dimensions shown to affect attachment, orientation and spreading. All concentration films were considered to be smooth. The solution concentration doesn't appear to affect the surface roughness of films cast on glass supports. The 3.0% chitosan films cast on lexan had parallel groove dimensions similar to those machined into the support for casting. These dimensions were on the μm scale suspected to influence cellular behavior. The average Ra values were very similar for equal concentration films with very low standard error in mean value, indicating that the films were cast in a reproducible manner.

6.1.3. Surface Free Energy Estimation by Contact Angle Measurement

The WIA contact angles of the three concentration chitosan films are in the reported optimum range of 60-90 degrees to support maximum cell adhesion[214]. All concentration chitosan films as well as polystyrene controls should support cell attachment and adhesion based on the reported WIA contact angles. The estimated SFE of the untreated chitosan films is in a range shown to promote fibroblast spreading[203]. Thus, all of these substrates should support the adhesion and spreading of 3T3 fibroblasts.

Exposing the 1.5% and 3.0% chitosan films to UV-IR radiation for varying times can change the increase SFE of the films. This may be due to crosslinking of the chitosan films due from the UV radiation. Also, the sterilization process may be changing the degree of deacetylation of the chitosan films, which may result in an increase in the

overall film SFE. These results suggest the possibility for optimizing cell spreading and growth of 3T3 fibroblasts on these chitosan films by changing the increasing SFE. Fibroblast spreading is greatest on substrates with surface energies greater than 55 erg/cm^2 (mJ/m^2)[203]. Further study of this behavior with SFE and UV-IR sterilization should include more time points between 0 and 12 hours of UV-IR treatment, as well as longer sterilization times. Experiments should be performed on films exposed to UV-IR radiation for times longer than 24 hours to determine whether the SFE of the chitosan films will continue to increase or approach an asymptotic value. Also, the effects of the UV and IR radiation should be studied separately. The treatment of films with IR radiation is not expected to significantly effect the films, because it is a low energy treatment.

6.1.4. Degree of Deacetylation

The degree of deacetylation for chitosan was characterized with FTIR measurements. The DDA of the Aldrich chitosan was best characterized using a modified baseline technique that was modeled after that outlined by Gupta and Kumar[74]. This technique gives accurate estimations of the DDA of chitosan samples. The DDA of chitosan samples sterilized with UV-IR should be estimated with this technique to determine whether the sterilization process is affecting the DDA of the films.

6.2. Cell Culture Experiments

6.2.1. Growth Cycle

The NIH-3T3 fibroblasts display the standard phases of cell growth, as depicted in Figure 19. The PDT and SD are important indicators of baseline NIH-3T3 cell

behavior. These parameters can be used to determine the seeding densities and sampling times of experiments on the attachment and growth of NIH-3T3 fibroblasts on chitosan films and controls. The SD and PDT should be used as a baseline for comparison to subsequent experiments of NIH-3T3 attachment and growth.

6.2.2. Attachment Experiments

All substrates support the attachment of NIH-3T3 fibroblasts. The polystyrene controls support greater fibroblast attachment than the 1.5% or 3.0% chitosan films. The 0.5% chitosan films and the polystyrene controls exhibit very similar attachment behavior. The rate of attachment for the 0.5% chitosan film and controls within the first 20 minutes is much greater than that for the next 40 minutes, indicating the attachment process to be very fast. The majority of fibroblasts that will attach do so within the first 60 minutes of inoculation. These results in conjunction with the WIA contact angle data from chapter 3 indicate that the WIA contact angle of chitosan films may be an indicator for the degree at which they will support fibroblast attachment, with lower WIA's implying better fibroblast attachment.

Based on the 95% confidence intervals of attachment data, the 0.5% chitosan films and the untreated polystyrene controls exhibit similar attachment and should not be considered statistically different. The 1.5% and 3.0% films supported similar cell attachment, at lower rates than the 0.5% film or controls. A higher variability in the 1.5% films compared to other concentrations or controls was not observed, as was reported for this films tensile properties, water-in-air contact angle and surface free energy in Chapter 3. Thus, the variability noticed in the physical parameters of the films doesn't appear to affect their biological function. Fibroblasts did not attach to grooved 3.0% chitosan films

cast on Lexan. Reasons for this are probably related to the Lexan support on which films were cast. Because the Lexan could not be autoclaved for sterilization, the resulting films cast on this support most likely contained contaminants from the support, which were toxic to cells. Future experimentation with a grooved film should utilize a support that can be autoclaved for sterilization. Lexan is not a suitable material for casting chitosan films.

6.2.3. Growth and Spreading Experiments

The chitosan films cast on glass support the growth of NIH-3T3 fibroblasts. The number of cells that will attach and grow during the first 12 hours in culture was lower than the number of cells that will attach to the films in the first 60 minutes. This may be due to cells initially attaching to the chitosan films but not subsequently spreading or growing. This is an interesting result indicating that even though the chitosan films were shown to support over 50% cell attachment within the first 60 minutes of inoculation, only a fraction of those cells attached actually continued to proliferate. This indicates that many initially attached cells did not grow and detached from the films.

The fibroblasts begin exponential growth on polystyrene controls after 12 hours in culture and on chitosan films after 24 hours in culture. This may represent the time required for viable attached fibroblasts to secrete ECM proteins which encourage subsequent proliferation. These results agree with previous studies which indicated that after 24 hours in culture, fibroblasts will have produced enough of their own ECM proteins to continue growth at rates comparable to other substrates [75]. Once in the exponential growth phase, fibroblasts cultured on chitosan films displayed slightly longer PDT's than ones cultured on polystyrene controls.

The chitosan films support the attachment, subsequent spreading and growth of NIH-3T3 fibroblasts. This data confirms the WIA and SFE data of Chapter 3 which indicated that all films and controls should support cell functions of attachment, spreading and growth. The NIH-3T3 fibroblasts initially attach to the films and controls in a random orientation, confirming the hypothesis that the Ra of the films would not affect the orientation of cells during attachment. The fibroblasts appear to prefer growth in colonies on all concentration chitosan films, which may be a result of increased collagen and fibronectin production by fibroblast colonies. This observation is very important, because these aggregates can be correlated to cell-cell interactions, cell differentiation, viability, migration and subsequent tissue formation. The aggregation of cells resembles the cell-cell interactions typically found in tissues, and cell function and survival can be improved in aggregate cultures. Also, chitosan films promoting these aggregates indicate potential tissue engineering aspects of these films, as they may act to enhance tissue function [197].

6.3. 3-D Scaffold Formation

The 1.5% chitosan matrices were formed with very similar porosities. The low error with this parameter indicates that 3-D matrices were formed in a reproducible manner. The surfaces of thin discs of the 3-D matrices supported NIH 3T3 cell attachment, spreading and proliferation as indicated by visual observation of cells on these samples. This method for 3-D matrix formation results in sponge-like matrices with very low porosities.

Future attempts to develop porous scaffolds from the gels described by the procedure in Section 5.2 might utilize some of the freezing methods described by

Madihally and Matthew[130], which are discussed in detail in Chapter7. In brief, a modification of the freezing conditions may introduce pores into a non-porous material, resulting in a structure with pores that possess a non-porous outer membrane. A 3-D matrix with controlled porous and non-porous components may have greater structural integrity than a completely porous matrix. Further characterization of porosity of samples should include SEM imaging. These tests provide a clear picture of the pore size and structure of porous matrices. Also, future tests should attempt to characterize matrix SFEs with cell spreading experiments.

Chapter 7

RECOMMENDATIONS FOR FUTURE WORK

7.1. Introduction

The results of this project indicate that NIH 3T3 fibroblasts will attach and grow on 2-D chitosan films. These results also indicate that the 2-D films were formed in a reproducible manner. One important chitosan film parameter characterized was the SFE of the films. This study indicates that treatment of films with UV-IR radiation can increase the overall SFE depending on the treatment time. The SFE has been identified as an important parameter corresponding to cell function on a substrate. The SFE of a substrate can affect cellular adhesion, spreading, migration and proliferation. This study briefly describes a method for the formation of non-porous 3-D chitosan sponges. This chapter suggests possible future experiments for the characterization of chitosan scaffolds for cell culture applications.

7.2. 3-D Scaffold Formation

The 3-D chitosan sponges developed in this project did not possess a significant pore structure. Cells were observed to attach and grow on the surfaces of these sponges, but not within the sponge matrix. For an implatation application, matrices should be porous (with pore dimensions greater than 10 μm) to allow for cellular migration and interaction, while not interfering with the diffusion of hormones, nutrients and metabolites into the matrix, which provide nourishment and initiate cellular responses [212]. Further studies should be performed to develop chitosan sponges using ionotropic gellation with pore structures that optimize cell attachment, spreading, growth and migration.

Madihally and Matthew[129] began preliminary investigations on the development of porous 3-D chitosan scaffolds using techniques similar to those described in chapter 5.2. These techniques appear promising for the development of scaffolds suitable for cell culture experiments. The resulting matrices had controlled mean pore diameters between 1-250 μm depending on the chitosan concentrations used as well as the freezing conditions of the method. These matrices also exhibited versatility with respect to controlling the overall scaffold shape. The results of Chapter 5 indicate that the 1.5% chitosan sponges had negligible porosities. Thus, a modification of the freezing conditions may introduce pores into a non-porous material, resulting in a structure with pores that possess a non-porous outer membrane. A 3-D matrix with controlled porous and non-porous components may have greater structural integrity than a completely porous matrix.

The techniques of Madihally and Matthew are briefly summarized here. Bulk scaffolds were prepared by freezing and lyophilizing chitosan solutions in pre-cooled, flat bottomed glass tubes. Freezing was accomplished by immersing the tubes, containing chitosan solution, in freezing baths maintained at –20 °C, -78 °C, and –196 °C. The samples were then lyophilized until dry. Planar scaffolds were formed by freezing chitosan solutions in polystyrene petri dishes. The dishes were placed with their bottom surfaces in contact with either liquid nitrogen or a dry ice slab (-78 °C), resulting in pores forming perpendicular to the sample plane. Also, pores approximately parallel to the sample plane were formed by filling a polystyrene mold with a chitosan solution followed by slow immersion into liquid nitrogen. After freezing, molds were opened to expose one frozen surface then lyophilized. Porous tubular scaffolds were formed by

injecting 1 or 2 wt % chitosan solutions into the annular space between concentric silicone or PTFE tubes and frozen by direct contact with dry ice (-78 °C). The outer tube was then removed and the assembly lyophilized. This method for porous tubular scaffolds was modified to create porous tubes with a non-porous inner membrane, by first coating the inner silicone tube with a chitosan film by dipping it into a 2% chitosan solution, gelling the film by brief immersion in an aqueous ammonia solution and drying at air temperature. Finally, the annular mold was assembled using the coated inner tube, filled with chitosan solution and processed as described above for porous tubular scaffolds. All lyophilized scaffolds were rehydrated and stabilized in either dilute NaOH or an ethanol series. Scaffolds were finally equilibrated with PBS [129]. These scaffolds were characterized with tensile testing, light and electron microscopy.

These methods provide a technique with control over the mean pore diameters within the range of 1 to 250 μm through variation of the freezing conditions, with lower freezing temperatures resulting in matrices with lower mean pore sizes. Also, the use of higher chitosan concentrations resulted in lower mean pore sizes. Hydrated porous samples exhibited extensions twice that as non-porous membranes under tensile conditions. The elastic moduli and tensile strengths of these membranes were about tenfold lower than non-porous membranes [129].

7.3. Surface Free Energy Experiments

The results of Chapter 3 indicate that exposing the chitosan films to UV-IR radiation for varying times can increase the SFE of the 1.5% and 3.0% films. Future study should further investigate the trends in the effects of UV-IR sterilization on the SFE of 2-D and 3-D chitosan materials. The goal would be to maximize the SFE of the chitosan-based

materials to improve fibroblast attachment, spreading and growth. The 2-D films can be studied with contact angle experiments similar to those outlined in Chapter 3. Studies on the SFE of 3-D films should be performed via fibroblast spreading experiments. A relationship between fibroblast spreading and substrate SFE can be established with substrates of varying SFE's. This relation could then be used to estimate the SFE of a porous matrix based on the extent of fibroblast spreading.

The effects of the UV treatment and the IR treatment on the films should be studied separately, because the UV treatment and the IR treatment might have unique effects on the overall SFE of chitosan films. Futher testing on tensile properties of films should be performed to characterize this proposed effect of UV and IR treatment on chitosan films. Any change in film properties due to UV or IR sterilization might be reflected in the film tensile properties. The effect of the wavelength of UV and IR radiation on the SFE of the chitosan films should also be investigated.

Other factors, including the film thickness, exposure time, distance from lamps to samples might also be considered. The thickness of the films might affect the respective change in SFE based on which side of the film is exposed to the UV-IR radiation. The exposure time was shown to be a key in the change in film SFE over time, so a more detailed study of these effects within the first 24 hours of treatment as well as for times greater than 24 hours should be investigated. Also, the distance that the UV-IR lamps are placed from the chitosan samples may have an effect on the change in SFE over time. There is currently a lack of information on the effect of sterilization on the SFE of chitosan films and matrices for tissue engineering applications.

7.4. Adhesion Experiments

The adhesion of a cell to a substrate is a very important characteristic. Certain tissue engineering applications require biomaterials to promote as well as inhibit cell contact. One example lies in the design of antithrombogenic grafts. Cell attachment is needed to seed endothelial cells on the inner wall to create a natural lining, while the inner lining should not allow the attachment of platelets or erythrocytes [46]. This may be achieved by introducing a specific attachment protein onto the chitosan substrate that is selective to endothelial cells by protein adsorption. The strength to which a cell can adhere to a substrate can affect its subsequent migration. A weak or moderate strength of attachment favors cell migration, and a strong attachment tends to immobilize the cell [192]. Cell adhesion experiments can be undertaken to investigate the strength of cellular attachment to various substrates.

One method to measure the force of cell adhesion utilizes radial flow detachment with a spinning disc, where fluid is circulated from the center to the periphery of the chamber radially, so that the shear force imparted on cells decreases with radial position from the center to the edge of the disc. This set up is useful because a range of shear forces on the attachment of cells can be studied simultaneously [87]. Another method for measuring cellular adhesion utilizes a parallel-plate flow chamber. This method utilizes a chamber in which cellular adhesion can be studied by exposing cells to a range of shear forces resulting from fluid passing through the chamber at different rates [197]. One study developed a parallel-plate flow chamber in which the cellular behavior could be continuously observed and recorded with a microscope connected to a video camera. The

detachment of adherent human skin fibroblasts on poly(methylmethacrylate) was shown to depend on time and shear stress [223].

7.5. Spreading Experiments

Another important function of NIH 3T3 fibroblasts is the extent of cell spreading on a substrate. Cell morphology, indicated by its spreading, is one index identifying cell behavior [211]. Experiments can be performed to characterize this important cellular parameter. Photographs of the cells can be taken at various times, and an image analysis software, such as Image-Pro Plus version 4.1, can be used to estimate the spreading area of individual cells. These images can be used to compare the influence of different substrates on cell spreading. A parallel-plate flow chamber or spinning disc apparatus can be fabricated to enable the study of cells under a characterized shear force as previously mentioned in section 7.4, which can also be related to the extent of cell spreading.

7.6. Protein Adsorption and Serum-Free Experiments

Serum proteins can greatly influence the attachment, spreading and growth of cells on a substrate. A damaged tissue will possess a significant amount of proteins due to the inflammatory stages of wound repair *in vivo*. The addition of serum to cell culture medium *in vitro* assists the cells in initial attachment and growth on substrates through protein adsorption by the substrate. Most substrates will adsorb a layer of serum proteins after a very short time of exposure to these proteins, both *in vitro* and *in vivo*. Thus, it is important to characterize the extent to which a biomaterial used for tissue culture applications will adsorb proteins *in vitro* and *in vivo*. A material that has a higher affinity

for protein adsorption may promote greater cell attachment, spreading and growth than one with a low protein adsorption capability. Methods for the characterization of extent of protein adsorption by chitosan films and matrices include IR spectroscopy. This procedure uses IR light at a glancing incidence to the sample plane, which is reflects back so the intensity of the light can be measured. The adsorption of thin protein layers will affect the returning IR light intensity [126]. Alternatively, a protein assay could be performed on a solution of proteins after detaching from the subtrate with the aid of an enzyme such as trypsin-EDTA to characterize the extent of protein adsoprtion.

Also, experiments should be performed in serum-free conditions to understand how the cells alone interact with the substrate without the aid of serum proteins for processes of attachment, spreading and growth. This gives an understanding of the surface properties of the substrate. A successful implantable biomaterial should exhibit properties favorable for fibroblast attachment to the substrate in the absence of serum proteins, but should also exploit the adsorption of serum proteins when present to maximize cell attachment, spreading and growth.

7.7. Modify Substrates with Proteins and Growth Factors

Another desirable trait for an implantable biomaterial is its potential for modification by the addition of bioactive molecules. An example of surface modification of a polymer to increase cell attachment and growth is glow-discharge treatment of polystyrene to increase the number of charged groups on the surface and the polymer's overall hydrophobicity [3]. Studies can be performed regarding the ability of chitosan films and matrices to sustain modification by the addition of growth factors or attachment proteins, which enhance cellular function. One possible study would investigate the

potential for fibronectin, or specifically the RGD attachment sequence, to be added to chitosan films or matrices by adsorption. The addition of specific growth factors and attachment proteins can greatly affect the function of cells, including the attachment, spreading, growth and differentiation of cells.

Examples of modifications of chitosan biomaterials include the anticoagulant membranes for blood ultra-filtration prepared by immobilizing important biological molecules like heparin on chitosan [30]. Also, the biodegradation of chitosan linked to BMP led to the controlled release of BMP. Quantitative measurement of the form of the tissue around the chitosan showed that bone tissue regeneration in a surgical bone defect is improved using this special chitosan [160]. Another study used chitosan gels to model the controlled release of bovine serum albumin (BSA) [185]. Furthermore, controlled-release studies of BSA from chitosan-alginate membranes have shown chitosan's potential for the delayed release of a protein [175]. These studies indicate chitosan has great potential to stimulate wound healing, which can be further enhanced by modifying the polysaccharide with proteins.

7.8. Summary

The current research has illustrated chitosan's ability to support NIH 3T3 fibroblast attachment, spreading and growth in 2-D culture applications. Because of the promise of 2-D chitosan films for cell culture applications, future research should further explore the potential of this polysaccharide for 3-D implantable tissue engineering applications. Some experiments that could be performed include further study of the relationship between SFE and UV-IR sterilization of films. Also, 3-D chitosan matrices should be characterized and investigated for NIH-3T3 fibroblast attachment, spreading and growth

as well as with other tissues vital to wound repair. These films and matrices may be modified with proteins and growth factors, which can improve the attachment, spreading and growth of cells, thereby improving the wound healing capability of these materials. Future cell culture experiments should include adhesion experiments to characterize the strength of cell adhesion to these substrates, cell spreading experiments and serum-free experiments to understand how the substrates alone are interacting with cells without the aid of attachment proteins.

BIBLIOGRAPHY

1. Allan, G., L. Altman, R. Bensinger, D. Ghosh, Y. Hirabayashi, A. Neogi, and S. Neogi. *Chitin, Chitosan and Related Enzymes*. New York: Academic Press, Inc., 1984.

2. Allen, R. F., N. C. Baldini, E. L. Gutman, J. G. Kramer, C. Leinweber, V. A. Mayer, and P. A. McGee, 102-7. *1998 Annual Book of ASTM Standards. Paper; Packaging; Flexible Barrier Materials; Business Imaging Products.* West Conshohocken, PA: American Society for Testing and Materials, 1998.

3. Amstein, C., and P. Hartman. "Adaptation of Plastic Surfaces for Tissue Culture by Glow Discharge." *Journal of Clinical Microbiology* 2 (1975): 46-54.

4. Andrade, J., and V. Hlady. "Protein Adsorption and Materials Biocompatibility: a Tutorial Review and Suggested Hypothesis." *Advanced Polymer Science* 79 (1986): 1-63.

5. Baier, R. "Surface Properties Influencing Biological Adhesion." *Adhesion in Biological Systems.* R. Manly, 15-45. New York: Academic Press, 1970.

6. Balassa, L., and J. Prudden. *MIT Sea Grant Report*, 78-7. 1978.

7. Barnes, D., and G. Sato. "Method for Growth of Cultures Cells in Serum-Free Medium." *Analytical Biochemistry* 102 (1980): 255-270.

8. Bell, E., B. Ivarson, and C. Merrill. "Production of a Tissue-Like Structure by Contraction of Collagen Lattices by Human Fibroblasts of Different Proliferative Potential *in Vitro*." *Cell Biology* 76 (1979): 1274-1278.

9. Ben-Ze'ev, A., G. Robinson, N. Bucher, and S. Farmer. "Cell-Cell and Cell-Matrix Interactions Differentially Regulate the Expression of Hepatic and Cytoskeletal Genes in Primary Culture of Rat Hepatocytes." *Proceedings of the Academy of Natural Sciences* 85 (1988): 2161-2165.

10. Bennet, N., and G. Schultz. "Growth Factors and Wound Healing: Part II. Role in Normal and Chronic Wound Healing." *American Journal of Surgery* 166 (1993): 74-81.

11. Berscht, P. C., B. Nies, A. Liebendorfer, and J. Kreuter. "Incorporation of Basic Fibroblast Growth Factor into Methylpyrrolidinone Chitosan Fleeces and Determination of the in Vitro Release Characteristics." *Biomaterials* 18, (1994): 593-600.

12. Bhatia, S. N., M. L. Yarmush, and M. Toner. "Controlling Cell Interactions by Micropatterning in Co-Cultures: Hepatocytes and 3T3 Fibroblasts." *Journal of Biomedical Materials Research* 34 (1997): 189-199.

13. Blackburn, C., P. Swank-Hill, and R. Schnaar. "Gangliosides support neural retina cell adhesion. " *Journal of Biological Chemistry* 261 (1986): 2873-2881.

14. Blumenthal, N., J. Ricci, and H. Alexander. "The Effects of Implant Surfaces on Bone Mineral Formation *in Vitro*." *Transactions of the Annual Meeting of the Society for Biomaterials* 12 (1989): 2.

15. Bodmeier, R., K. H. Oh, and Y. Pramar. "Preparation and Evaluation of Drug-Containing Chitosan Beads." *Drug Development and Industrial Pharmacy* 15, 9 (1989): 1475-1494.

16. Bohnert, A., J. Hornung, I. Mackenzie, and N. Fusenig. "Epithelial-Mesenchymal Interaction Control Basement Membrane Production and Differentiation in Cultured and Transplanted Mouse Keratinocytes." *Cell Tissue Research* 244 (1986): 413-429.

17. Bourin, M., and U. Lindahl. "Glycosaminoglycans and the regulation of blood coagulation. " *Biochemical Journal* 289 (1993): 313-330.

18. Bradford, M. "A Rapid and Sensitive Method for the Quantitation of Microgram Quantities of Protein Using the Principle of Protein-Dye Binding." *Analytical Biochemistry* 72 (1976): 248-254.

19. Brandley, B. K., O. A. Weisz, and R. L. Schnaar. "Cell Attachment and Long-Term Growth on Derivatizable Polyacrylamide Surfaces." *Journal of Biological Chemistry* 262, 13 (1987): 6431-6437.

20. Broadley, K., A. Aquino, and B. Hicks. "Growth Factors BFGF and TGF-β Accelerate the Rate of Wound Repair in Normal and Diabetic Rats." *International Journal of Tissue Reactions - Experimental and Clinical Aspects* 6 (1988): 345-353.

21. Brunauer, S., P. H. Emmett, and E. J. Teller. "BET Surface Area Calculations." *American Chemical Society*, 60 (1938): 309.

22. Brunette, D. "Fibroblasts on Micromachined Substrata Orient Hierarchically to Grooves of Different Dimensions." *Experimental Cell Research* 164 (1986): 11-26.

23. Burke, J., I. Yannas, W. Quimby, C. Bondoc, and W. Jung. "Successful Use of a Physiologically Acceptable Artificial Skin in the Treatment of Extensive Burn Injury." *Annals of Surgery* 194 (1981): 413-428.

24. Burridge, K., and L. Connell. "A New Protein of Adhesion Plaques and Ruffling Membranes." *Journal of Cell Biology* 97 (1983): 359.

25. Cancer Web, and D. Howe, site designer. Web page, 1998 [accessed August 2001]. Available at http://www.graylab.ac.uk/omd/.

26. Carreno-Gomez, B., and R. Duncan. "Evaluation of the Biological Properties of Soluble Chitosan and Chitosan Microspheres." *International Journal of Pharmaceutics* 148 (1997): 231-240.

27. Casser-Bette, M, A. B. Murray, E. I. Closs, V. Erfle, and J. Schmidt. "Bone Formation by Osteoblast Like Cells in a Tree-Dimensional Cell Culture." *Calcified Tissue International* 46 (1990): 46-56.

28. Castellot, J., M. Karnovsky, and B. Spiegelman. "Differentiation-Dependent Stimulation of Neovascularization and Endothelial Cell Chemotaxis by 3T3 Adipocytes." *Proceedings of the National Academy of Sciences of the United States of America* 79 (1982): 5597-5601.

29. Cavari, S., and M. Ruggiero. "Antiproliferative Effects of Heparin on Normal and Transformed NIH/3T3 Fibroblasts." *Cell Biology International* 17 (1993): 781-786.

30. Chandy, T., and C. Sharma. "Bioactive Molecules Immobilized to Liposome Modified Albumin Blended Chitosan Membranes - Antithrombotic and Permeability Properties." *Journal of Colloid and Interfacial Science* 130, (1989): 331-340.

31. Chandy, T., and C. Sharma. "Chitosan - As a Biomaterial." *Biomaterials, Artificial Cells, Artificial Organs* 18, (1990): 1-24.

32. Chandy, T., and G. H. R. Rao. "Evaluation of Heparin Immobilized Chitosan-PEG Microbeads for Charcoal Encapsulation and Endotoxin Removal." *Artery Cells, Blood Substitutes, and Immobilization Biotechnology* 28, no. 1 (2000): 65-77.

33. Chesmel, K., C. Clark, and J. Black. "Culture Surface Morphology and Chemistry Have a Synergistic Effect on Bone Cell Protein Synthesis." *Transactions of the Annual Meeting of the Society for Biomaterials* 12 (1989): 1.

34. Chevallay, B., N. Abdul-Malak, and D. Herbage. "Mouse Fibroblasts in Long-Term Culture Within Collagen Three-Dimensional Scaffolds: Matrix Reorganization, Growth, Biosynthetic and Proteolytic Activities." *Journal of Biomedical Materials Research* 49 (2000): 448-459.

35. Chevallay, B., and D. Herbage. "Collagen-Based Biomaterials As 3D Scaffold for Cell Cultures: Applications for Tissue Engineering and Gene Tharapy." *Medical and Biological Engineering and Computing 2000b* 38 (2000): 211-218.

36. Chicquet, M., E. Puri, and D. Turner. "Fibronectin Mediates Attachment of Chicken Myoblasts to a Gelatin-Coated Substratum." *Journal of Biological Chemistry* 254 (1979): 5475-5482.

37. Chuang, W.-Y., T.-H. Young, C.-H. Yao, and W.-Y. Chiu. "Properties of the Poly(Vinyl Alcohol)/Chitosan Blend and Its Effect on the Culture of Fibroblast *In Vitro* ." *Biomaterials* 20 (1999): 1479-1487.

38. Cima, L., D. Ingber, J. Vacanti, and R. Langer. "Hepatocyte Culture on Biodegradable Polymeric Substrates." *Biotechnology and Bioengineering* 38 (1991): 145-158.

39. Clark, D. S. "Can Immobilization Be Exploited to Modify Enzyme Activity?" *TIBTECH* 12 (1994): 439-443.

40. Collumbel, C., O. Damour, C. Gagnieu, F. Poinsignon, C. Echinard, and J. Marichy, "Biomaterials for Artificial Skin and Implants Containing Acetylated Chitosan, Collagens and GAGs." Europe Patent Applications, Assignee. France IP 296,078. 1988.

41. Cook, J., B. Crute, and L. Patrone. "Microporosity of the Substratum Regulates Differentiation of MDCK Cells *in Vitro*." *In Vitro Cellular Developmental Biology* 25 (1989): 914-922.

42. Couchman, J., M. Hook, D. Rees, and R. Timpl. "Adhesion, Growth and Matrix Production by Fibroblasts on Laminin Substrates." *Journal of Cell Biology* 96 (1983): 177-183.

43. Culp, L. "Adhesion of Fibroblasts to Artificial Substrata." *Biocompatible Polymers, Metals and Composites*, M. Szycher, 701-21. Lancaster, PA: Technomic Publishing Inc., 1983.

44. D'agnese, J. "Brothers With Heart." *Discover* (2001): 36-43, 102.

45. Damour, O., P. Y. Gueugniaud, P. Berthin-Maghit, P. Rousselle, F. Berthod, F. Sahuc, and C. Collumbel. "A Dermal Substrate Made of Collagen-GAG-Chitosan for Deep Burn Coverage: First Clinical Uses." *Clinical Materials* 15 (1994): 273-276.

46. Desai, N. P., and J. A. Hubbell. "The Short-Term Blood Biocompatibility of Poly(Hydroxyethylmethacrylate-Co-Methyl Methacrylate) in an *in Vitro* Flow System Measured by Videomicroscopy." *Journal of Biomaterials Science-Polymer Edition* 1, no. 2 (1989): 123-146.

47. Diamantstein, T., M. Klos, H. Osawa, and Z. Chen. "Chitin: an immunological adjuvant and a polyclonal B-lymphocyte activator. " *International Archives of Allergy and Applied Immunology* 68 (1982): 377-381.

48. Dongxu, P., C. Xiaodong, M. Lijiang, H. Yuanjie, X. Wenshu, S. Ruihuan, and Z. Ying. "Study on Nerve Cell Affinity of Polymer Hydrogel Films." *3rd Far-Eastern Symposium on Biomedical Materials.* China.

49. Ehrlich, H., D. Buttle, and D. Bernanke. "Physiological Variables Affecting Collagen Lattice Contraction by Human Dermal Fibroblast." *Experimental and Molecular Pathology* 50 (1989): 220-229.

50. Elghannam, A., P. Ducheyne, and I. M. Shapiro. "Bioactive Material Template for *in Vitro* Synthesis of Bone." *Journal of Biomedical Materials Research* 29 (1995): 357-370.

51. Engvall, E., and E. Ruoslahti. "Binding of Soluble Form of Fibroblast Surface Protein, Fibronectin, to Collagen." *International Journal of Cancer* 20 (1977): 1-5.

52. Fager, G., G. Hansson, P. Ottosson, B. Dahllof, and G. Bondjers. "Human Arterial Smooth Muscle Cells in Culture. Effects of Platelet-Derived Growth Factor and Heparin on Growth *in Vitro*." *Experimental Cell Research* 176 (1988): 319-335.

53. Foidart, J., J. Berman, S. Paglia, S. Rennard, S. Abe, A. Perantoni, and G. Martin. "Synthesis of Fibronectin, Laminin, and Several Collagens by a Liver-Derived Epithelial Cell Line." *Laboratory Investigation* 42 (1980): 525-532.

54. Folkman, J., and A. Moscona. "Role of Cell Shape in Growth Control." *Nature* 273 (1976): 345-349.

55. Fox, H., and W. Zisman. "The Spreading of Liquids on Low Energy Surfaces. I. Polytetraflouroethylene." *Journal of Colloid Science* 5 (1950): 514-531.

56. Freed, L. E., and G. Vunjak-Novakovic. "Culture of Organized Cell Communities." *Advanced Drug Delivery Reviews* 33 (1998): 15-30.

57. Freshney, R. I. *Culture of Animal Cells. A Manual of Basic Technique.* 2nd Edition. New York: Alan R. Liss, Inc., 1987.

58. Frisch, S., and H. Francis. "Disruption of Epithelial Cell-Matrix Interactions Induces Apoptosis." *Journal of Cell Biology* 124 (1994): 619-626.

59. Gauss-Muller, V., H. Kleinman, G. Martin, and E. Schiffmann. "Role of Attachment and Attractants in Fibroblast Chemotaxis." *Journal of Laboratory and Clinical Medicine* 96 (1980): 1071-1080.

60. Geiger, B. "A 130K Protein From Chicken Gizzard: Its Localization at the Terminal of Microfilament Bundles in Cultured Chicken Cells." *Cell* 18 (1979): 193.

61. Giannobile, W., R. Finkelman, and Lynch S. "Comparison of Canine and Non-Human Primate Animal Models for Periodontal Regenerative Therapy: Results Following a Single Administration of PDGF/IGF-I." *Journal of Periodontology* 65 (1994): 1158-1168.

62. Gimenez-Gallego, G., G. Conn, V. Hatcher, and K. Thomas. "Human Brain-Derived Acidic and Basid Fibroblast Growth Factors: Amino Terminal Sequences and Specific Mitogenic Activities." *Biochemical and Biophysical Research Communications* 135 (1986): 541-548.

63. Goldberg, S., R. Doyle, and M. Rosenberg. "Mechanism of Enhancement of Microbial Cell Hydrophobicity by Cationic Polymers." *Journal of Bacteriology* 172 (1990): 5650-5654.

64. Good, R. J., and C. J. van Oss. "The Modern Theory of Contact Angles and the Hydrogen Bond Components of Surface Energies." *Modern Approaches to Wettability. Theory and Applications.* 1st Edition. M. E. Schrader, and G. I. Loeb, 1-19. New York: Plenum Press, 1992.

65. Goosen, M. F. A., O-W Achaw, and E. W. Grandmaison. "Chitosan-Alginate Affinity Microcapsules for Isolation of Bovine Serum Albumin." *Applications of Chitin and Chitosan.* M. F. A. Goosen, 233-254. Lancaster, PA: Technomic Publishing Company, Inc., 1997.

66. Gospodarowicz, B., G. Greenburg, and C. R. Birdwell. "Determination of Cellular Shape by the Extracellular Matrix and Its Correlation With the Control of Cellular Growth." *Cancer Research* 38 (1978): 4155-4171.

67. Gospodarowicz, D., and J. Cheng. "Heparin Protects Basic and Acidic FGF From Inactivation." *Journal of Cellular Physiology* 128 (1986): 475-484.

68. Graves, D., Y. Kang, and K. Kose. "Growth Factors in Periodontal Regeneration." *Compendium on Continuing Education for the Practicing Veterinarian* 18 (1994): S672-S677.

69. Green, H., J. G. Rheinwald, and T. Sun. "Properties of an Epithelial Cell Type in Culture: the Epodermal Keratinocyte and Its Dependance on Products of the Fibroblast." *Cell Shape and Surface Architecture* (1977): 493-500.

70. Grinnell, F. "Cellular Adhesiveness and Extracellular Substrata." *International Review of Cytology - a Survey of Cell Biology* 53 (1978): 65-144.

71. Grinnell, F., and M. Field. "Initial Adhesion of Human Fibroblasts in Serum-Free Medium: Possible Role of Secreted Fibronectin." *Cell* 17 (1979): 117-128.

72. Grinnell, F., M. Field, and D. Minter. "Fibroblast Adhesion to Fibrinogen and Fibrin Substrates; Requirement for Cold-Insolube Globulin (Plama Fibronectin)." *Cell* 19 (1980): 517-525.

73. Guarnaccia, S., and R. Schnaar. "Hepatocyte adhesion to immobilized carbohydrates. II. Cellular modification of the carbohydrate surface. " *Journal of Biological Chemistry* 257 (1982): 14288-14292.

74. Gupta, K. C., and P. Kumar. "Structural Changes and Release Characteristics of Crosslinked Chitosan Beads in Response to Solution PH." *Journal of Medical Science - Pure Applied Chemisty* A36, no. 5&6 (1999): 827-841.

75. Gutshe, A. T., P. Parsons-Wingerter, D. Chand, W. M. Saltzman, and K. W. Leong. "N-Acetylglucosamine and Adenosine Derivated Surfaces for Cell Culture: 3T3 Fibroblast and Chicken Hepatocyte Response." *Biotechnology and Bioengineering* 43 (1994): 801-809.

76. Haipeng, G., Z. Yinghui, L. Jianchun, G. Yandao, Z. Nanming, and Z. Xiufang. "Studies on Nerve Cell Affinity of Chitosan-Derived Materials." *Journal of Biomedical Materials Research* 52 (2000): 285-895.

77. Hamano, T., D. Chiba, A. Teramoto, Y. Kondo, and K. Abe. "Effects of Polyelectrolyte Complex (PEC) on Human Periodontal Ligament Fibroblast (HPLF) Functions in the Presence of Glucocorticoids." *Journal of Biomaterials Science Polymer Edition* no. 9 (1998): 985-1000.

78. Hasson, J., D. Wiebe, and W. Abbott. "Adult Human Vascular Endothelial Cell Attachment and Migration on Novel Bioadsorbable Polymers." *Archives of Surgery* 122 (1987): 428-430.

79. Hay, E. *Cell Biology of Extracellular Matrix*. E. Hay. New York: Plenum Press, 1981.

80. Hayashi, M., and K. Yamada. "Domain Structure of the Corboxylterminal Half of Human Plama Fibronectin." *Journal of Biological Chemistry* 258 (1983): 3332-3340.

81. Hebda, P., C. Klingbeil, J. Abraham, and J. Fiddes. "Basic Fibroblast Growth Factor Stimulation of Epidermal Wound Healing in Pigs." *Journal of Investigative Dermatology* 95 (1990): 626-631.

82. Heck, D. E., D. L. Laskin, C. R. Gardner, and J. D. Laskin. "Epidermal Growth Factor Suppresses Nitric Oxide and Hydrogen Peroxide Production by Keratinocytes. Potential Role for Nitric Oxide in the Regulation of Wound Healing." *Journal of Biological Chemistry* 267 (1992): 21227-21280.

83. Hewitt, A., H. Kleinman, J. Pennypacker, and G. Martin. "Identification of an Adhesion Factor for Chondrocytes." *Proceedings of the National Academy of Sciences of the United States of America* 77 (1980): 385-388.

84. Hong, H., and D. Brunette. "Effect of Cell Shape on Proteinase Secretion by Epithelial Cells." *Journal of Cell Science* 87 (1987): 259-267.

85. Hook, M., K. Rubin, A. Oldberg, B. Obrink, and A. Vaheri. "Cold-Insoluble Globulin Mediates the Adhesion of Rat Liver Cells to Plastic Petri Dishes." *Biochemical and Biophysical Research Communications* 79 (1977): 726-731.

86. Horbett, T. A., and M. B. Schway. "Correlations Between Mouse 3T3 Cell Spreading and Serum Fibronectin Adsorption on Glass and Hydroxyethylmethacrylate-Ethylmethacrylate Copolymers." *Journal of Biomedical Materials Research* 22 (1988): 763-793.

87. Horbett, T. A., J. J. Waldburger, B. D. Ratner, and A. S. Hoffman. "Cell Adhesion to a Series of Hydrophilic-Hydrophobic Copolymers Studies With a Spinning Disc Apparatus." *Journal of Biomedical Materials Research* 22 (1988): 383-404.

88. Horbett, T., M. Schway, and B. Ratner. "Hydrophilic-Hydrophobic Copolymers As Cell Substrates: Effect on 3T3 Cell Growth Rates." *Journal of Colloid and Interface Science* 104 (1985): 28-39.

89. Horvath, G., and K. Kawazoe. "Method for the calculation of effective pore distribution in molecular sieve carbon. " *Journal of Chemical Engineering of Japan* 16, no. 6 (1983): 470.

90. Hubbell, Jeffrey A. "Biomaterials in Tissue Engineering." *Bio-Technology* 13 (1995): 565-576.

91. Humphries, M. "The Molecular Basis and Specificity If Integrin-Ligand Interactions." *Journal of Cell Science* 97 (1990): 585-592.

92. Ikada, Y. "Surface Modification of Polymers for Medical Applications." *Biomaterials* 15, no. 10 (1994): 726-736.

93. Ikeda, K., V. P. Michelangeli, T. J. Martin, and D. M. Findlay. "Type I Collagen Substrate Increased Calcitonin and Parathyroid Hormone Receptor-Mediated Signal Transduction in UMR 106-06 Osteoblast-Like Cells." *Journal of Cellular Physiology* 156 (1993): 130-137.

94. Ingber, D. "Fibronectin Controls Capillary Endothelial Cell Growth by Modulating Cell Shape." *Proceedings of the National Academy of Sciences of the United States of America* 87 (1990): 3579-3583.

95. InteliHealth Inc. "Merriam Webster Online Medical Dictionary." Web page, 2001 [accessed August 2001]. Available at http://www.intelihealth.com/IH/ihtIH/WSIHW000/9276/9276.html?k=tnavx 408x9276.

96. Ishizaki, Y., J. Burne, and M. Raff. "Autocrine Signals Enable Chondrocytes to Survive in Culture." *Journal of Cell Biology* 126 (1994): 1069-1077.

97. Ishuag, S., G. Crane, M. Miller, A. Yasko, M. Yaszemski, and A. Mikos. "Bone Formation by Three-Dimensional Stromal Osteoblast Culture in Biodegradable Polymer Scaffolds." *Journal of Biomedical Materials Research* 36 (1997): 17-28.

98. Iwig, M., D. Glaesser, and M. Bethge. "Cell Shape-Mediated Growth Control of Lens Epithelial Cells Grown in Culture." *Experimental Cell Research* 131 (1981): 47-55.

99. Jacoby, M. "Custom-Made Biomaterials." *Chemical and Engineering News* 79, no. 6 (2001): 30-35.

100. Jameela, S., A. Misha, and A. Jayakrishinan. "Crosslinked Chitosan Microspheres As Carriers for Prolonged Delivery of Macromolecular Drugs." *International Journal of Pharmaceutics* 6, no. 7 (1994): 621-632.

101. Jauregui, H. O. "Cell Adhesion to Biomaterials - The Role of Several Extracellular Matrix Components in the Attachment of Non-Transformed Fibroblasts and Parenchymal Cells." *Trans American Society of Artifical Internal Organs* 33, no. 2 (1987): 66-74.

102. Jianchun, L., Z. Yinghui, G. Haipeng, G. Yandao, Z. Nanming, and Z. Xiufang. "A Primary Study of Using Chitosan for Nerve Repair Conduit."*5th IUMRS International Conference on Advanced Materials* China: 1999.

103. Kabat, D., B. Gliniak, and L. Rohrschneider. "Cell Anchorage Determines Whether Mammary Tumor Virus Glycoproteins Are Processed for Plasma Membranes or Secretion." *Journal of Cell Biology* 101 (1985): 2274-2283.

104. Kas, H. "Review: Chitosan: Properties, Preparations and Application to Microparticulate Systems." *Journal of Microencapsulation* 14, no. 6 (1997): 689-711.

105. Kibune, K., Y. Yamaguchi, and K. Motosugi. "Manufacture of Bandages From Chitin Fibers." Japan Kokai Tokkyo Koho, Assignee. Japan JP 63,209,661. 1988.

106. Kienzle-Sterzer, C., D. Rodriquez-Sanchez, and C. Rha. "Mechanical Properties of Chitosan Films: Effect of Solvent Acid." *Makromolecular Chemistry* 183 (1982): 1353-1359.

107. Kim, S., and C. Rha. "Chitosan for the Encapsulation of Mammalian Cell Culture." *Chitin and Chitosan - Sources, Chemistry, Biochemistry, Physical Properties and Applications.* G. Skyak-Brack, T. Anthonsen, and P. Sanford, 617-626. London: Elsevier, 1989.

108. Klebe, R. "Isolation of a Collagen-Dependent Cell Attachment Factor." *Nature* 250 (1974): 248-251.

109. Kleinman, H. K., R. J. Klebe, and G. R. Martin. "Review: Role of Collagenous Matrices in the Adhesion and Growth of Cells." *Journal of Cell Biology* 88 (1981): 473-485.

110. Klokkevold, P., L. Vandemark, E. Kennedy, and G. Bernard. "Osteogenesis Enhanced by Chitosan (Poly-N-Acetyl Glucosaminoglycan) *in Vitro*." *Journal of Periodontology* 67 (1996): 1170-1177.

111. Koller, M., and E. T. Papoutsakis. "Cell Adhesion in Animal Cell Culture: Physiological and Fluid Mechanical Implications." *Bioprocess Technology* 20 (1995): 61-110.

112. Koyano, T., N. Minoura, M. Nagura, and K. Kobayashi. "Attachment and Growth of Cultured Fibroblast Cells in PVA/Chitosan-Blended Hydrogels." *Journal of Biomedical Materials Research* 39 (1998): 486-490.

113. Krajewska, B. "Chitosan Membranes With Immobilized Urease." *Chitin Enzymology* (1993): 493-498.

114. Kratz, G., C. Arnander, J. Swedenborg, M. Back, C. Falk, I. Gouda, and O. Larm. "Heparin-Chitosan Complexes Stimulate Wound Healing in Human Skin." *Scandinavian Journal of Plastic and Reconstructive Surgery and Hand Surgery* 31 (1997): 119-123.

115. Kurita, K. "Graft Copolymers." *Applications of Chitin and Chitosan.* M. F. A. Goosen, 297-305. Lancaster, PA: Technomic Publishing Company, Inc., 1997.

116. Lahiji, A., A. Sohrabi, D. S. Hungerford, and C. G. Frondoza. "Chitosan Supports the Expression of Extracellular Matrix Proteins in Human Osteoblasts and Chondrocytes." *Journal of Biomedical Materials Research* 51 (2000): 586-595.

117. Laurencin, C., M. Attawia, H. Elgendy, and K. Herbert. "Tissue Engingineered Bone-Regeneration Using Degradable Polymers: The Formation of Mineralized Matrices." *Bone* 19, Supplement (1996): 93S-99S.

118. Lazarides, E., and K. Burridge. "α-Actin: Immunoflourescent Localization of a Muscle Structural Protein in Nonmuscle Cells." *Cell* 6 (1975): 289.

119. Leahy, D., W. Hendrickson, I. Aukhil, and H. Erickson. *Science* 258 (1992): 987-991.

120. Lee, E., W. Lee, C. Kaetzel, G. Parry, and M. Bissell. "Interaction of Mouse Mammary Epithelial Cells With Collagen Substrata: Regulation of Casein Gene Expression and Secretion." *Proceedings of the National Academy of Sciences of the United States of America* 82 (1985): 1419-1423.

121. Lee, Y. M., Y. J. Park, S. J. Lee, Y. Ku, S. B. Han, S. M. Choi, P. R. Klokkevold, and C. P. Chung. "Tissue Engineering Bone Formation Using Chitosan/Tricalcium Phosphate Sponges." *Journal of Periodontology* 71, no. 3 (2000a): 410-417.

122. Lee, Y. M., Y. J. Park, S. J. Lee, Y. Ku, S. B. Han, S. M. Choi, P. R. Klokkevold, and C. P. Chung. "The Bone Regenerative Effect of Platelet Derived Growth Factor-BB Delivered With a Chitosan/Tricalcium Phosphate Sponge Carrier." *Journal of Periodontology* 71 (2000b): 418-424.

123. Li, Q., E. T. Dunn, E. W. Grandmaison, and M. F. A. Goosen. Applications and Properties of Chitosan. M. F. A. Goosen, New York: Academic Press, 1997.

124. Lieberman, M. "Density-dependent regulation of cell growth: an example of a cell-cell recognition phenomenon. " *Journal of Membrane Biology* 63 (1981): 1-11.

125. Luker, A., I. Crane, C. Scully, and S. Prime. "The Effect of 3T3 Fibroblasts on the Expression of Anchorage Independence and Cornification of Oral Keratinocytes." *Virchows Archiv - Cells Molecules and Pathology* 57 (1989): 19-26.

126. Lundstrom, I. "Protein Conformation at Surfaces." *Oral Interfacial Reactions of Bone, Soft Tissue and Saliva.* Editors, P. O. Glantz, S. A. Leach, and T. Ericson, 9-23. Oxford, England: IRL Press Limited, 1985.

127. Lynch, S., R. Williams, and A. Polson. "A Combination of Platelet-Derived Growth Factor and Insulin-Like Growth Factors Enhances Periodontal Regeneration." *Journal of Clinical Periodontology* 16 (1989): 545-548.

128. Macarak, E., E. Kirby, T. Kirk, and N. Kefalides. "Synthesis of Cold-Insoluble Globulin by Cultured Calf Endothelial Cells." *Proceedings of the National Academy of Sciences of the United States of America* 75 (1978): 2621-2625.

129. Madihally, S. V., and H. W. T. Matthew. "Porous Chitosan Scaffolds for Tissue Engineering." *Biomaterials* 20 (1999): 1135-1142.

130. Maghami, G. G., and G. A. F. Roberts. "Studies on the Adsorption of Anionic Dyes on Chitosan." *Makromolecular Chemistry* 189 (1988): 2239-2243.

131. Main, A., T. Harvey, M. Baron, J. Boyd, and I. Campbell. "The three-dimensional structure of the tenth type III module of fibronectin: an insight into RGD-mediated interactions. " *Cell* 71 (1992): 671-678.

132. Malette, W., Inventor. "Method of Altering Growth and Development and Suppressing Contamination Micro-Organisms in Cell or Tissue Culture." USA 4605623. 1986.

133. Malette, W., H. Quigley, R. Gaines, N. Johnson, and W. Rainer. "Chitosan: a new hemostatic. " *Annals of Thoracic Surgery* 36 (1983): 55.

134. Manly, R. S., *Adhesion in Biological Systems.* New York: Academic Press, 1970.

135. Markwald, R., R. Runyan, G. Kitten, F. Funderberg, D. Bernauke, and P. Brouer. "Use of Collagen Gel Cultures to Study Heart Development: Proteoglycan and Glycoprotein Interactions During the Formation of Endorcardial Cushion Tissue." *The Role of Extracellular Matrix in Development.* R. Trelstad, 323-350. New York: A.R. Lyss, Inc., 1984.

136. Maurer, A., Z. Han, D. Dhermy, and T. Briere. "Glycosaminoglycans Enhance Human Leukemic Cell Growth *in Vitro* ." *Leukemia Research* 18 (1994): 837-842.

137. McDonald, J. "Receptors for Extracellular Matrix Components." *American Journal of Physiology* 257 (1989): L331.

138. McPherson, J. "The Utility of Collagen-Based Vehicles in Delivery of Growth Factors for Hard and Soft Tissue Wound Repair." *Clinical Materials* 9 (1992): 225-234.

139. McPherson, J., P. Ledger, and G. Ksander. "The Influence of Heparin on the Wound Healing Response to Collagen Implants *in Vivo*." *Collagen Related Research* 8 (1988): 83-100.

140. Meyle, J., K. Gultig, and W. Nisch. "Variation in Contact Guidance by Human Cells on a Microstructured Surface." *Journal of Biomedical Materials Research* 29 (1995): 81-88.

141. Mima, S., M. Miya, R. Iwamoto, and S. Yoshikawa. "Highly Deacetylated Chitin and Its Properties." *Proceedings of the Second International Conference on Chitin and Chitosan.* S. Hirano, and S. Tokura. Tottori, Japan: The Japanese Society of Chitin and Chitosan, 1982.

142. Minami, S., Y. Okamoto, K. Miyatake, A. Matsuhashi, Y. Kitamura, T. Tanigawa, Y. Tanaka, and Y. Shigemasa. "Chitin Induces Type IV Collagen and Elastic Fiber in Implanted Non-Woven Fabric of Polyester." *Carbohydrate Polymers* 29 (1996): 295-99.

143. Minami, S., Y. Okamoto, and S. Tanioka. "Effects of Chitosan on Wound Healing." *Carbohydrates and Carbohydrate Polymer.* M. Yalpani. Chicago, IL: ATL Press, 1993.

144. Minuth, W. W., M. Sitiinger, and S. Kloth. "Tissue Engineering: Generation of Differentiated Artificial Tissues Fro Biomedical Applications." *Cell Tissue Resource* 291 (1998): 1-11.

145. Miyazaki, S., K. Ishii, and T. Nadai. "The Use of Chitin and Chitosan As Drug Carriers." *Chemical Pharmaceutical Bulletin* (1981): 3067-3069.

146. Moore, G. H., and G. A. F. Roberts. *MIT Sea Grant Report* 78-7 (1978): 406.

147. Mori, T, M Okumura, M Matsuura, K Ueno, S Tokura, Y Okamoto, S Minami, and T Fujinaga. "Effects of Chitin and Its Derivatives on the Proliferation and Cytokine Production of Fibroblasts in Vitro." *Biomaterials* 18 (1997): 947-951.

148. Motosugi, K., Y. Yamaguchi, and K. Kibune, inventors. "Chitosan Sponges As Surgical Dressings." Japan Kokai Tokkyo Koho, Assignee. Japan JP 63,90,507. 1988.

149. Muzzarelli, R. A. A. "Depolymerization of Methyl-Pyrrolidinone Chitosan by Lysozyme." *Carbohydrate Polymers* 19 (1992): 29-34.

150. Muzzarelli, R. A. A. "Biochemical Significance of Exogenous Chitins in Animals and Patients." *Carbohydrate Polymers* 20 (1993): 7-16.

151. "Morphogenetic Actions of Chitosan and Growth Factors - Fibroblast Encapsulation in Chitosan Gel." Handout from Workshops on Cell Cultures, Italy (1994).

152. Muzzarelli, R. A. A. "New Derivatives of Chitin and Chitosan: Properties and Applications." *New Developments in Industrial Polysaccharides.* V. Crescenzi, I. C. M. Dea, and S. S. Stivala, 207-231. New York: Gordon and Breach Science Publishers, 1984.

153. Muzzarelli, R. A. A."Chitin." *The Polysaccharides.* 3rd Edition., G. O. Aspinall, 417-450. New York: Academic Press, Inc., 1985.

154. Muzzarelli, R. A. A., G. Biagini, M. Bellardini, L. Simonelli, C. Castaldini, and G. Fratto. "Osteoconduction Exerted by N-Methylpyrrolidione Chitosan Used in Dental Surgery." *Biomaterials* 14, no. 1 (1993): 39-43.

155. Muzzarelli, R. A. A., M. Mattioli-Belmonte, A. Pugnaloni, and G Biagini. "Biochemistry, Histology and Clinical Uses of Chitins and Chitosans in Wound Healing." *Chitin and Chitinases.* P. Jolles, and R. A. A. Muzzarelli, 251-264. Basel, Switzerland: Birkhauser Verlag, 1999.

156. Muzzarelli, R. A. A., M. Mattioli-Belmonte, C. Tietz, R. Biagini, G. Ferioli, M. A. Brunelli, M. Fini, R. Giardino, P. Iilari, and G. and Biagini. "Stimulatory Effect on Bone Formation Exerted by a Modified Chitosan." *Biomaterials* 15, no. 13 (1994): 1075-1081.

157. Muzzarelli, R. A. A., F. Tanfani, G. Scarpini, and G Laterza. "The Degree of Acetylation of Chitins by Gas Chromatography and Infrared Spectroscopy." *Journal of Biochemical and Biophysical Methods* , no. 2 (1980): 299-306.

158. Muzzarelli, R A. A., V Baldassarre, F Conti, P Ferrara, G Biagini, G Gazzanelli, and V Vasi. "Biological Activity of Chitosan Ultrastructural Study." *Biomaterials* 9 (1988): 247-252.

159. Muzzarelli, R. A. A., and G. Biagini. "Role and Fate of Exogenous Chitosans in Human Wound Tissues." *Chitin Enzymology*, R. A. A. Muzzarelli, 187-196. Grottammare: Atec, 1993.

160. Muzzarelli, R. A. A., G. Biagini, M. Mattioli-Belmonte, O. Talassi, M. Gandolfi, R. Solmi, S. Carreno, R. Giardino, M. Fini, and N. Nicoli-Aldini. "Osteoconduction by Chitosan-Complexed BMP: Morpho-Structural Responses in an Osteoporotic Model." *Journal of Bioactive and Compatible Polymers* 12 (1997): 321-329.

161. Muzzarelli, R. A. A., G. Biagini, A. Pugnaloni, O. Fillippini, V. Baldassarre, C. Castaldini, and C. Rizzoli. "Reconstruction of Parodontal Tissue With Chitosan." *Biomaterials* 10 (1989): 598-603.

162. Nakagawa, S., P. Pawelek, and F. Grinnell. "Long Term Culture of Fibroblasts in Contracted Collagen Gel: Effect on Cell Growth and Biosynthetic Activity." *Journal of Investigative Dermatology* 93 (1989): 792-798.

163. Neufelt, G., D. Gospodarowicz, L. Dodge, and D. Fujii. "Heparin Modulation of the Neurotropic Effects of Acidic and Basic Fibroblast Growth Factors and Nerve Growth Factor on PC12 Cells." *Journal of Cellular Physiology* (1987): 131-140.

164. Nimni, M. "Polypeptide Growth Factors; Targeted Delivery Systems." *Biomaterials* 18 (1997): 1201-1225.

165. Nishimura, K., S. Nishimura, H. Seo, N. Nishi, S. Tokura, and I. Azuma. "Macrophage Activation With Multiporous Beads Prepared From Partially Deacetylated Chitin." *Journal of Biomedical Materials Research* 20 (1986): 1359-1372.

166. Ogawa, K., T. Yui, and M. Miya. "Dependence on the Preparation Procedure of the Polymorphism and Crystallinity of Chitosan Membranes." *Bioscience, Biotechnology, Biochemistry* 56, no. 6 (1992): 858-862.

167. Okamoto, Y., S. Minami, A. Matsuhashi, H. Sashiwa, H. Saimoto, Y. Shigemasa, T. Tanigawa, Y. Tanaka, and S. Tokura. "Polymeric N-Acetyl-D-Glucosamine (Chitin) Induce Histionic Activation in Dogs." *Journal of Veterinary Medical Science* 55 (1993): 743-747.

168. Palapura, S., and J. Kohn. "Trends in the Development of Bioresorbable Polymers for Medical Application." *Journal of Biomaterial Applications* 6 (1992): 216-250.

169. Peluso, G., O. Petillo, M. Ranieri, M. Santin, L. Ambrosio, C. Daniela, B. Avallone, and G. Balsamo. "Chitosan-Mediated Stimulation of Macrophage Function." *Biomaterials* 15, no. 15 (1994): 1215-1220.

170. Pena, S., and R. Hughes. "Fibronectin-Plasma Membrane Interactions in the Adhesion and Spreading of Hamster Fibroblasts." *Nature* 276 (1978): 80.

171. Pieper, J. S., T. Hafmans, J. H. Veerkamp, and T. H. van Kuppevelt. "Development of Tailor-Made Collagen-Glycosaminoglycan Matrices: EDC/NHS Crosslinking, and Ultrastructural Aspects." *Biomaterials* 21 (2000): 581-593.

172. Pieper, J. S., A. Oosterhof, P. J. Dijkstra, J. H. Veerkamp, and T. H. van Kuppevelt. "Preparation and Characterization of Porous Crosslinked Collagenous Matrices Containing Bioavailable Chondroitin Sulfate." *Biomaterials* 20 (1999): 847-858.

173. Pierschbacker, M., and E. Ruoslahti. "Variants of the Cell Recognition Site of Fibronectin That Retain Attachment Promoting Activity." *Proceedings of the National Academy of Sciences of the United States of America* 81 (1984): 5985-5988.

174. Pless, D., D. Lee, S. Roseman, and R. Schnaar. "Specific Cell Adhesion to Immobilized Glycoproteins Demonstrated Using New Reagents for Protein and Glycoprotein Immobilization. " *Journal of Biological Chemistry* 258 (1983): 2340-2349.

175. Polk, A., B. Amsden, K. De Yao, T. Peng, and M. Goosen. "Controlled Release of Albumin From Chitosan-Alginate Microcapsules." *Journal of Pharmaceutical Sciences* 83, no. 2 (1984): 178-185.

176. Pouchert, C. " *The Aldrich Library of FT-IR Spectra.* 2nd Edition. C. Pouchert, 1238A. Milwaukee, WI: Aldrich, 1997.

177. Prasitsilp, M., R. Jenwithisuk, K. Kongsuwan, N. Damrongchai, and P. Watts. "Cellular Responses to Chitosan *In Vitro*." *Journal of Material Science: Materials and Medicine* 11 (2000): 773-778.

178. Prud'homme, C. "Chitosan in PH Sensitive Coatings for Rumen Protected Amino Acids." *Proceedings of the International Symposium on Controlled Release Bioactive Materials* 21 (1994): 112-113.

179. Pullan, S., J. Wilson, A. Metcalfe, G. Edwards, N. Goberdhan, J. Tilly, J. Hickman, C. Dive, and C. Streuli. "Requirement of Basement Membrane for the Supression of Programmed Cell Death in Mammary Epithelium." *Journal of Cell Science* 109 (1996): 631-642.

180. Rabinowitch, M., and M. DeStefano. "Manganese Stimulates Adhesion and Spreading of Mouse Sarcoma I Ascites Cells." *Journal of Cell Biology* 59 (1973): 165-76.

181. Raff, M. "Social Controls on Cell Survival and Cell Death." *Nature* 356 (1992): 397-400.

182. Raff, M., B. Barres, J. Burne, H. Coles, Y. Ishizaki, and M. Jacobson. "Programmed Cell Death and the Control of Cell Survival: Lessons From the Nervous System." *Science* 262 (1993): 695-700.

183. Reddi A. H., R. Gay, S. Gay, and E. J. Miller. "Transitions in Collagen Types During Matrix-Induced Cartilage, Bone, and Bone Marrow Formation." *The Proceedings of the National Academy of Sciences of the United States of America* no. 12 (1977): 5580-5592.

184. Remes, A., and D. Williams. "Immune Response in Biocompatibility." *Biomaterials* 13 (1992): 731-743.

185. Remunan-Lopez, C., and M. Lorenzo. "Development of New Microencapsulated Chitosan Gel Cores for the Controlled Release of Hydrophilic Macromolecules."*Proceeding of the 10th International Symposium on Microencapsulation.* Austin, TX: The University of Texas at Austin Press, 1995.

186. Rheinwald, J., and H. Green. "Serial Cultivation of Strains of Normal Human Epidermal Keratinocytes: the Formation of Keratinizing Colonies From Single Cells." *Cell* 6 (1975): 331-334.

187. Rigby, G., Inventor. "Process for the Preparation of Films and Filaments and Products Thereof."USA 2,030,880. 19 May 1936.

188. Rigby, G. Inventor. "Substantially Undegraded Deacetylated Chitin and Processes for Producing the Same." USA 2,040,879. 19 May 1936.

189. Risbud, M., A. Hardikar, and R. Bhonde. "Growth Modulation of Fibroblasts by Chitosan-Polyvinyl Pyrrolidone Hydrogel: Implications For Wound Management?" *Journal of Bioscience* 25, no. 1 (2000): 25-31.

190. Rollins, B., M. Cathcart, and L. Culp. "Fibronectin-Proteoglycan Binding As the Molecular Basis for Fibroblast Adhesions to ECMs." *The Glycoconjugates*, M. Horowitz, 289. New York: Academic Press, 1982.

191. Ruoslahti, E., E. Engvall, and E. Hayman. "Fibronectin: Current Concepts of Its Structure and Functions." *Collagen and Related Research* 1 (1981): 95-128.

192. Ruoslahti, E., and B. Obrink. "Review: Common Principles in Cell Adhesion." *Experimental Cell Research* 227 (1996): 1-11.

193. Ruoslahti, E., and A. Vaheri. "Novel Human Serum Protein From Fibroblast Plasma Membranes." *Nature* 248 (1974): 789-791.

194. Ruoslahti, E., and Y. Yamaguchi. "Proteoglycans As Modulators of Growth Factor Activities." *Cell* 64 (1991): 867-869.

195. Rutherford, R., C. Niekrash, J. Kennedy, and M. Charette. "Platelet-Derived and Insulin-Like Growth Factor Stimulate Regeneration of Periodontal Attachment in Monkeys." *Journal of Periodontal Research* 27 (1992): 285-290.

196. Saintigny, G., M. Bonnard, O. Damour, and C Collombell. "Reconstruction of Epidermis on a Chitosan Cross Linked Collagen-GAG Latice: Effect of Fibroblast." *Acta Derm Venereol* 73 (1993): 175-180.

197. Saltzman, M. W. "Cell Interactions With Polymers." *Principles of Tissue Engineering.* R. Lanza, R. Langer, and W. Chick, 225-246. New York: R. G. Landes Company, 1997.

198. Samuels, R. J. "Solid State Characterization of the Structure of Chitosan Films." *Journal of Polymer Science* 19 (1981): 1081-1105.

199. San-Antonio, J., O. Jacenko, M. Yagami, and R. Tuan. "Polyionic Regulation of Cartilage Development Promotion of Chondrogenesis in Vitro by Polylysine Is Associated With Altered Glycosaminoglycan Biosynthesis and Distribution." *Developmental Biology* 152 (1992): 323-325.

200. Sashiwa, H., K. Saito, H. Saimoto, S. Minami, Y. Okamoto, A. Matsuhashi, and Y. Shigemasa. "Enzymatic Degradation of Chitin and Chitosan." *Chitin Enzymology.* R. A. A. Muzzarelli, 177-186. Ancona: European Chitin Society, 1993.

201. Schakenraad, J. M., H. J. Busscher, C. R. H. Wildevuur, and J. Arends. "The Influences of Substratum Surface Free Energy on Growth and Spreading of Human Fibroblasts in the Presencee and Absence of Serum Proteins." *Journal of Biomedical Materials Research* 20 (1986): 773-784.

202. Schlessinger, J., I. Lax, and M. Lemmon. "Regulation of Growth Factor Activation by Proteoglycans: What Is the Role of the Low Affinity Receptors?" *Cell* 83 (1995): 357-360.

203. Schmidt, J., and A. von Recum. "Macrophage Response to Microtextured Silicone." *Biomaterials* 12 (1992): 385-389.

204. Sengel, P. *Morphogenesis of the Skin*. New York: Cambridge University Press, 1976.

205. Shoshan, S., and J. Gross. "Review: Biosynthesis and Metabolism of Collagen and Its Role in Tissue Repair Processes." *Israel Journal of Medical Science* 10, no. 5 (1974): 537-561.

206. Singhvi, R., G. Stephanopoulos, and D. I. C. Wang. "Review: Effects of Substratum Morphology on Cell Physiology." *Biotechnology and Bioengineering* no. 43 (1994): 764-771.

207. Sirca, A., and R. Woodman. "Selective aggregation of L1210 leukemia cells by the polycation chitosan. " *Journal of the National Cancer Institute* 47, no. 2 (1971): 377-388.

208. Sittinger, M., J. Bujia, W. Minuth, C. Hammer, and G. Burmeister. "Engineering of Cartilage Tissue Using Bioresorbable Polymer Carriers in Perfusion Culture." *Biomaterials* 15 (1994): 451-456.

209. Soranno, T., and E. Bell. "Cytostructural Dynamics of Spreading and Translocating Cells." *Journal of Cell Biology* 91 (1982): 127-136.

210. Sporns, O., G. Edelman, and K. Crossin. "The Neural Cell Adhesion Molecule (N-CAM) Inhibits Proliferation in Primary Cultures of Rat Astrocytes." *Proceedings of the National Academy of Sciences of the United States of America* 82 (1995): 542-546.

211. Tamada, Y, and Y Ikada. "Fibroblast Growth on Polymer Surface and Biosynthesis of Collagen." *Journal of Biomedical Materials Research* 28 (1994): 783-789.

212. Tan, W., R. Krishnaraj, and T. A. Desai. "Evaluation of Nanostructured Composite Collagen-Chitosan Matrices for Tissue Engineering." *Tissue Engineering* 7 (2001): 203-210.

213. Taylor, S., and J. Folkman. "Protamine is an Inhibitor of Angiogenesis." *Nature* 297 (1982): 307-312.

214. Thomas, K., and S. Cook. "An Evaluation of Variables Influencing Implant Fixation by Direct Bone Apposition." *Journal of Biomedical Materials Research* 19 (1985): 875-901.

215. Tokura, S., M. Itoyama, and S. Hiroshi, inventors. "Partially Sulfated Chitosan Goods." Japan Kokai Tokkyo Koho, Assignee. Japan JP 63,89,167. 1988.

216. Trinkaus, J. *Cells into Organs*. Englewood Cliffs, NY: Prentice-Hall, 1984.

217. Uhlrich, S., O. Lagente, M. Lenfant, and Y. Courtois. "Effect of Heparin on the Stimulation of Non-Vascular Cells by Human Acidic and Basic FGF." *Biochemical and Biophysical Research Communications* 137 (1986): 1205-1213.

218. Uragami, T., H. Mori, and Y. Noishiki. *Jinko Zoki* 17, no. 2 (1988): 511-514.

219. Usami, Y., Y. Okamoto, S. Minami, A. Matsuhashi, N. Kumazawa, S. Tanioka, and Y. Shigemasa. "Chitin and Chitosan Induce Migration of Bovine Polymorphonuclear Cells." *Journal of Veterinary Medical Science* 56 (1994): 761-762.

220. Usami, Y., Y. Okamoto, S. Minami, Matsuhashi A., and Y. Shigemasa. "Influence of Chain Length of *N*-Acetyl-D-Glucosamine and D-Glucosamine Residues on Direct and Complement-Mediated Chemotactic Activities for Canine Polymorphonuclear Cells." *Carbohydrate Polymers* 32 (1997): 115-122.

221. Vaissiere, G, B Chevallay, D Herbage, and O Damour. "Comparative Analysis of Different Collagen-Based Biomaterials As Scaffolds for Long-Term Culture of Human Fibroblasts." *Medical and Biological Engineering and Computing* 38 (2000): 205-210.

222. van der Valk, P., A. W. J. van Pelt, H. J. Busscher, H. P. de Jong, Ch. R. H. Wildevuur, and J. Arends. "Interaction of Fibroblasts and Polymer Surfaces: Relationship Between Surface Free Energy and Fibroblast Spreading." *Journal of Biomedical Materials Research* 17 (1983): 807-817.

223. van Kooten, T. G., J. M. Schakenraad, H. C. van der Mei, and H. J. Besscher. "Development and Use of a Parallel Plate Flow Chamber for Studying Cellular Adhesion to Solid Surfaces." *Journal of Biomaterials Research* 26, no. 6 (1992): 725-738.

224. van Oss, C. J., and H. J. Busscher. "Estimation of the Polar Surface Tension Parameters of Glycerol and Formamide, for Use in Contact Angle Measurements on Polar Solids." *Journal of Dispersion Science and Technology* 11 (1990): 75-81.

225. van Wachem, P. B., T. Beugeling, J. Feijen, A. Bantjes, J. P. Detmers, and W. G. van Aken. "Interaction of Cultured Human Endothelial Cells With Polymeric Surfaces of Different Wettabilities." *Biomaterials* 6 (1985): 403-408.

226. van Wachem, P., A. Hogt, T. Beugeling, J. Feijen, A. Bantjes, J. Detmers, and W. van Aken. "Adhesion of Cultured Human Endothelial Cells Onto Methacrylate Polymers With Varying Surface Wettability and Charge." *Biomaterials* 8 (1987): 323-328.

227. Weiss, L. "Principles of Adhesion in Biological Systems. "*Adhesion in Biological Systems.* R. Manly, 1-12. New York: Academic Press, 1970.

228. Williams, A., and A. Barclay. "The immunoglobulin superfamily--domains for cell surface recognition. " *Annual Review of Immunology* 6 (1988): 381-405.

229. Yamada, K., and J. Weston. "Isolation of a Major Cell Surface Glycoprotein From Fibroblasts." *Proceedings of the National Academy of Sciences of the United States of America* 71 (1974): 3492-3496.

230. Yoshika, T., R. Hirano, T. Shioya, and M. Kako. *Biotechnology and Bioengineering* 35 (1990): 66-72.

231. Zhang, Z., K. Vuori, J. C. Reed, and E. Ruoslahti. "The Alpha 5 Beta 1 Integrin Supports Survival of Cells on Fibronectin and Up-Regulates Bcl-2 Expression." *Proceedings of the National Academy of Sciences of the United States of America* 92 (1995): 6161-6165.

232. Zielinski, B. A., and P. Aebischer. "Chitosan As a Matrix for Mammalian Cell Encapsulation." *Biomaterials* 15, no. 13 (1994): 1049-1056.

APPENDICES

Appendix A

Statistical Methods

Equation A 1. Mean value

Equation A 2. Variance

Equation A 3. Standard Deviation

Equation A 4. Coefficient of determination

Equation A 5. Standard Error

Equation A 6. Confidence interval for mean μ

Equation A 7. Standard normal variate

Appendix A. Statistical Methods

Common statistical methods were applied to the experimental data of this report. The common values reported are the average and the standard error. The mean, standard deviation and standard error were all calculated according to the following equations:

A 1. Mean value

$$Average = \overline{X} = \frac{X_1 + X_2 + ... + X_n}{n}$$

where X_1 = measurement 1, and n is the number of measurements.

A 2. Variance

$$Variance = s^2 = \frac{\left|\left(X_1 - \overline{X}\right)^2 + \left(X_2 - \overline{X}\right)^2 + ... + \left(X_n - \overline{X}\right)^2\right|}{(n-1)}$$

A 3. Standard deviation

$$\text{Standard deviation} = s = \sqrt{s^2}$$

The coefficient of determination (R^2) was used to compare the linear relationship between two variables (X and Y). The equation used to calculate R^2 is as follows:

A 4. Coefficient of determination

$$R^2 = \left(\frac{n\left(\sum_n X_n Y_n\right) - \left(\sum_n X_n\right)\left(\sum_n Y_n\right)}{\sqrt{\left[n\sum_n X^2 - \left(\sum_n X\right)^2\right]\left[n\sum_n Y^2 - \left(\sum_n Y\right)^2\right]}} \right)^2$$

The standard error is reported in 3-5 was calculated from equation A.5

A 5. Standard error

$$\text{Standard Error} = \frac{s}{\sqrt{n}}$$

The standard error is calculated under the assumption that the distribution of sample values follows a standard bell curve. The standard error is an estimation of the error of the mean.

The 95% confidence intervals for the mean value μ, were estimated from the Equation A.6.

A 6. Confidence interval for mean μ

$$\langle \mu \rangle_{1-\alpha} = \left(\bar{x} - k_{\alpha/2} \frac{s}{\sqrt{n}}; \bar{x} + k_{\alpha/2} \frac{s}{\sqrt{n}} \right)$$

- $(1-\alpha)$ = confidence interval
- $<\mu>_{1-\alpha}$ = mean with a given confidence interval
- $k_{\alpha/2}$ = standard normal variate with cumulative probability levels of $\alpha/2$ and $(1-\alpha/2)$ respectively

The standard normal variate, $k_{\alpha/2}$ is given by Equation A.7 and determined from a table of normal probablility. For 95% confidence, $k_{\alpha/2} = 1.96$.

A 7. Standard normal variate

$$k_{\alpha/2} = \Phi^{-1}\left(1 - \frac{\alpha}{2}\right)$$

Appendix B

Bradford Assay for Measurement of Total Protein Concentrations

Appendix B. Bradford Assay for Measurement of Total Protein Concentrations

The Bradford assay utilizes the following materials:

Dye Stock: Coomassie Blue G (C.I. # 42655) (100 mg) is dissolved in 50 mL of methanol. (If turbid, the solution is treated with Norit (100 mg) and filtered through a glass-fiber filter.) The solution is added to 100 mL of 85% H_3PO_4, and diluted to 200 mL with water. The solution should be dark red, and have a pH of –0.01. The final reagent concentrations are 0.5 mg/mL Coomassie Blue G, 25% methanol, and 42.5% H_3PO_4. The solution is stable indefinitely in a dark bottle at 4 °C.

Assay Reagent: The assay reagent is prepared by diluting 1 volume of the dye stock with 4 volumes of distilled H_2O. The solution should appear brown, and have a pH of 1.1. It is stable for weeks in a dark bottle at 4 °C.

Protein Standards: Protein standards should be prepared in the same buffer as the samples to be assayed. A convenient standard curve can be made using bovine serum albumin (BSA) with concentrations of 0, 250, 500, 1000, 1500, 2000 μg/mL for the standard assay.

The following method describes the standard protein assay procedure used for the determination of the total protein content of cell suspensions (200-2000 μg/mL protein):

Prepare six standard solutions (1 mL each) containing 0, 250, 500, 1000, 1500 and 2000 μg/mL BSA. Set the spectrophotometer to collect the spectra at 595 nm and over and absorbance range of 0 to 2 Absorbance units. Use a 4 mL plastic cuvette filled with distilled water to blank the spectrophotometer over this wavelength range.

- Empty the plastic cuvette into a test tube and shake out any remaining liquid. Then add in the following order;

- 2.0 mL Assay reagent
- 40 μL of protein standard solution, starting with the lowest protein concentration and working up, or one of the samples to be assayed.
- Mix thoroughly.

- Record the absorbance spectrum of the sample at 595 nm.
- Repeat the steps above for each of the protein samples and for the samples to be assayed.

Examine the spectra of the standards and samples. If any spectrum has an absorbance at 595 nm greater than 2 Å, dilute the sample by a known amount and repeat the assay. Prepare a graph of Absorbance at 595 nm vs. protein concentration for the BSA protein standards. Examine the graphed points and decide if any should be rejected. (Often a single point can be rejected without invalidating the standard curve, but if more than one point appears questionable the assay should be repeated.) The Bradford assay gives a hyperbolic plot for absorbance versus protein concentration, but within a range of relatively low protein concentrations, the hyperbolic curve can be approximated reasonably well by a straight line. Use a best-fit straight line to fit the points if you feel it will give a good fit. If not, draw a smooth curve that falls on or near each of the data points.

To determine the protein concentration of a sample from its absorbance, use the standard curve to find the concentration of standard that would have the same absorbance of the sample.

The calibration curve for cell concentration corresponding to total protein concentration is depicted in Figure B.1. A calibration curve was established by

solubilizing various known cell concentrations (determined by a hemocytometer count) and determining the total protein content. These protein contents were then correlated to standard bovine serum albumin (BSA) protein measurements to create the calibration curve.

Figure B 1. Calibration curve for cell concentration versus BSA concentration

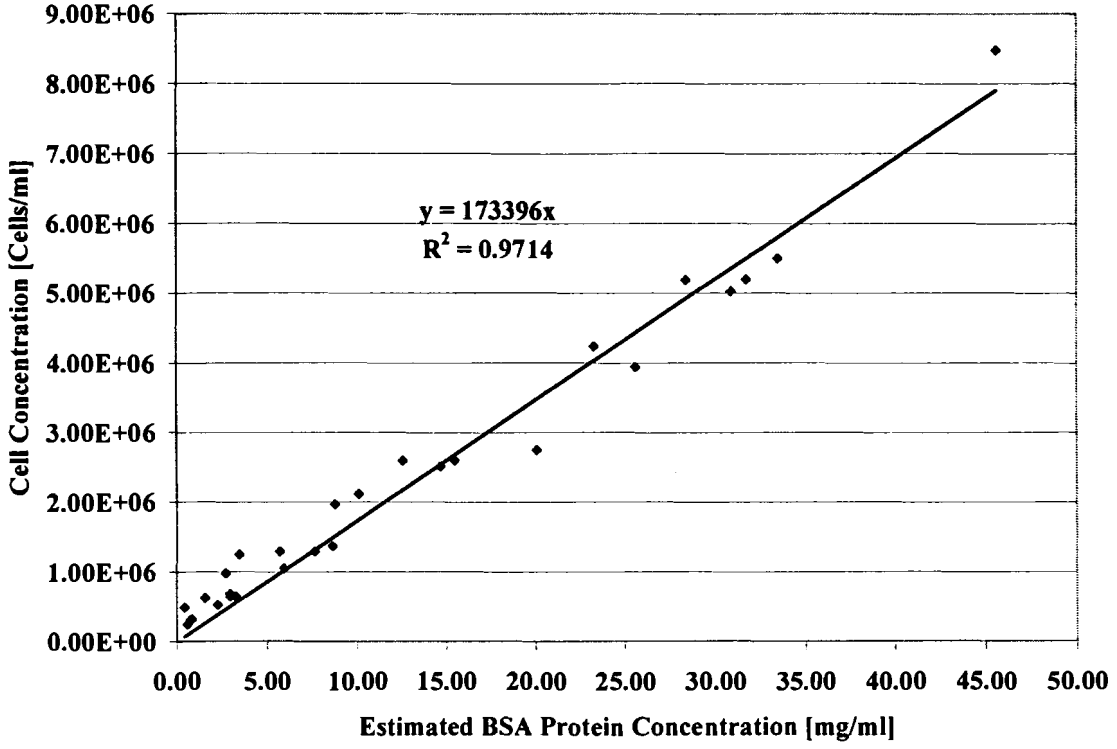

Appendix C

Surface Tension Components for Liquids Utilized in Contact Angle Measurements

Table C.1. Surface tension components of fluids

Appendix C. Surface Tension Components for Liquids Utilized in Contact Angle Measurements

The surface tension components of water, ethylene glycol and glycerol were characterized by Good and Van Oss [64 224]. These parameters are depicted in Table C.1

Table C 1. Surface tension components of fluids

Fluid	γ_l	γ_l^{LW}	γ_l^{AB}	γ_l^+	γ_l^-
Water	72.8	21.8	51.0	25.5	25.5
Glycerol	64.0	34.0	30.0	3.9	57.4
Ethylene Glycol	48.0	29.0	19.0	1.9	47.0

BIOGRAPHY OF THE AUTHOR

Michael Katalinich was born on May 7, 1975 in Denver, Colorado. He was raised in Longmont, Colorado, where he graduated from Skyline High School in 1993. He attended Fort Lewis College in Durango, Colorado from 1993 to 1994. He then transferred to The University of Colorado, Boulder, majoring in civil engineering with an environmental emphasis. He attained his Bachelor of Science degree in December 1998. While at the University of Colorado, he acted as the Vice President of Chi Epsilon Civil Engineering Honor Society from August 1997 to May 1998. In addition, he acted as both Vice President and President of the American Society of Civil Engineers Student Chapter (ASCE) from August 1996 to December 1998. During his undergraduate college career, he also worked as a research assistant on fuel cell technologies for Los Alamos National Laboratory in the summer of 1998. In addition, he worked as a quality control and quality assurance technician for a geotechnical engineering firm, Terracon Consultants, from 1997 to 1999. Following his graduation from the University of Colorado, he joined the Department of Chemical Engineering at the University of Maine, Orono. Michael is a candidate for the Master of Science degree in Chemical Engineering from The University of Maine in December, 2001.